**CLARA SUPRANI MARQUES**

# DEVELOPMENT, CHARACTERIZATION, APPLICATION, AND DEGRADATION OF SUSTAINABLE ACTIVE PACKAGING: CELLULOSE ACETATE AND ZEIN FILMS INCORPORATED WITH GARLIC ESSENTIAL OIL

Thesis submitted to the Graduate Program in Food Science of the Universidade Federal de Viçosa in partial fulfillment of the requirements for the degree of *Doctor Scientiae*.

Adviser: Nilda de Fátima Ferreira Soares

Co-advisers: Marali Vilela Dias
Maria Cristina Dantas Vanetti

**VIÇOSA – MINAS GERAIS**
**2022**

**Ficha catalográfica elaborada pela Biblioteca Central da Universidade Federal de Viçosa - Campus Viçosa**

T

M357d
2022

Marques, Clara Suprani, 1986-

Development, characterization, application, and degradation of sustainable active packaging: cellulose acetate and zein films incorporated with garlic essential oil / Clara Suprani Marques. – Viçosa, MG, 2022.

1 tese eletrônica (99 f.): il. (algumas color.).

Texto em inglês.

Orientador: Nilda de Fátima Ferreira Soares.

Tese (doutorado) - Universidade Federal de Viçosa, Departamento de Tecnologia de Alimentos, 2022.

Inclui bibliografia.

DOI: https://doi.org/10.47328/ufvbbt.2022.507

Modo de acesso: World Wide Web.

1. Alimentos - Conservação. 2. Alimentos - Armazenamento. 3. Polímeros - Biodegradação. 4. Essências e óleos essenciais. I. Soares, Nilda de Fátima Ferreira, 1960-. II. Universidade Federal de Viçosa. Departamento de Tecnologia de Alimentos. Programa de Pós-Graduação em Ciência e Tecnologia de Alimentos. III. Título.

CDD 22. ed. 664.028

Bibliotecário(a) responsável: Euzébio Luiz Pinto CRB-6/3317

**CLARA SUPRANI MARQUES**

# DEVELOPMENT, CHARACTERIZATION, APPLICATION, AND DEGRADATION OF SUSTAINABLE ACTIVE PACKAGING: CELLULOSE ACETATE AND ZEIN FILMS INCORPORATED WITH GARLIC ESSENTIAL OIL

Thesis submitted to the Graduate Program in Food Science of the Universidade Federal de Viçosa in partial fulfillment of the requirements for the degree of *Doctor Scientiae*.

APPROVED: July 22, 2022

Assent:

Clara Suprani Marques
Author

Nilda de Fátima Ferreira Soares
Adviser

## ACKNOWLEDGEMENTS

The author acknowledges the Coordenação de Aperfeiçoamento de Pessoal de Nível Superior – Brasil (CAPES) – Código de Financiamento 001, and Conselho Nacional de Desenvolvimento Científico e Tecnológico (CNPq) for financial support (grant number 142564/2018-4).

## ABSTRACT

MARQUES, Clara Suprani, D.Sc., Universidade Federal de Viçosa, July 2022. **Development, characterization, application, and degradation of sustainable active packaging: cellulose acetate and zein films incorporated with garlic essential oil**. Adviser: Nilda de Fátima Ferreira Soares. Co-advisers: Marali Vilela Dias and Maria Cristina Dantas Vanetti.

Biodegradable polymers obtained from renewable sources are considered potential substitutes for conventional plastics. In the present work, cellulose acetate (CA) and zein films containing garlic essential oil (GEO) and different plasticizers (glycerol and tributyrin) were manufactured, characterized, and evaluated as active films aiming food preservation, as well as investigated regarding their degradation in soil. In the first chapter, CA and zein blends were manufactured by adding glycerol or tributyrin as plasticizers, and GEO, complexed or not with β-cyclodextrin. Blends plasticized with tributyrin exhibited a more homogeneous surface than those containing glycerol. The blends underperformed the CA films at mechanical properties and water vapor permeability. However, they were more flexible than the zein brittle films. The films added with GEO presented in vitro activity against *Listeria innocua* and *Staphylococcus aureus*. These findings suggest that the mixture of CA and plasticizers could increase the range of application of zein as a sustainable packaging component, while GEO acts as a natural preservative. In the second chapter, CA-based films containing GEO were tested *in vitro* against *L. innocua* to verify the occurrence of sub-lethal injury and/or homologous resistance to GEO. Two conditions were tested: 7 ºC for 10 days, and 37 ºC for 24 h. The active films were also tested on food. The *in vitro* trials showed that the incubation under low temperature enhanced the active films properties: log reductions of 4.3 and 5.7 were obtained for films containing 1% and 10% of GEO, respectively. Moreover, 86.3% of *L. innocua* cells were injured at sub-lethal level when exposed to films with 10% of GEO for 10 days at 7 ºC. Despite this, no occurrence of homologous resistance was found. When the active films were tested on food, they resulted in fewer contaminants. This work suggested that GEO is a safe active compound from the point of view of homologous resistance. In the third chapter, the degradation in soil of blend films and CA-based films was studied. Films were buried for 150 days and were studied in terms of weight loss, macro and micro changes, molecular alterations, and thermal degradation profile. The polymer mass loss was more noticeable in CA:zein blend films and in films produced through glycerol incorporation. Also, there was significant interaction between the plasticizer choice and

presence of GEO: incorporation of GEO in glycerol-added films reduced the mass loss due to polymer degradation, while, when tributyrin was used, no impact was observed. FTIR spectra evidenced plasticizer loss, as well as degradation of zein in blend films and oxidation of the CA remaining hydroxyls. This study showed that the polymeric film's degradation in soil can be dependent on the polymer matrix, the type of plasticizer, and the presence of antimicrobial agent. Overall, the present study showed that the plasticizer choice can impact on the antimicrobial property of active films, and that additives as well as the polymer type affect the degradation rate of biodegradable films. Additionally, GEO, acting as antimicrobial agent in films, did not cause homologous resistance in *L. innocua* cells.

Keywords: Food preservation. Food Packaging. Polymers. Microbiology. Bacterial resistance. Degradation.

## RESUMO

MARQUES, Clara Suprani, D.Sc., Universidade Federal de Viçosa, julho de 2022. **Desenvolvimento, caracterização, aplicação e degradação de embalagem ativa sustentável: filmes de acetato de celulose e zeína incorporados com óleo essencial de alho**. Orientadora: Nilda de Fátima Ferreira Soares. Coorientadoras: Marali Vilela Dias e Maria Cristina Dantas Vanetti.

Polímeros biodegradáveis provenientes de fontes renováveis são investigados como potenciais substitutos dos plásticos convencionais. Neste trabalho, filmes de acetato de celulose (AC) e zeína contendo óleo essencial de alho (OEA) e diferentes plastificantes (tributirina e glicerol) foram elaborados, caracterizados e avaliados como filmes ativos em alimentos, bom como quanto à degradação em solo. No primeiro capítulo, blendas de AC e zeína foram elaboradas com os plastificantes e OEA complexado ou não com β-ciclodextrina. Blendas com tributirina apresentaram aspecto mais homogêneo. Em relação às propriedades mecânicas e barreira ao vapor de água, as blendas mostraram desempenho inferior aos filmes AC. Entretanto, em comparação ao filme quebradiço de zeína, as blendas mostraram-se mais flexíveis. Os filmes incorporados com OEA não complexado tiveram ação *in vitro* frente a *Listeria innocua* e *Staphylococcus aureus*. Os resultados indicam que AC e plastificantes podem ampliar o leque de aplicações de zeína na área de embalagens, e OEA atuaria como um potencial conservante natural. No segundo capítulo, filmes AC contendo OEA foram testados *in vitro* contra *L. innocua* para verificar se o contato com o filme ativo ocasionaria injúria subletal e/ou resistência homóloga ao OEA. Duas condições foram utilizadas: 7 ºC por 10 dias, e 37 ºC por 24 h. Os filmes também foram testados em alimento. A incubação sob baixa temperatura favoreceu a ação dos filmes, sendo verificadas reduções logarítmicas de 4,3 e 5,7 (1% e 10% de OEA, respectivamente). Além disso, 86,3% das células de *L. innocua* sofreram injúria subletal após 10 dias em contato com filme com 10% de OEA a 7 ºC. Também não foi verificada ocorrência de resistência homóloga. Quando aplicados no alimento, a presença dos filmes ativos reduziu em quase 1 ciclo log a contagem de microrganismos. Os resultados obtidos sugerem que OEA seja um composto seguro do ponto de vista de resistência homóloga. No terceiro capítulo, as blendas e filmes de AC foram investigados quanto a degradação em solo. Os filmes foram enterradas por 150 dias e avaliadas quanto à perda de massa, alterações macro e microscópicas, alterações moleculares e perfil de decomposição térmica. Perda de massa do polímero foi mais perceptível nas

blendas e nos filmes incorporados com glicerol. Houve interação significativa entre o tipo de plastificante e presença de OEA: filmes contendo OEA e glicerol tiveram menor perda de massa do polímero, ao passo que, quando tributirina foi utilizado, não foi verificada efeito do OEA. Os espectros de FTIR evidenciaram ocorrência de perda de plastificante, bem como perda de zeína, além de oxidação de hidroxilas remanescentes no AC. O estudo indicou que a degradação pode depender da matriz polimérica, do tipo de plastificante e da presença de agente antimicrobiano. De forma geral, o estudo mostrou que a atividade antimicrobiana dos filmes foi impactada pelo tipo de plastificante usado, e que os aditivos e o material polimérico influenciaram a taxa de degradação de filmes biodegradáveis. Além disso, OEA, como agente ativo em filmes, não promoveu aumento de resistência homóloga em *L. innocua*, o que foi desejável.

Palavras-chave: Conservação de alimentos. Embalagem de alimentos. Polímeros. Microbiologia. Resistência microbiana. Degradação.

**SUMMARY**

1 GENERAL INTRODUCTION ..... 11
2 REFERENCES ..... 12
3 ARTICLE 1: DEVELOPMENT AND INVESTIGATION OF ZEIN AND CELLULOSE ACETATE POLYMER BLENDS INCORPORATED WITH GARLIC ESSENTIAL OIL AND B-CYCLODEXTRIN FOR POTENTIAL FOOD PACKAGING APPLICATION13
3.1 Introduction ..... 13
3.2 Materials and Methods ..... 14
3.2.1 Materials ..... 14
3.2.2 Preparation of GEO:βCD inclusion complex ..... 15
3.2.3 Inclusion complex's characterization ..... 15
3.2.3.1 Entrapment efficiency (EE%) ..... 15
3.2.3.2 Thermal stability ..... 15
3.2.3.3 X-Ray diffraction (XRD) ..... 16
3.2.4 Elaboration of polymer blends ..... 16
3.2.5 Polymer blends' characterization ..... 17
3.2.5.1 Scanning electron microscopy ..... 17
3.2.5.2 Thickness and mechanical properties ..... 17
3.2.5.3 Water vapor permeability (WVP) ..... 17
3.2.6 Investigation of antibacterial property ..... 18
3.2.6.1 Inocula preparation ..... 18
3.2.6.2 Minimal inhibitory concentration (MIC) ..... 18
3.2.6.3 Films antibacterial activity by indirect contact ..... 19
3.2.7 Statistical analysis ..... 19
3.3 Results and Discussion ..... 19
3.3.1 Inclusion complex characterization ..... 19
3.3.2 Polymer blends aspect ..... 20
3.3.3 Thermogravimetric analysis ..... 23
3.3.4 Mechanical and water vapor barrier properties ..... 24
3.3.3 Antibacterial investigation ..... 27
3.4 Conclusion ..... 30
3.5 References ..... 30

4 ARTICLE 2: EXPOSURE TO CELLULOSE ACETATE FILMS INCORPORATED WITH GARLIC ESSENTIAL OIL DOES NOT LEAD TO HOMOLOGOUS RESISTANCE IN *Listeria innocua* ATCC 33090 ..... 39
4.1 Introduction ..... 39
4.2 Material and Methods ..... 40
4.2.1 Materials ..... 40
4.2.2 Initial assessment of GEO ..... 41
4.2.2.1 Gas chromatography (GC) ..... 41
4.2.2.2 Minimal inhibitory concentration (MIC) ..... 41
4.2.2.3. Pre-exposure of *L. innocua* to sub-lethal concentrations of GEO and investigation of homologous resistance ..... 42
4.2.3 Active films elaboration ..... 42
4.2.4 Films characterization ..... 43
4.2.4.1 Scanning Electron Microscopy (SEM) ..... 43
4.2.4.2 Thermogravimetric analysis (TGA) ..... 43
4.2.4.3 Thickness, density, and grammage ..... 43
4.2.4.4 Mechanical properties ..... 43
4.2.4.5 Water vapor permeability (WVP) ..... 44
4.2.5 Pre-exposure to GEO-films and investigation of sub-lethal injury and homologous resistance in *L. innocua* ..... 44
4.2.6 Test as interfold packaging ..... 46
4.2.7 Statistical analyses ..... 47
4.3. Results and Discussion ..... 47
4.3.1. Assessment of GEO ..... 47
4.3.2 Films characterization ..... 48
4.3.3 *In vitro* assessment of active films ..... 53
4.3.4 Active films as interfold packaging ..... 56
4.4. Conclusion ..... 59
4.5 References ..... 59
5 ARTICLE 3: DEGRADATION IN SOIL OF CELLULOSE ACETATE AND ZEIN BLEND FILMS INCORPORATED WITH DIFFERENT PLASTICIZERS AND GARLIC ESSENTIAL OIL ..... 69
5.1 Introduction ..... 69
5.2 Material and Methods ..... 70
5.2.1 Material ..... 70
5.2.2 Experimental design and films elaboration ..... 71
5.2.3 Degradation assay ..... 72

5.2.3.1 Subjective visual analysis ..... 72
5.2.3.2 Scanning Electron Microscopy ..... 72
5.2.3.3 Mass loss ..... 73
5.2.3.4 Thermogravimetric analysis (TGA) ..... 73
5.2.3.5 Fourier Transform Infrared Spectroscopy (FTIR) ..... 73
5.2.3.6 Statistical analysis ..... 73
5.3 Results and Discussion ..... 73
5.3.1 Macro and microscopic changes in films ..... 74
5.3.2 Mass loss ..... 78
5.3.3 FTIR ..... 83
5.4 Conclusion ..... 87
5.5 References ..... 88
5.6 Supplementary Material ..... 93
6 GENERAL CONCLUSION ..... 99

# 1. GENERAL INTRODUCTION

The invention of plastic was a major breakthrough in many areas, from military to the textile industry. The food packaging area has also benefited enormously from this revolutionary discovery, since plastic packaging present a set of features suitable for food preservation. However, despite the advantages, the pollution generated from the improper disposal of these materials results in serious environmental problems.

Sustainable packaging research is a trend focused on strategies and changes in the packaging sector aiming for a positive impact on the environment. For instance, the study of bio-based polymers is an interesting approach oriented toward developing biodegradable packaging materials from renewable sources. In this sense, cellulose, starch, proteins, and other biopolymers are widely studied as potential materials to replace conventional plastics in packaging development. Conversely, the films obtained from bio-based polymers underperform the traditional plastics in terms of mechanical, barrier and thermal properties, which is a problem to their implementation and consolidation on the market (MANGARAJ et al., 2019). To enhance these properties, some strategies are proposed, such as blending two or more biopolymers and incorporating plasticizers.

Moreover, another significant trend in the food packaging sector is the development of active packaging. Besides the usual functions expected from packaging, such as containing and protecting the product from external hazards, active packaging has additional features that play a role in food preservation. Antimicrobial packaging is a type of active packaging with antimicrobial agents capable of inhibiting the growth of spoilage and/or pathogenic microorganisms, contributing to food preservation and safety. During the ongoing COVID-19 pandemic, the interest in this kind of packaging increased, and it is expected to continue growing post COVID-19 (PASCUTA, VODNAR, 2022).

Despite the benefits of this technology, it is worth mentioning that several stress factors used in the food industry to preserve food can lead to the development of resistance in microorganisms. The use of antimicrobial compounds, such as food preservatives, for example, can induce homologous resistance in bacteria, in other words, the microorganism can become more resistant to the same stressing agent used (CEBRIÁN et al., 2010). Although there is a lack of studies about active antimicrobial packaging and the development of bacterial resistance, it is important to verify if the active material is safe or if it could induce the emergence of resistant strains, which would be a risk to public health. Additionally, since antimicrobial packaging contains antimicrobial agents, and since the

degradation phenomenon involves the soil microbiota, it is therefore necessary to study whether the presence of these compounds can alter the material degradation rate.

In this sense, the present work investigated the proposed themes: the development of a sustainable blend, the occurrence of homologous resistance in bacteria after contact with active films, and, at last, the material degradation rate when buried in soil. Cellulose acetate and zein were the polymers selected for the blend manufacture due to their hydrophobicity, glycerol and tributyrin were the plasticizers investigated, and garlic essential oils was the natural antimicrobial used. In chapter Article 1, the blend preparation and characterization are presented. In chapter Article 2, *Listeria innocua* cells were exposed to active films elaborated with cellulose acetate, glycerol and garlic essential oil to verify the occurrence of cell injury and homologous resistance. After, the films were also tested on food. Finally, in chapter Article 3, the degradation of both blend films and cellulose acetate films was explored.

## 2. REFERENCES

CEBRIÁN, G.; SAGARZAZU, R.; PAGÁN, R.; CONDÓN, S.; MAÑAS, P. Development of stress resistance in *Staphylococcus aureus* after exposure to sub-lethal environmental conditions. **International Journal of Food Microbiology**, v. 140, p. 26–33, 2010.

MANGARAJ, S.; YADAV, A.; BAL, L.M.; DASH, S.K.; MAHANTI, N.K. Application of biodegradable polymers in food packaging industry: a comprehensive review. **Journal of Packaging Technology and Research**, vol. 3, p. 77-96, 2019.

PASCUTA, M. S.; VODNAR, D. C. Nanocarriers for sustainable active packaging: An overview during and post COVID-19. **Coatings**, v. 12, n. 1, 102, 2022.

# 3. ARTICLE 1: DEVELOPMENT AND INVESTIGATION OF ZEIN AND CELLULOSE ACETATE POLYMER BLENDS INCORPORATED WITH GARLIC ESSENTIAL OIL AND B-CYCLODEXTRIN FOR POTENTIAL FOOD PACKAGING APPLICATION

This article was published in *Polysaccharides* (March 2022, doi: 10.3390/polysaccharides3010016).

## 3.1 Introduction

Plastics revolutionized the food packaging sector since they are available at low cost, flexible, durable, versatile, and have distinct mechanical and barrier properties, suitable for food preservation [1,2]. However, the rampant consumption and improper disposal of plastics has resulted in a worldwide problem, causing damage to the environment and human health. In order to reduce the manufacture and use of materials from nonrenewable sources, various strategies are proposed, such as recycling and the total or partial replacement of conventional plastics with bio-based materials [2–9].

Derived from several renewable sources (i.e., agroindustrial byproducts and feed-stock), bio-based materials have become increasingly popular among researchers from the packaging area since they fulfill the requirements for sustainable development [2,10]. In this context, several bio-based polymers extracted from different sources have been investigated as potential compounds for packaging. Cellulose derivatives, such as cellulose acetate (CA), and plant proteins, such as zein, are examples of hydrophobic polymers of natural origin that are already approved by the FDA to be used as food contact substances (CA) or listed as GRAS (zein) [4,11–13].

However, despite the growing trend, studies have revealed that films elaborated with bio-based polymers leave much to be desired when compared with the petroleum- based ones. Regarding food packaging and its role in food preservation, the higher water vapor permeability and lower mechanical properties that bio-based films usually present may impair their application as packaging components [2,10]. Aiming at improving the polymers' performance as a packaging material, several strategies are considered.

The blend or mixture of two or more polymers for obtaining a new material with distinct characteristics is one of these proposed strategies [14,15]. The incorporation of different additives can also allow the elaboration of films with improved properties and/or

functions [4, 5,16–18]. Plasticizers, such as glycerol, for example, are widely used since they can enhance films' flexibility. They are usually low-molecular weight compounds with low or no volatility, and able to increase polymer chain mobility [16,17].

Essential oils (EOs) are another example of additives for food packaging due to their bioactive properties and natural appeal. Some EOs show antimicrobial activity, which could grant to the packaging a preservative action, contributing to food safety and shelf-life extension [5,6,19,20]. However, the direct incorporation of EOs into polymer matrices is not recommended due to several issues (EOs are prone to thermal and light degradation, for instance) [21]. Thus, their complexation with cyclodextrins (CDs), followed by their addition into polymeric matrices, is considered an interesting way to protect the EOs' active compounds from the degradation caused by light, temperature exposure, and oxygen presence, as well as to minimize their sensorial impact [18]. βCD, for example, is a low-cost natural CD recognized as safe and already used in food items and drugs [18–20].

Within this context, the present work aimed to obtain, characterize, and compare blends of CA and zein with two different plasticizers, glycerol and tributyrin. Although CA:zein blends have already been studied as nanofibers in the biomedical area, their potential as a food packaging material is not elucidated in the literature [ 22 , 23 ]. In addition, GEO was added into the films, free or as an inclusion complex (IC) with βCD, aiming at elaborating active films with antibacterial action. Two hypotheses were investigated: (1) that there would be an improvement in the properties of the new material compared with those of the individual polymers; and (2) that the incorporation of the EO in the complexed form would ensure a better antibacterial action by the films when compared with the ones with added non-complexed EO.

## 3.2 Materials and Methods

### 3.2.1 Materials

CA (SD = 2.5, and average molar mass of 2024000 $g.mol^{-1}$) was donated by Rhodia Solvay Group (Brazil). Zein was donated by Flo Chemical Corp (F4400, molecular mass of 15-26 kDa) (USA). Glycerol (LabSynth, Brazil) and tributyrin (98% purity degree, Acros Organics, India) were the plasticizers investigated. Anhydrous ethanol (99.8% purity degree, Neon, Brazil) and acetone (99.5% purity degree, LabSynth, Brazil) were the solvents used for polymers dispersion. GEO suitable for food was purchased from Empório Laszlo (Brazil), and βCD (97% purity degree) was acquired from Sigma-Aldrich (USA).

### 3.2.2 Preparation of GEO:βCD inclusion complex

IC was prepared by kneading method following the mass proportion of 88% of βCD and 12% of GEO [19], which approximately matches the 1:1 molar ratio when considering the GEO compounds average molar mass. The IC preparation was performed according to Marques et al. [20] methodology, with modifications. In a porcelain mortar, 880 mg of βCD were added to 880 µL of hydroalcoholic solution (1:3 v/v ethanol:water) and homogenized for 5 minutes. Subsequently, 120 mg of GEO were added to the obtained paste and the mixture was manually macerated for up to 30 minutes. Samples were dried in desiccator containing silica gel for 48 h at 25 ºC, ground and stored. Physical mixture (PM) was prepared for comparison purposes mixing briefly 880 mg of βCD and 120 mg of GEO in a mortar.

### 3.2.3 Inclusion complex's characterization

#### 3.2.3.1 Entrapment efficiency (EE%)

Determination of GEO amounts in the IC was performed spectrophotometrically according to Hill, Gomes, and Taylor [24] with modifications. Initially, calibration curve was obtained from GEO solutions ranging from 0.0010 µL.mL$^{-1}$ to 0.0088 µL.mL$^{-1}$ in isopropanol:acetonitrile (3:2 v/v) at 209 nm of UV absorbance (UV1800, Shimadzu, Japan). 20 mg of ICs samples were dispersed in 20 mL of isopropanol:acetonitrile and mixed for 48 h. After, samples were centrifuged at 3200 x g (model 4K-15, Sigma, Germany), for 15 min. The supernatant was measured at 209 nm of UV absorbance. The percentage of GEO entrapped in ICs was calculated as equation 1:

$$EE\% = \frac{GEO_R}{GEO_T}\ x\ 100 \quad \text{(Eq. 1)}$$

in which $GEO_R$ and $GEO_T$ represent the real and the theoretical amount of GEO entrapped in the IC, respectively.

#### 3.2.3.2 Thermal stability

Thermogravimetric analysis (TGA) was performed on a thermogravimetric analyzer, (Model DTG-60H, Shimadzu, Japan), under a nitrogen atmosphere (50 mL.min-$^{1}$). Approximately 3 mg of samples were weighed and heated from 25 ºC to 360 ºC at a rate of 10 ºC.min$^{-1}$. TG curves were obtained for βCD, IC, PM, and GEO.

The thermal stability of the elaborated films and their components was verified as well. The parameters were the same, with the exception of the final temperature, which was 550 ºC.

#### 3.2.3.3 X-Ray diffraction (XRD)

X-Ray diffractograms for βCD, IC, and PM were obtained through a BRUKER X-ray diffractometer (model D8 Discover) equipped with an X-ray tube (Cu-Kα radiation, λ=0.1514 nm), in a 2θ range from 5° to 70° with a scanning rate of 0.05° $s^{-1}$.

### 3.2.4 Elaboration of polymer blends

Aiming the obtainment of a CA:zein blend, each polymer was, at first, dispersed separately. CA was dispersed in acetone (1:10 wt/v) and let to rest for 24 h. Zein was dispersed in ethanol 80% (v/v), ratio of 1:10 (wt/v), stirring at 500 rpm under 65 ºC for 10 min. After cooled back to room temperature (approximately 25 ºC), the dispersions were mixed together following the proportion of 60:40 CA:zein (wt/wt), since previous tests conducted in the laboratory revealed that this ratio allowed the obtainment of a more homogeneous film when compared to the others (Figure 1S of Supplementary Material). The plasticizer (glycerol or tributyrin) was also added to the mixed dispersion in the proportion of 30% (wt/wt) based on the polymer mass, as well as the bioactive agents: GEO (10% wt/wt) or IC (10% wt/wt), also based on the polymer mass. The dispersion was homogenized at 5,000 rpm for 2 min (model T25, Ultra Turrax, IKA), let to rest for 30 min, poured onto a glass plate with machine casting (K-Paint applicator, USA) and allowed to dry at room temperature. A blend without bioactive agent and a blend containing 10% of βCD were also investigated as control samples. Therefore, four different blends and four CA-films for each plasticizer were obtained, resulting in 16 assays, as described in Table 1. For comparison purpose, films with only CA and only zein were elaborated as well (Figure 2S of Supplementary Material).

**Table 1.** Elaborated films with different plasticizers and additives: cellulose acetate and zein blends (BL) (ratio 60:40 CA:zein wt/wt) and their respective controls cellulose acetate-based (CA).

| Sample | Plasticizer (30% wt/wt) | Additive (10% wt/wt) |
|---|---|---|
| BL-T-CNT | Tributyrin | - |
| BL-T-βCD | Tributyrin | β-cyclodextrin |
| BL-T-GEO | Tributyrin | Garlic essential oil |
| BL-T-IC | Tributyrin | Inclusion complex |
| CA-T-CNT | Tributyrin | - |

| | | |
|---|---|---|
| CA-T-βCD | Tributyrin | β-cyclodextrin |
| CA-T-GEO | Tributyrin | Garlic essential oil |
| CA-T-IC | Tributyrin | Inclusion complex |
| BL-G-CNT | Glycerol | - |
| BL-G-βCD | Glycerol | β-cyclodextrin |
| BL-G-GEO | Glycerol | Garlic essential oil |
| BL-G-IC | Glycerol | Inclusion complex |
| CA-G-CNT | Glycerol | - |
| CA-G-βCD | Glycerol | β-cyclodextrin |
| CA-G-GEO | Glycerol | Garlic essential oil |
| CA-G-IC | Glycerol | Inclusion complex |

### 3.2.5 Polymer blends' characterization

#### 3.2.5.1 Scanning electron microscopy

Micrographs of films' surface and films' cross-sectional area, after liquid-nitrogen brittle fracture, were obtained with a scanning electron Tabletop Microscope (model TM3000, Hitachi High-Technologies, Japan) with secondary electron detector and operating under low-vacuum. Uncoated samples were attached on stubs' surface with a double-sided carbon tape aid, and the accelerating voltage of 15 KV was used.

#### 3.2.5.2 Thickness and mechanical properties

Film thickness was measured, in μm, with a digital micrometer (model 547-401, Mitutoyo, Japan). Ten specimens of each treatment were analyzed in ten random points per sample [5]. The films' mechanical properties were also evaluated, which factors analyzed were tensile strength (TS, in MPa), elongation at break (E, in %), and modulus of elasticity (Young's modulus, YM, in MPa) using a Universal Testing Machine (model 3367, Instron Corporation, USA) equipped with a 1 kN load cell. Five rectangular specimens of each treatment (175 mm x 25 mm) were tested. The initial distance of grids' separation was 125 mm, and the rate of separation rate was 50 $mm.min^{-1}$ [25].

#### 3.2.5.3 Water vapor permeability (WVP)

WVP was investigated by the gravimetric method according to ASTM E96/E96M (2010) [26] (with a few modifications), which allow the calculation of the water vapor transmission rate (WVTR) as a function of weight gain. The films were cut into circles (Ø =

83 mm) and sealed with parafilm in poly(methyl methacrylate) cups containing a saturated solution of lithium chloride (12% ± 5 % RH at 25 ºC ± 2 ºC). After, the cups were placed in desiccators containing a saturated solution of sodium chloride (75% ± 5 % RH at 25 ºC ± 2 ºC). The cups were periodically weighted to provide at least ten data points. Graphs expressing the gain of mass over time allowed the determination of the WVTR according to equation 2:

$$\mathrm{WVTR} = \frac{m}{t.A} \quad \text{(Eq. 2)}$$

in which m/t is the slope of gain of mass (g) over time (h), and A is the permeation area (m²). After, the WVP was obtained according to equation 3:

$$\mathrm{WVP} = \frac{\mathrm{WVTR}.X_T}{P_S.(RH_1 - RH_2)} \quad \text{(Eq. 3)}$$

in which $X_T$ is the film thickness, $P_S$ is the saline water saturation pressure, $RH_1$ is the relative humidity in the desiccator containing NaCl, and $RH_2$ is the relative humidity on the desiccator containing LiCl. WVP was expressed as $g.Pa^{-1}.s^{-1}.m^{-1}$ .

### 3.2.6 Investigation of antibacterial property

The antibacterial activity of GEO was initially investigated against Gram-positive bacteria *Staphylococcus aureus* and *Listeria innocua*, and Gram-negative bacteria *Escherichia coli*, *Pseudomonas fluorescens*, and *Salmonella* Choleraesuis. Since the EO only showed activity against the Gram-positive ones, *L. innocua* and *S. aureus* were used for investigation of minimal inhibitory concentration of GEO and IC, as well as for evaluation of the films. *P. fluorescens* was selected as negative control.

#### 3.2.6.1 Inocula preparation

Selected colonies of the bacteria were taken from a non-selective medium (plate count agar, PCA, Oxoid, England) and were suspended in 0.85% (m/v) saline solution until visual suspension density similar to 0.5 McFarland turbidity standard (around 1-2 x $10^7$ $CFU.mL^{-1}$) then diluted 1:10 once [22].

#### 3.2.6.2 Minimal inhibitory concentration (MIC)

The agar dilution method, with few modifications, was used to investigate the MIC of GEO and IC [27]. Samples of both bioactive agents were dispersed in 10 mL of liquefied Brain Heart Infusion (BHI, Himedia, India) agar (~45 ºC), resulting in the final concentrations of 2,650 $\mu g.mL^{-1}$, 1,272 $\mu g.mL^{-1}$, 636 $\mu g.mL^{-1}$, 318 $\mu g.mL^{-1}$, 159 $\mu g.mL^{-1}$, 79.5 $\mu g.mL^{-1}$, and

39.75 µg.mL$^{-1}$ for GEO, and 9,600 µg.mL$^{-1}$, 4,800 µg.mL$^{-1}$, 2,400 µg.mL$^{-1}$, 1,200 µg.mL$^{-1}$, 600 µg.mL$^{-1}$, and 300 µg.mL$^{-1}$ for IC. Negative controls were BHI agar and BHI agar with 9,600 µg.mL$^{-1}$ of βCD. After allowing the agar to set and solidify, aliquots of 20 µL of the inoculum (Section 3.2.6.1) were dispensed on the dried agar surface, resulting in a final bacterial concentration of approximately $10^4$ CFU.mg$^{-1}$ per spot. The plates were incubated at 37 ± 1 ºC for 24 h. MIC was determined based on the lowest concentration capable of growth inhibition.

**3.2.6.3 Films antibacterial activity by indirect contact**

The elaborated films were cut into (2x4) cm² shape and fixed onto the lids of Petri dishes. The plates were previously prepared with BHI agar and inoculated with *S. aureus* or *L. innocua* (Section 3.2.6.1) with a swab aid [6]. The incubation conditions were 24 h at 37 ºC ± 1 ºC (*S. aureus* and *L. innocua*) and 10 days at 7 ºC ± 1 ºC (*L. innocua*). The presence or absence of microbial growth was evaluated after the incubation period.

**3.2.7 Statistical analysis**

Analysis of variance (ANOVA) was carried out and followed by Tukey's test at 5% probability, if suitable. The statistical software R was used [28].

**3.3 Results and Discussion**

**3.3.1 Inclusion complex characterization**

The IC preparation of GEO with βCD was achieved by the kneading method, which was chosen due to the practicality and quality of the technique [20,29]. To calculate the GEO entrapped in ICs, the calibration curve was obtained (equation 4) with a R² adjusted of 0.9942.

$$Y_{209\,nm} = 0.0299 + 69.052X_{GEO} \quad \text{(Eq. 4)}$$

in which $Y_{209}$ is the measured absorbance at 209 nm and $X_{GEO}$ is the EO concentration. The entrapment efficiency calculated was 87.5%.

The thermogravimetric curves, as well as their derivatives, plus the X-ray diffractograms of IC and pristine materials are displayed in the Supplementary Material, Figure 3S and Figure 4S, respectively. Regarding the thermal analyses, the βCD mass losses, exhibited in the TG curve, occurred in two steps: at 25-120 ºC, losing 12.6%, due to water loss, and above 309 ºC, corresponding to 76.7% of material decomposition, corroborating with Giordano et al. [30]. The EO mass loss displayed in the GEO TG curve started at room

temperature (~25 ºC) and achieved around 95% of loss until 200 ºC. A similar behavior was observed by Piletti et al. [31] when studying the thermal protection of complexed GEO.

Three stages were observed for the TG curve of PM: at 25-120 ºC, losing 14.5%, at 120-250 ºC (4.0%), and above 300 ºC, with 66.2% of material degradation. In the first and second stages, PM exhibited an intermediary behavior between βCD and GEO mass loss under temperature increase. The initial mass loss of PM system was higher than the one of βCD, which may have occurred due to water molecules loss besides non-complexed EO volatilization.

IC TG curve, in turn, presented an initial mass loss of 7%, a lower value than the verified for βCD and PM. This occurrence is discussed in the literature as an indication that the complexation was successfully achieved [31,32]. It can also be observed that ~5% IC mass loss occurred at 100-250 ºC, which can be attributed to the degradation of non-complexed EO [20,31]. The material degradation occurred near 300 ºC, with 62% of mass loss. A small peak, slightly before material degradation, can be observed in the IC DTG curve, emphasized by a red arrow in Figure 3S. This can be attributed to complexed GEO volatilization, which occurred in a higher temperature than non-complexed GEO, indicating greater thermal stability of IC compound [31].

Regarding the XRD analyses (Figure 4S), βCD diffractogram exhibited the characteristic peaks for βCD at 2θ = 9.0º, 12.4º, 16.9º, 22.6º, 27.1º, 31.9º, 34.6º and 35.5º [33]. PM diffractogram presented peaks similar to βCD, albeit in lesser intensity. On the other hand, in IC diffractogram, it is possible to observe greater changes in XDR profile, such as broadening, appearance, and disappearance of some peaks [20,32]. The decrease in the degree of crystallinity, as can be observed when comparing the IC diffractogram with βCD and PM diffractograms, with the disappearance of some well-defined and narrow peaks (pointed out with black arrows in Figure 4S) can be a result of changes that occurred in the βCD's molecular organization, an indicative that the complexation with GEO was achieved [32,34].

### 3.3.2 Polymer blends aspect

The manufactured CA:zein blends and the CA-films incorporated with tributyrin or glycerol as plasticizers and the additives (GEO, IC, or βCD) are displayed in Figure 1. The blends presented a yellowish color and a porous appearance when compared to the transparent CA-films, probably due to the zein addition (Figure 1 and Figure 2S). The films' aspect also changed as a function of the plasticizer kind used. Tributyrin incorporation resulted in blends

with a more homogeneous surface than glycerol added-blends, which in turn presented serious defects.

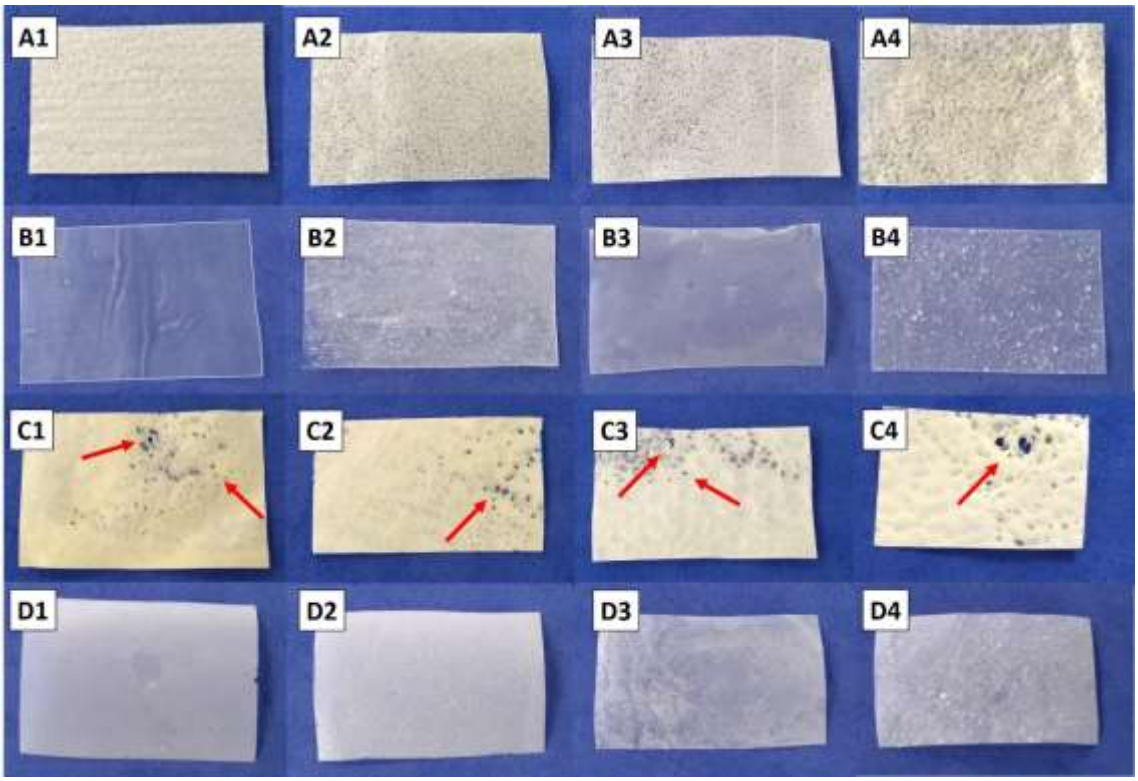


**Figure 1.** Images of the obtained blends and cellulose acetate (CA) films. Blends (line A) and their respective CA-films (line B) incorporated with tributyrin and additives: control (no additive, A1 and B1), βCD (A2 and B2), GEO (A3 and B3), and inclusion complex (A4 and B4). Blends (line C) and their respective CA-films (line D) incorporated with glycerol and additives: control (no additive, C1 and D1), βCD (C2 and D2), GEO (C3 and D3), and inclusion complex (C4 and D4). Red arrows indicate presence of macro-holes and tears.

In addition, SEM micrographs revealed the presence of micro-sized globules in the glycerol added-blends' cross-sectional area, which were not observed in tributyrin added-blends, suggesting a poor compatibility between glycerol and the polymers (Figure 2). Tributyrin is a triglyceride of butyric acid more hydrophobic than glycerol, and since both polymers (CA and zein) used have a more hydrophobic nature, the obtained result is coherent [35]. The incorporation of βCD or IC into blends or CA-films also resulted in major changes in films' appearance and thickness, exhibiting more irregular surface than the control samples and the ones containing GEO. The presence of lumps and aggregates indicates poor compatibility among these additives and the polymers.

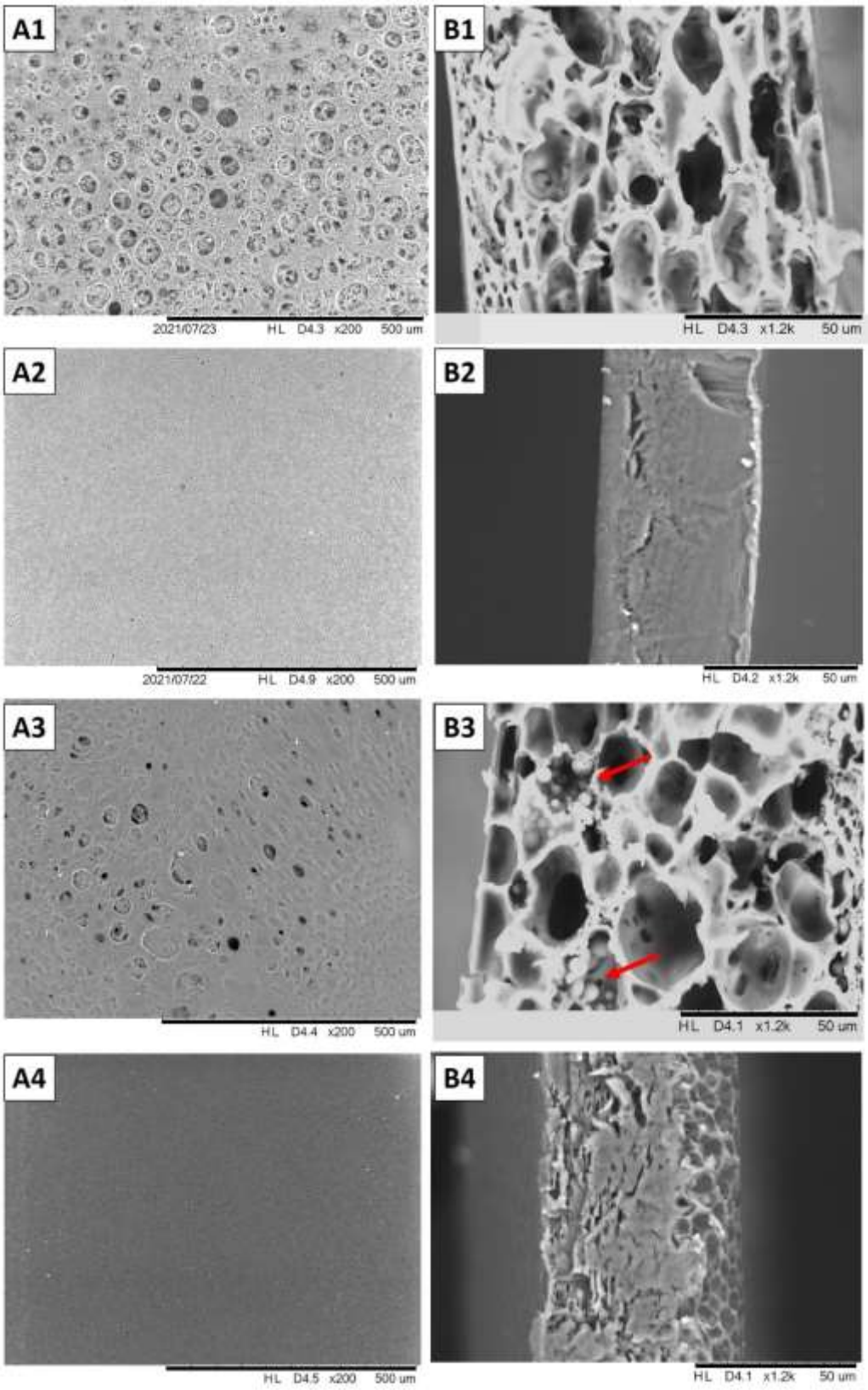


**Figure 2.** Scanning Electron micrographs of surface (A) and cross-section (B) of blends and cellulose acetate (CA) films. CA:zein blend incorporated with tributyrin (A1 and B1); CA-film with tributyrin (A2 and B2); CA:zein blend incorporated glycerol (A3 and B3), and CA-film with glycerol (A4 and B4). Red arrows show glycerol micro-globules.

### 3.3.3 Thermogravimetric analysis

The results obtained from the thermal analysis support the ones observed in the SEM micrographs. TG curves and their respective derivatives of pure materials, CA-films, and CA:zein blends are displayed in Figure 3. Moreover, TG curves and their derivatives of all 16 films can be found in the Supplementary Material (Figure 5S).

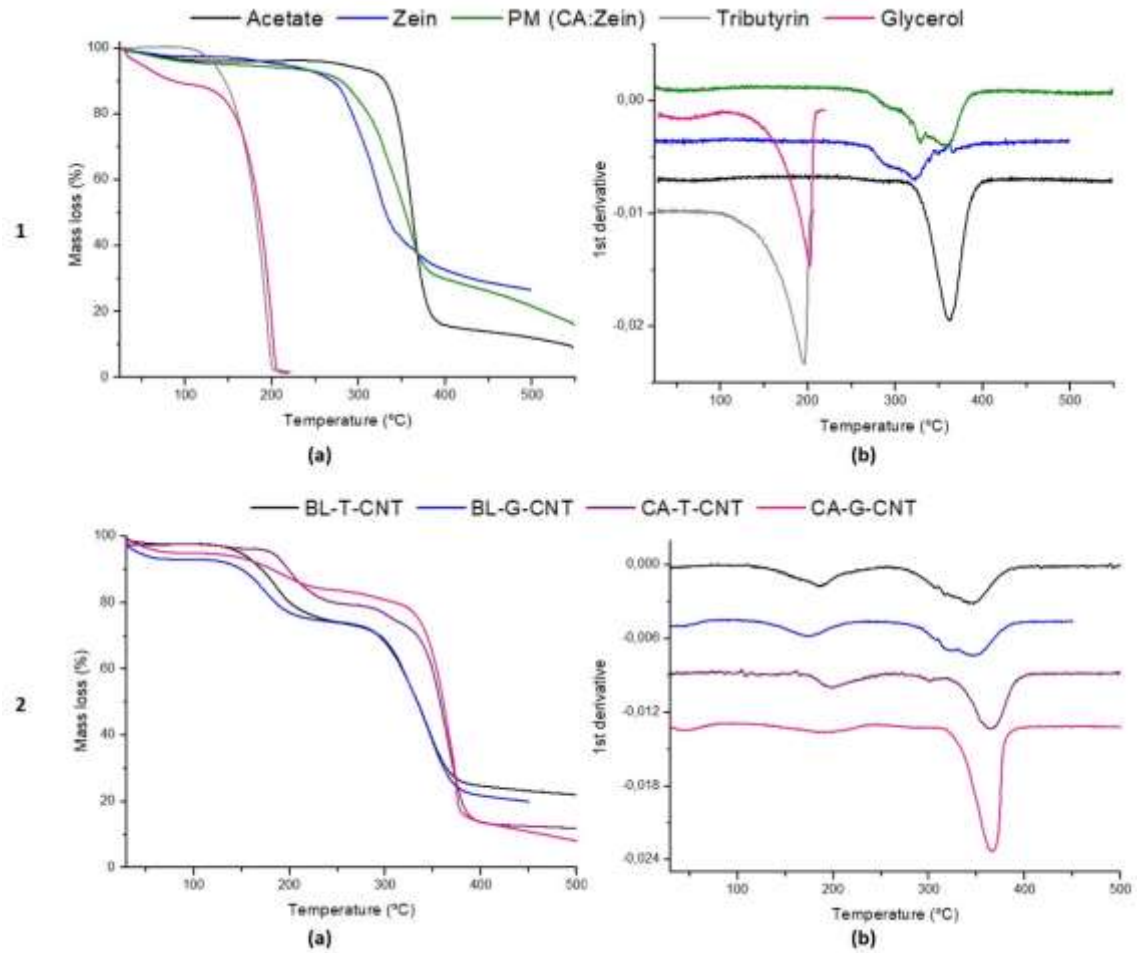


**Figure 3.** Thermogravimetric curves (a) and their respective 1st derivative (b) of: 1) pristine polymers (cellulose acetate and zein) and their physical mixture (PM), plus pristine plasticizers (tributyrin and glycerol); 2) control blends with tributyrin (BL-T-CNT) or glycerol (BL-G-CNT) and cellulose acetate films with tributyrin (CA-T-CNT) or glycerol (CA-G-CNT).

Both plasticizers lost approximately 100% of their mass close to 200 ºC. Regarding the polymers, CA and zein exhibited around 3% of mass loss at 100 ºC due to water molecules loss [36]. The peak-temperature degradation was 320 ºC and 360 ºC for zein and CA, respectively. A physical mixture (PM) of zein and CA was also prepared and

investigated. In the DTG curve, it is possible to distinguish two peaks in the range of 320-360 ºC (Figure 3-1b), indicating that the degradation of each polymer occurred separately from the other. In contrast, when observing the DTG curves of the blends (Figure 3-2b), a single peak around 350 ºC is verified for the tributyrin added-blend, while a slightly double-peak can be seen in DTG of the glycerol added-blend. This observation is a possible indication that the zein-CA-tributyrin compatibility was higher than the zein-CA-glycerol compatibility. Both CA-films and blends containing tributyrin lost mass slower than those plasticized with glycerol, and the mass losses matched around 240 ºC. Films plasticized with tributyrin exhibited only two stages of mass loss (plasticizer degradation and polymer degradation), while three stages were observed for glycerol added-films (water loss, plasticizer degradation, and polymer degradation).

### 3.3.4 Mechanical and water vapor barrier properties

The blends compatibility can also be evaluated from the quality of the polymer mixing states and classified as synergism, additivity, or incompatibility [37,38]. Through the mechanical analysis, it was observed that TS, YM and E% parameters of the blends were lower than those of CA-films, as displayed in Table 2. This behavior is justified by the additivity rule, in which the properties exhibited by the mixed material corresponded with the properties average of isolated components. In this case, the addition of a polymer to another does not entail positive (synergism) nor negative (incompatibility) changes to the polymers. It needs to be emphasized that pure zein films, with or without plasticizers, were brittle and difficult to handle, which hindered the obtainment of the specimens required for both the mechanical and permeability assays. The tributyrin added-blends, in turn, were more flexible, allowing the samples to be characterized. Although glycerol added-blends were also more flexible than zein films, the presence of macro-holes and tears on the films' surface (Figure 1) impaired the obtainment of specimens for the conduction of these assays.

**Table 2.** Thickness, mechanical properties (tensile strength, TS, elongation at break, E, and Young's modulus, YM), and water vapor permeability (WVP) of blends (BL) and control films (CA) plasticized with tributyrin (T) or glycerol (G) and incorporated with garlic essential oil (GEO), β-cyclodextrin (βCD) or inclusion complex (IC).

| **Sample** | **Thickness (μm)** | **TS (MPa)** | **E (%)** | **YM (MPa)** | **WVP ($10^{-10}$g.Pa$^{-1}$.s$^{-1}$.m$^{-1}$)** |
|---|---|---|---|---|---|
| BL-T-CNT | 121.6 (7.8) $^{abc}$ | 4.7 (0.5) $^{a}$ | 3.3 (0.4) $^{a}$ | 313 (6) $^{a}$ | 11.9 (1.3) $^{c}$ |
| BL-T- βCD | 136.7 (18.1) $^{abc}$ | 5.1 (0.3) $^{a}$ | 2.6 (0.1) $^{a}$ | 306 (39) $^{a}$ | 11.8 (0.6) $^{c}$ |
| BL-T-GEO | 136.2 (18.5) $^{abc}$ | 5.9 (0.8) $^{a}$ | 2.7 (0.1) $^{a}$ | 338 (16) $^{a}$ | 14.0 (1.2) $^{c}$ |
| BL-T-IC | 250.8 (83.4) $^{d}$ | 5.3 (0.5) $^{a}$ | 3.3 (0.3) $^{a}$ | 283 (33) $^{a}$ | 27.6 (3.8) $^{d}$ |
| CA-T-CNT | 58.8 (4.3) $^{a}$ | 28.9 (4.9) $^{c}$ | 7.7 (0.8) $^{b}$ | 1,203 (203) $^{b}$ | 4.7 (0.2) $^{a}$ |
| CA-T-βCD | 112.4 (46.0) $^{abc}$ | 16.1 (5.5) $^{b}$ | 2.8 (0.4) $^{a}$ | 969 (287) $^{b}$ | 10.8 (0.7) $^{bc}$ |
| CA-T-GEO | 66.7 (13.1) $^{a}$ | 29.1 (3.1) $^{c}$ | 6.9 (0.4) $^{b}$ | 1,273 (97) $^{b}$ | 6.5 (1.5) $^{ab}$ |
| CA-T-IC | 155.9 (48.2) $^{bc}$ | 7.7 (1.7) $^{a}$ | 3.6 (0.5) $^{a}$ | 389 (52) $^{a}$ | 12.3 (1.9) $^{c}$ |
| BL-G-CNT | 122.2 (5.8) $^{abc}$ | np | np | np | np |
| BL-G- βCD | 180.2 (8.8) | np | np | np | np |
| BL-G-GEO | 152.2 (4.2) $^{bc}$ | np | np | np | np |
| BL-G-IC | 258.5 (49) $^{d}$ | np | np | np | np |
| CA-G-CNT | 59.4 (0.9) $^{a}$ | np | np | np | np |
| CA-G-βCD | 111 (3.6) $^{abc}$ | np | np | np | np |
| CA-G-GEO | 76.8 (4) $^{ab}$ | np | np | np | np |
| CA-G-IC | 182.6 (23.5) $^{cd}$ | np | np | np | np |

np: not performed due to their high number of defects, restricting the obtaining of specimens in the dimensions required by the methodologies [25,26];
Means followed by the standard deviation between parentheses;
Mean values followed by the same letter, within the same column, are not significantly different according to Tukey's test ($P > 0.05$).

Besides, the incorporation of IC or βCD into CA-films significantly reduced TS, YM, and E% parameters compared to the control and the film containing GEO. This is justified by the insertion of defects in the matrix and interruption of secondary interactions between polymer chains [39]. However, the same effect was not observed when comparing the mechanical performance among the blends. This suggests that IC and βCD did not impair the structural cohesion between the polymers in the blend.

The elaborated CA:zein blends also underperformed the CA control and GEO films at WVP (Table 2), probably due to their more porous nature when compared to the more solid appearance of the CA-films (Figure 2). Presence of IC or βCD also impaired the water vapor barrier property of the films, making them more permeable than the controls. According to Oliveira et al. [3], film's thickness heterogeneity may lead to problems on mechanical and barrier properties, which, in fact, was verified herein, since the films presenting the most irregular surfaces performed significantly worse on these assays.

WVP and mechanical properties are important parameters that must be considered when choosing an appropriate packaging for food. WVP, for example, is crucial for food preservation, while TS refer to material endurance and resilience. Although hydrophobic polymers, such as zein and CA, act as a better water vapor barrier than the hydrophilic ones, they are still below the conventional plastics [40,41]. The mechanical properties of the biopolymers evaluated, measured in terms of TS and YM, need to be improved to achieve petrochemical polymer performance. Features such as brittleness, stiffness, and fragility limit or even prevent their application [16,42]. To overcome these problems, strategies are proposed, such as the investigation of new polymers nanocomposite-based films [5,14], incorporation of plasticizers [4,17], and mixing two or more polymers aiming the obtainment of altered materials [15].

In the present work, we verified that the blends resulting from the mixing of zein and CA with tributyrin, despite underperforming the CA-control films, showed improvements when compared to the zein films. Incorporation of the nanoparticles βCD and IC impaired the film appearance and performance, while the addition of non-complexed GEO did not affect

the films' properties. Although the direct incorporation of EOs into polymer matrices is not recommended, IC incorporation harmed the films' performance. Perhaps the choice of a natural βCD may not have been the best due to its insolubility in several organic solvents, such as acetone and ethanol, the solvents used for the filmogenic dispersion preparation [43]. Maybe a derivative CD with hydrophobic nature or a higher solubility in polar organic solvents should solve the problem [43,44].

We also investigated two kinds of plasticizers: glycerol, widely used to plasticize biopolymer films, and tributyrin, a glycerol ester with three butyric acids of natural occurrence in milkfat [4,17,35,45]. It was observed that the plasticizer choice had an impact on the CA-zein blends. The glycerol has been incorporated into hydrophobic CA-films, as reported by Dias et al. [5], Gonçalves et al. [4] and Teixeira et al. [17]. However, its polar nature may have been the cause of the poor compatibility with the polymeric matrices blends, CA and zein, as verified by SEM micrographs and TG curves. Opposite behavior was observed when tributyrin was added as plasticizer, resulting in films with a better performance and a more homogeneous appearance.

### 3.3.3 Antibacterial investigation

*S. aureus* is an important foodborne pathogen, being considered one of the most significant threats to public health [46]. This bacterium is often responsible for foodborne intoxications through the production of heat-stable enterotoxins in various food products [47]. On the other hand, *L. innocua* has been used by many researchers as a surrogate for *Listeria monocytogenes* (considered a significant causative agent responsible for severe diseases in both humans and animals) in many food systems [48,49]. Therefore, both microorganisms were chosen to evaluate IC and GEO antibacterial activity. IC and GEO exhibited inhibitory activity against both bacteria, although GEO antibacterial properties stood out (Table 3). However, it is essential to emphasize that the amount of EO present in IC correspond to around 10% of the IC total weight (approximately 480 $\mu g.mL^{-1}$), thus, reducing the discrepancy between the MIC values found for them.

**Table 3.** Garlic essential oil (GEO) and inclusion complex (IC) minimal inhibitory concentration (MIC) against *S. aureus*, *L. innocua* and *P. fluorescens* (control) after incubation at 37 ºC for 24 h.

| **Bacteria** | **MIC (µg.mL$^{-1}$)** | |
|---|---|---|
| | **GEO** | **IC** |
| *S. aureus* | 78.12 | 4800 |
| *L. innocua* | 156.25 | 4800 |
| *P. fluorescens* | > 2650 | > 9600 |

Regarding the films, their antibacterial activity was evaluated by the indirect contact methodology, also using *S. aureus* and *L. innocua* as target microorganisms at their optimal growth temperature (37 ºC). Furthermore, *L. innocua* was tested under refrigeration conditions (7 ºC) since this microorganism has the ability to growth under refrigeration. The polymer matrix did not exert significant influence on the antibacterial properties of the films, and a similar pattern was observed when evaluating CA-films and the blends. However, the kind of plasticizer used and the complexation or not of EO compounds did influenced the outcomes. The results are displayed in Figure 4.

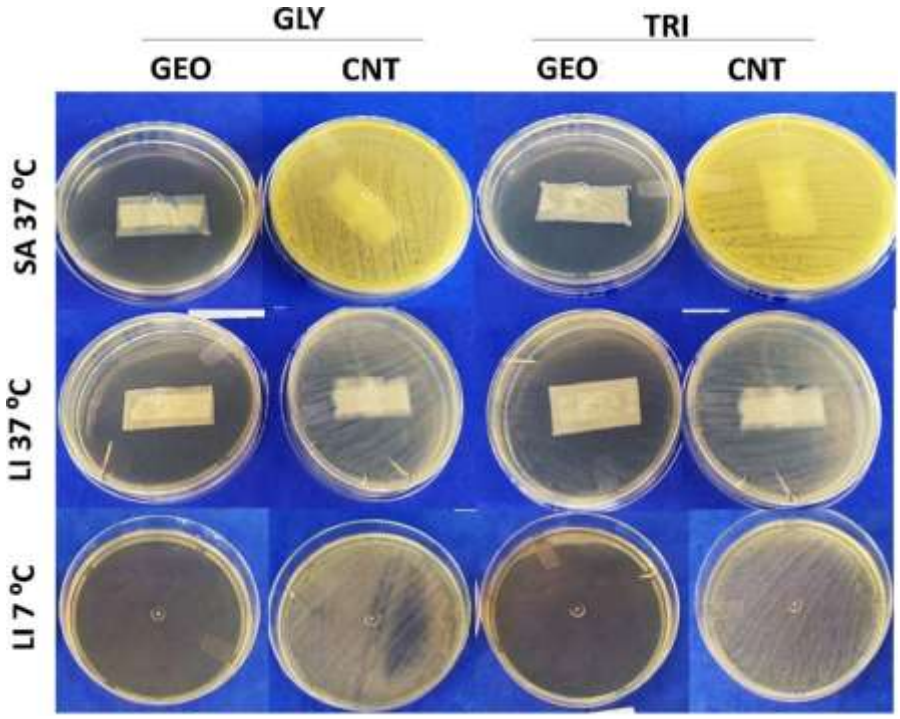


**Figure 4.** Antibacterial properties of active cellulose acetate films incorporated with 10% of garlic essential oil (GEO) and control films (CNT), produced with glycerol (GLY) and

tributyrin (TRI) as plasticizers, tested by indirect contact against *S. aureus* (SA) and *L. innocua* (LI) at 37 ºC/24 h and 7 ºC/10 d. Plates in the last row are presented without the lid.

The plasticized films incorporated with GEO completely inhibited the growth of *S. aureus* after 24 h at 37 ºC. On the other hand, differences in the kind of plasticizer were observed in *L. innocua* growth, tested under the same conditions. The active films produced with tributyrin (BL-T-GEO and CA-T-GEO) only partially inhibited the target bacteria, while the glycerol added-films completely inhibited *L. innocua* growth. The plasticized films containing the IC, in turn, did not affect bacteria growth, showing a similar outcome than the control films.

The differences found for plasticizer type can be attributed to the hydrophobic character of tributyrin [35]. This non-polar profile of tributyrin may enhance the entrapment of the GEO into the film matrix and, therefore, reduce the release of antibacterial agents. As a result, the films produced with this plasticizer exhibited lower antibacterial performance during the tests. Corroborating with this hypothesis, the GEO MIC results indicated higher susceptibility of *S. aureus* to GEO components, which may explain the complete inhibition achieved with the active film; meanwhile, *L. innocua* exhibited a certain resistance, being partially inhibited [50,51].

Under refrigeration (7ºC/10 d), *L. innocua*, a psychrotrophic bacteria, did not exhibit visual growth when incubated in the presence of films incorporated with 10% GEO, independent of the plasticizer (Figure 4). In this case, despite the ability to grow under refrigeration temperatures [52], the cold conditions contributed to the GEO antibacterial activity. GEO thermal stability at lower temperatures was not assessed in the present research; however, low temperatures were already associated with stabilizing some GEO compounds [53]. This improved activity minimized the possible entrapment effect of tributyrin, and the films were able to control the bacteria growth during the incubation period. In addition, films incorporated with IC once again underperformed the GEO added-films and only partially inhibited *L. innocua* growth when under refrigerated condition (results not shown). These results are in agreement with the MIC values found, since it was verified that a much higher concentration of IC was necessary to inhibit microbial growth, indicating that more IC should be added to the filmogenic dispersion in order to obtain films with a similar active property than the GEO added-films. However, this would hardly be viable.

## 3.4 Conclusion

In the present work, CA:zein active blends were successfully manufactured by the incorporation of GEO, as the bioactive agent, and tributyrin, as the plasticizer, into bio-based polymeric matrices. Despite the blends underperforming the CA control films, they showed considerable improvements over zein films, which were brittle and fragile to the extent of impair their manipulation. This could open a wider range of applications of zein as a food packaging component. Besides that, the results indicated that the films elaborated with non-complexed GEO could be used as a potential ally in food preservation, assisting in maintaining the microbiological quality and safety of food products. Films incorporated with IC, on the other hand, underperformed the GEO-added ones regarding the antibacterial activity.

## 3.5 References

1. Kato, L.S.; Conte-Junior, C.A. Safety of plastic food packaging: The challenges about non-intentionally added-substances (NIAS) discovery, identification and risk assessment. *Polymers* **2021**, *13*, 2077.
2. Mangaraj, S.; Yadav, A.; Bal, L.M.; Dash, S.K.; Mahanti, N.K. Application of Biodegradable Polymers in Food Packaging Industry: A Comprehensive Review. *J Package Technol Res* **2019**, *3*, 77-96.
3. Oliveira, T.V.; Freitas, P.A.V.; Pola, C.C.; Silva, J.O.R.; Diaz, L.D.A.; Ferreira, S.O.; Soares, N.F.F. Development and optimization of antimicrobial active films produced with a reinforced and compatibilized biodegradable polymers. *Food Packag Shelf Life* **2020**, *24*, 100459.
4. Gonçalves, S.M.; Santos, D.C.; Motta, J.F.G.; Santos, R.R.; Chávez, D.W.H.; Melo, N.R. Structure and functional properties of cellulose acetate incorporated with glycerol. *Carbohydr Polym* **2019**, *209*, 190-197.
5. Dias, M.V.; Sousa, M.M.; Lara, B.R.B.; Azevedo, V.M.; Soares, N.F.F.; Borges, S.V.; Queiroz, F. Thermal and morphological properties and kinetics of diffusion of antimicrobial films on food and a simulant**.** *Food Packag Shelf Life* **2018**, *16*, 15–22.
6. Pola, C.C.; Medeiros, E.A.A.; Pereira, O.L.; Souza, V.G.L.; Otoni, C.G.; Camilloto, G.P.; Soares, N.F.F. Cellulose acetate active films incorporated with oregano (*Origanum*

*vulgare*) essential oil and organophilic montmorillonite clay control the growth of phytopathogenic fungi. *Food Packag Shelf Life* **2016**, *9*, 69-78.

7. Malm, M.; Liceaga, A.M.; San Martin-Gonzalez, F.; Jones, O.G.; Garcia-Bravo, J.M.; Kaplan, I. Development of Chitosan Filmsfrom Edible Crickets and Their Performance as a Bio-Based Food Packaging Material. *Polysaccharides* **2021**, *2*, 744–758.
8. Atta, O.M.; Manan, S.; Shahzad, A.; Ul-Islam, M.; Ullah, M.W.; Yang, G. Biobased materials for active packaging: a review. *Food Hydrocoll*. **2022**, *125*, 107419.
9. Atta, O.M.; Manan, S.; Ul-Islam, M.; Ahmed, A.A.Q.; Ullah, M.W.; Yang, G. Development and characterization of plant oil-incorporated carboxymethyl cellulose/bacterial cellulose/glycerol-based antimicrobial edible films for food packaging applications. *Adv. Compos. Hybrid Mater*. **2022**, https://doi.org/10.1007/s42114-021-00408-9.
10. Yuvarai, D.; Iyyappan, J.; Gnanasekaran, R.; Ishwarya, G.; Harshini, R.P.; Dhithya, V.; Chandran, M.; Kanishka, V.; Gomathi, K. Advances in bio food packaging – An overview. *Heliyon* **2021**, e07998.
11. Aytac, Z.; Huang, R.; Vaze, N.; Xu, T.; Eitzer, B.D.; Krol, W.; MacQueen, K.A.; Chang, H.; Bousfield, D.W.; Chan-Park, M.B.; Ng, K.W.; Parker, K.K.; White, J.C.; Demokritou, P. Development of Biodegradable and Antimicrobial Electrospun Zein Fibers for Food Packaging. *ACS Sustainable Chem Eng* **2020**, *8*, 40, 15354–15365.
12. US Food and Drug Administration. Available online: <https://www.cfsanappsexternal.fda.gov/scripts/fdcc/index.cfm?set=FCN&id=2043&sort=FCN_No&order=DESC&startrow=1&type=basic&search=cellulose%20acetate> (accessed on 20 January 2022).
13. US Food and Drug Administration. Available online: <https://www.accessdata.fda.gov/scripts/cdrh/cfdocs/cfcfr/CFRSearch.cfm?fr=184.1984> (accessed on 20 January 2022).
14. Lara, B.R.B.; Andrade, P.S.; Guimarães Junior, M.; Dias, M.V.; Alcântara, L.A.P. Novel Whey Protein Isolate/Polyvinyl Biocomposite for Packaging: Improvement of Mechanical and Water Barrier Properties by Incorporation of Nano-silica. *J Polym Environ* **2021**, *29*, 2397-2408.

15. Moraes, A.R.F.; Pola, C.C.; Bilck, A.P.; Yamashita, F.; Tronto, J.; Medeiros, E.A.A.; Soares, N.F.F. Starch, cellulose acetate and polyester biodegradable sheets: Effect of composition and processing conditions. *Mater Sci Eng C* **2017**, *78*, 932-941.
16. Sanyang, M.L.; Sapuan, S.M.; Jawaid, M.; Ishak, M.R.; Sahari, J. Effect of plasticizer type and concentration on physical properties of biodegradable films based on sugar palm (*Arenga pinnata*) starch for food packaging. *J Food Sci Technol* **2016**, *53*, 1, 326-336.
17. Teixeira, S.C.; Silva, R.R.A.; Oliveira, T.V.; Stringheta, P.C.; Pinto, M.R.M.; Soares, N.F.F. Glycerol and triethyl citrate plasticizer effects on molecular, thermal, mechanical, and barrier properties of cellulose acetate films. *Food Bioscience* **2021**, *42*, 101202.
18. Arruda, T.R.; Marques, C.S.; Soares, N.F.F. Native Cyclodextrins and Their Derivatives as Potential Additives for Food Packaging: A Review. *Polysaccharides* **2021**, 2, 825–842.
19. Ayala-Zavala, J.F.; González-Aguilar, G.A. Optimizing the use of garlic oil as antimicrobial agent on fresh-cut tomato through a controlled release system. *Journal of Food Science* **2010**, *75*, 7.
20. Marques, C.S.; Carvalho, S.G.; Bertoli, L.D.; Villanova, J.C.O.; Pinheiro, P.F.; dos Santos, D.C.M.; Yoshida, M.I.; Freitas, J.C.C.; Cipriano, D.F.; Bernardes, P.C. β-Cyclodextrin inclusion complexes with essential oils: Obtention, characterization, antimicrobial activity and potential application for food preservative sachets. *Food Research International* **2019**, *119*, 499-509.
21. Mukurumbira, A. R.; Shellie, R. A.; Keast, R.; Palombo, E. A.; Jadhav, S. R. Encapsulation of essential oils and their application in antimicrobial active packaging. *Food Control*. **2022**, *136*, 108883.
22. Ali, S.; Khatri, Z.; Oh, K. W.; Ki, I. S.; Kim, S. H. Zein/cellulose acetate hybrid nanofibers: electrospinning and characterization. *Macromol. Res*. **2014***, 22*, 971-977.
23. Liu, F.; Li, X.; Wang, L.; Yan, X.; Ma, D.; Liu, Z.; Liu, X.; Sesamol incorporated cellulose acetate-zein composite nanofiber membrane: as efficient strategy to accelerate diabetic wound healing. *Int. J. Biol. Macromol***. 2020***, 149*, 627-638.
24. Hill, L.E.; Gomes, C.; Taylor, T.M. Characterization of beta-cyclodextrin inclusion complexes containing essential oils (trans-cinnamaldehyde, eugenol, cinnamon bark, and clove bud extracts) for antimicrobial delivery application. *LWT* **2013**, *51*, 86-93.

25. ASTM. ASTM D882-12. Standard Test Method for Tensile Properties of Thin Plastic Sheeting. ASTM: American Society for Testing and Materials, West Conshohocken, PA, USA, 2012.
26. ASTM. ASTM E96/E96M-10. Standard test method for water vapor transmission of materials. ASTM: American Society for Testing and Materials, West Conshohocken, PA, USA, 2010.
27. CLSI. Methods for Dilution Antimicrobial Susceptibility Tests for Bacteria that Grow Aerobically; Approved Standard-Ninth Edition. M07-A7. CLSI: Clinical and Laboratory Standards Institute, 2012.
28. R Core Team. R: A language and environment for statistical computing. R Foundation for Statistical Computing, Vienna, Austria, **2021**. Available online: https://www.R-project.org/
29. Santos, E.H.; Kamimura, J.A.; Hill, L.E.; Gomes, C.L. Characterization of carvacrol beta-cyclodextrin inclusion complexes as delivery systems for antibacterial and antioxidant applications. *LWT* **2015**, *60,* 1, 583-592.
30. Giordano, F.; Novak, C.; Moyano, J.R. Thermal analysis of cyclodextrins and their inclusion compounds. *Thermochim Acta* **2001**, *380*, 123-151.
31. Piletti, R.; Zanetti, M.; Jung, G.; Melo, J.M.M.; Dalcanton, F.; Soares, C.; Riella, H.G.; Fiori, M.A. Microencapsulation of garlic oil by β-cyclodextrin as thermal protection method for antibacterial action. *Mater Sci Eng C* **2019**, *94*, 139-149.
32. Abarca, R.L.; Rodríguez, F.J.; Guarda, A.; Galotto, M.J.; Bruna, J.E. Characterization of beta-cyclodextrin inclusion complexes containing an essential oil component. *Food Chemistry* **2016**, *196*, 968-975.
33. Narayanan, G.; Boy, R.; Gupta, B.S.; Tonelli, A.E. Analytical techniques for characterizing cyclodextrins and their inclusion complexes with large and small molecular weight guest molecules. *Polym Test* **2017**, *62*, 402-439.
34. Takahashi, A.I.; Veiga, F.J.B.; Ferraz, H.G. A literature review of cyclodextrin inclusion complexes characterization - Part II: X-ray diffraction, infrared spectroscopy and nuclear magnetic resonance. *Int J Pharm Sci Rev Res* **2012**, *1*, 8-15.
35. Iglesias Montes, M.L.; D'amico, D.A.; Manfredi, L.B.; Cyras, V.P. Effect of Natural Glyceryl Tributyrate as Plasticizer and Compatibilizer on the Performance of Bio-Based Polylactic Acid/Poly(3-Hydroxybutyrate) Blends. *J. Polym. Environ.* **2019**, *27* (7), 1429–1438.

36. Freitas, P.A.V.; Silva, R.R.A.; Oliveira, T.V.; Soares, R.R.A.; Junior, N.S.; Moraes, A.R.F.; Pires, A.C.S.; Soares, N.F.F. Development and characterization of intelligent cellulose acetate-based films using red cabbage extract for visual detection of volatile bases, *LWT* **2020**, *132*, 109780.
37. Meister, J. *Polymer Modification: Principles, Techniques, and Applications*, 1st ed.; CRC Press: Florida, USA, 2000. 914 pp.
38. Shanks, R.A. Concepts and classification of compatibilization processes. In *Compatibilization of polymer blends*, 1st ed.; Ajitha, A.R., Thomas, S, Eds; Elsevier: Amsterdam, Netherlands, 2020, pp. 31-56.
39. Callister Jr, W.D.; Rethwisch, D.G. *Materials Science and Engineering: An introduction*. 8th ed.; John Willey & Sons: New Jersey, USA, 2010, 992 pp.
40. Farhan, A.; Hani, N.M. Characterization of edible packaging films based on semi-refined kappa-carrageenan plasticized with glycerol and sorbitol. *Food Hydrocoll* **2017**, *64*, 48-58.
41. Togashi, Y.; Hara, M. Water vapor permeability of polypropylene. *Fusion Sci Technol* **2011**, *60*, 4, 1471-1474.
42. Hazrol, M.D.; Sapuan, S.M.; Zainudin, E.S.; Zuhri, M.Y.M.; Abdul Wahab, N.I. Corn Starch (*Zea mays*) Biopolymer Plastic Reaction in Combination with Sorbitol and Glycerol. *Polymers* **2021**, *13*, 242.
43. Miranda, J.C.; Martins, T.E.A.; Veiga, F.; Ferraz, H.G. Cyclodextrins and ternary complexes: Technology to improve solubility of poorly soluble drugs. Braz J Pharm Sci **2011**, 47, 4, 665-681.
44. Przybyla, M.A.; Yilmaz, G.; Becer, R. Natural cyclodextrins and their derivatives for polymer synthesis. *Polym Chem* **2020**, *11*, 7582-7602.
45. Vazquez, R.; Nogueira, R.; Orfão, M.; Mata, J.L.; Saramago, B. Stability of triglyceride liquid films on hydrophilic and hydrophobic glasses. *J Colloid Interface Sci* **2006**, *299*, 274-282.
46. Rubab, M.; Shahbaz, H.M.; Olaimat, A. N.; Oh, D. H. Biosensors for Rapid and Sensitive Detection of *Staphylococcus aureus* in Food. *Biosens. Bioelectron.* **2018**, *105* (November 2017), 49–57.
47. Hennekinne, J. A.; De Buyser, M. L.; Dragacci, S. *Staphylococcus aureus* and Its Food Poisoning Toxins: Characterization and Outbreak Investigation. *FEMS Microbiol. Rev.* **2012**, *36* (4), 815–836.

48. Shamloo, E.; Hosseini, H.; Moghadam, A.Z.; Larsen, H.M.; Haslberger, A.; Alebouyeh, M. Importance of *Listeria Monocytogenes* in Food Safety: A Review of Its Prevalence, Detection, and Antibiotic Resistance. *Iran. J. Vet. Res.* **2019**, *20* (4), 241–254.
49. Friedly, E. C.; Crandall, P.G.; Ricke, S.; O'Bryan, C.A.; Martin, E.M.; Boyd, L.M. Identification of *Listeria Innocua* Surrogates for *Listeria Monocytogenes* in Hamburger Patties. *J. Food Sci.* **2008**, *73* (4), 174–178.
50. Münchberg, U.; Anwar, A.; Mecklenburg, S.; Jacob, C. Polysulfides as Biologically Active Ingredients of Garlic. *Org. Biomol. Chem.* **2007**, *5* (10), 1505–1518.
51. Arbach, M.; Santana, T.M.; Moxham, H.; Tinson, R.; Anwar, A.; Groom, M.; Hamilton, C.J. Antimicrobial Garlic-Derived Diallyl Polysulfanes: Interactions with Biological Thiols in *Bacillus Subtilis*. *Biochim. Biophys. Acta - Gen. Subj.* **2019**, *1863* (6), 1050–1058.
52. Sheng, L.; Shen, X.; Su, Y.; Xue, Y.; Gao, H.; Mendoza, M.; Green, T.; Hanrahan, I.; Zhu, M.-J. Effects of 1-Methylcyclopropene and Gaseous Ozone on *Listeria Innocua* Survival and Fruit Quality of Granny Smith Apples during Long-Term Commercial Cold Storage. *Food Microbiol.* **2022**, *102*.
53. Fujisawa, H.; Suma, K.; Origuchi, K.; Seki, T.; Ariga, T. Thermostability of Allicin Determined by Chemical and Biological Assays. *Biosci. Biotechnol. Biochem.* **2008**, *72* (11), 2877–2883

### 3.6 Supplementary Material

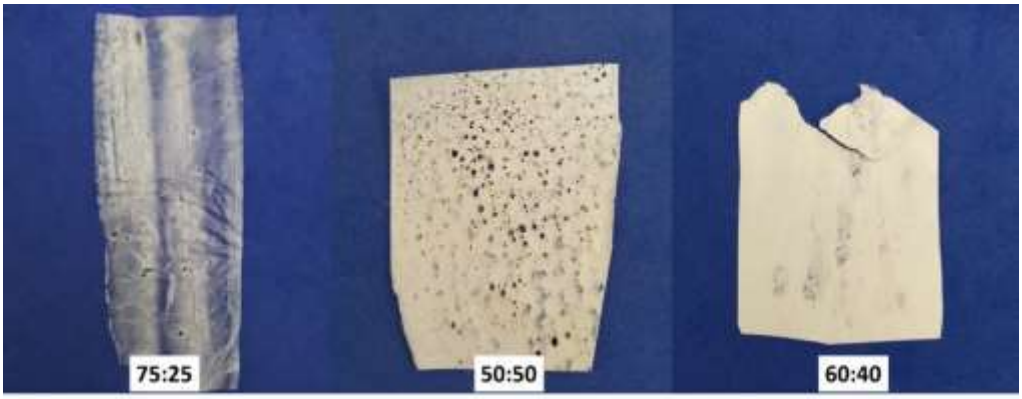


**Figure S1.** Cellulose acetate and zein blends prepared with different polymer ratios (wt/wt).

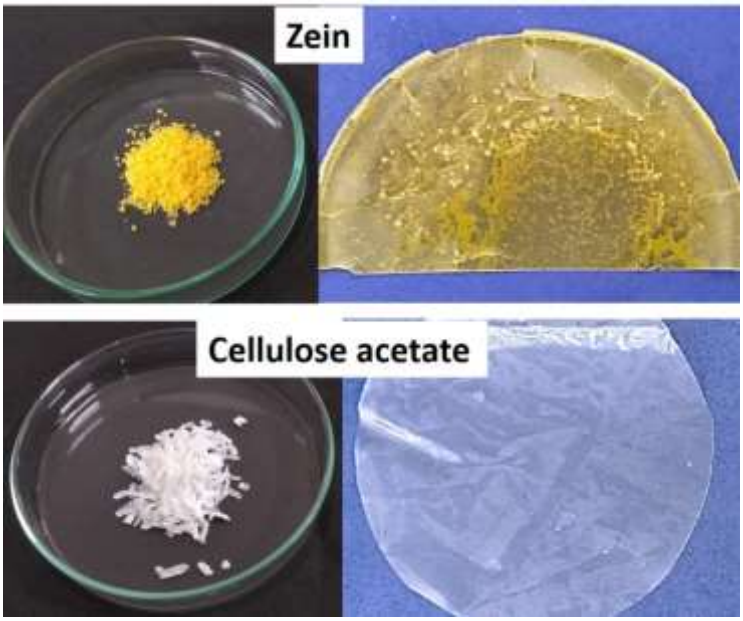


**Figure S2.** Cellulose acetate and zein as pellets and films.

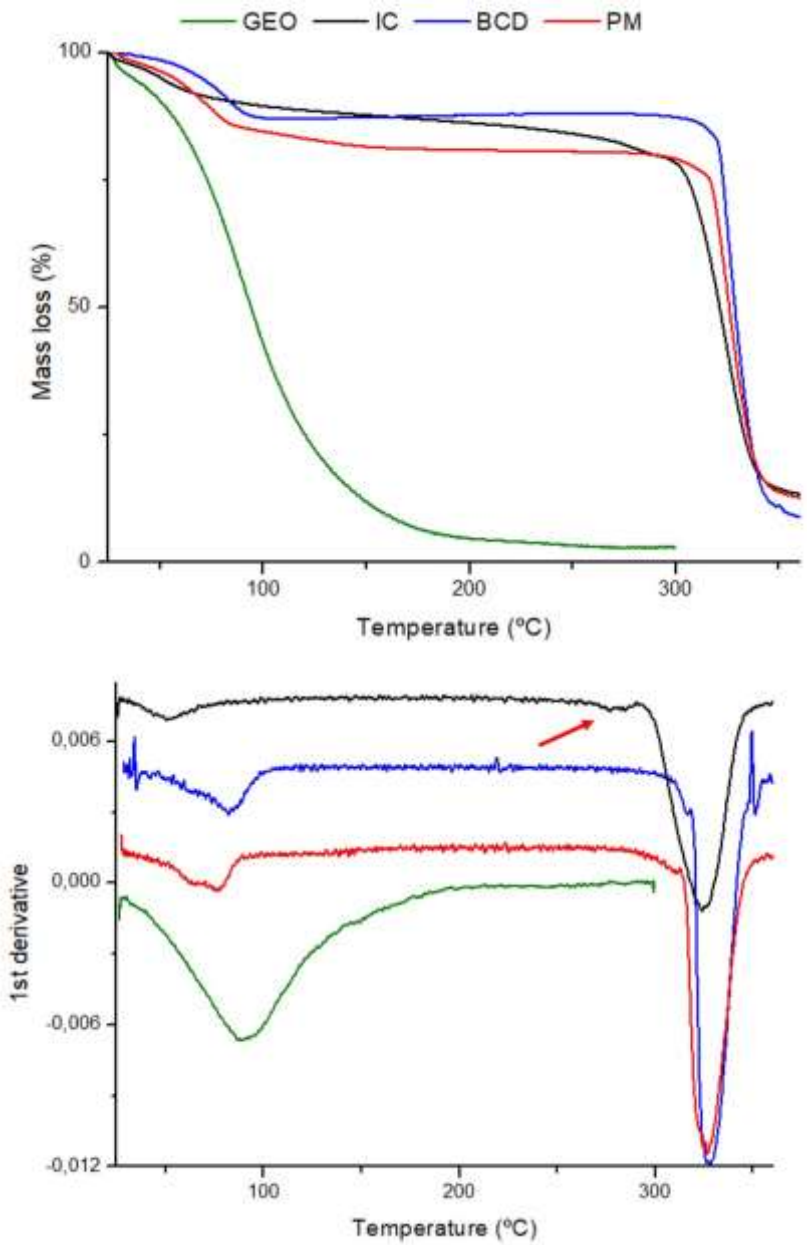


**Figure S3.** Thermogravimetric (TG) curves and their derivative (DTG) of βCD, inclusion complex (IC), garlic essential oil (GEO), and physical mixture (PM). *The red arrow indicates GEO loss in the inclusion complex.

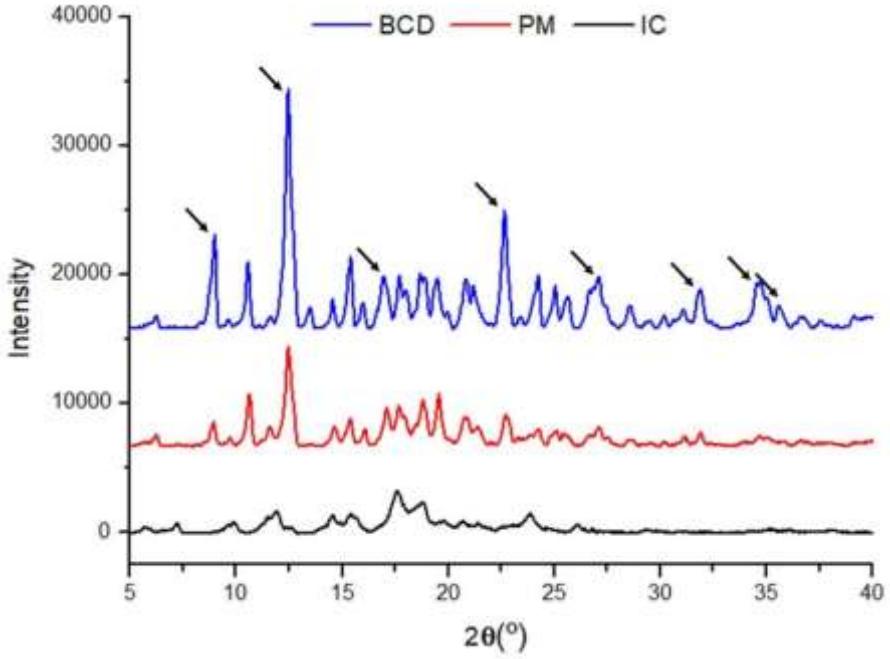


**Figure S4.** X-ray diffractograms of βCD, inclusion complex (IC), and physical mixture (PM). *Black arrows indicate the characteristic peaks for βCD.

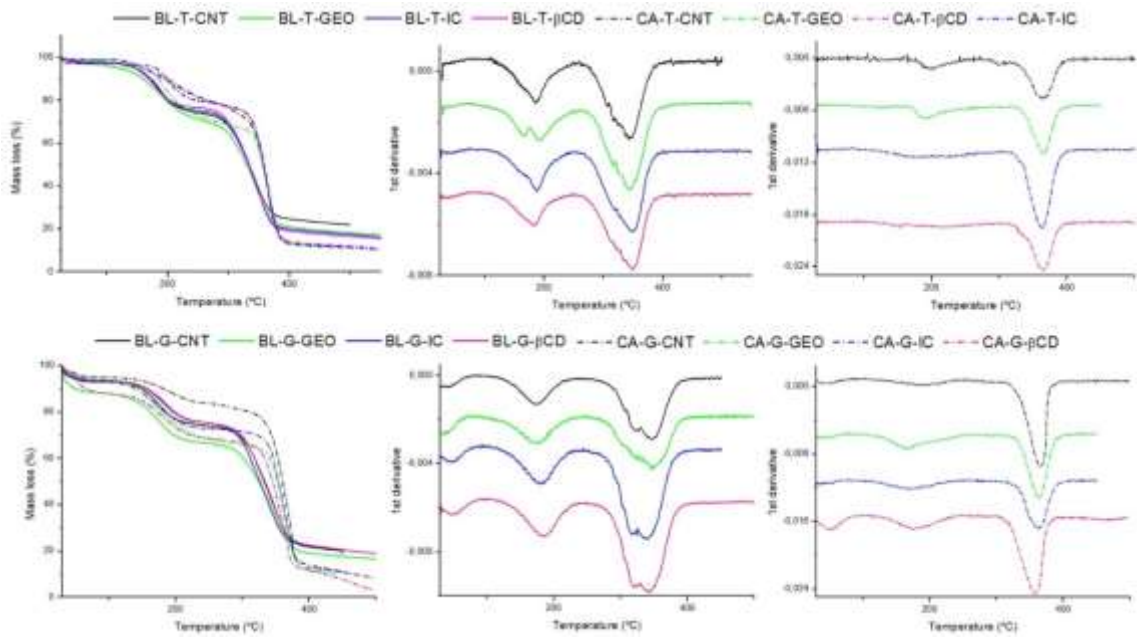


**Figure S5**. Thermogravimetric (TG) curves and their derivative (DTG) of cellulose acetate (CA) films and CA:zein blends incorporated with tributyrin (T) or glycerol (G) as plasticizers, and garlic essential oil (GEO), β-cyclodextrin (βCD), or inclusion complex (IC).

# 4. ARTICLE 2: EXPOSURE TO CELLULOSE ACETATE FILMS INCORPORATED WITH GARLIC ESSENTIAL OIL DOES NOT LEAD TO HOMOLOGOUS RESISTANCE IN *Listeria innocua* ATCC 33090

This article was published in Food Research International (July 2022, doi: 10.1016/j.foodres.2022.111676)

## 4.1 Introduction

Essential oils (EOs) have been widely studied as natural food preservatives due to their bioactive properties. These compounds can be applied in active antimicrobial sustainable food packaging, which encourages an eco-friendly trend in the sector (Motelica et al., 2020). Conversely, due to their strong and characteristic odor, these can negatively affect the sensorial properties of foods and, consequently, impair consumers' acceptance. Because of this, low doses are recommended (Ahmed et al., 2021). However, recent studies show that exposure to sub-inhibitory concentrations of EOs and their constituents can increase antimicrobial resistance in certain microorganisms, which can lead to emergent resistant strains, potentially resulting in a public health issue (Chueca et al., 2016; Berdejo et al., 2020; 2021).

Bacterial resistance is a term often linked to antibiotic resistance since it is a topic of particular importance and extensively studied in the medical and pharmaceutical fields. Nevertheless, any stressing agent, such as those used in food preservation, can lead to bacterial resistance. The use of acids, sanitizers, low temperatures, and high concentrations of solutes are examples of common stressing factors in the food industry that can provoke several stress responses in the surviving microbial population, resulting in adaptive responses and possible gain of resistance (Al-Nabulsi et al., 2015).

The development of bacterial resistance can be homologous, which happens when the microorganism becomes more resistant to the same stressing agent used, or cross-protection (or cross-resistance), when the exposure to one specific stressor can lead to resistance against other stressing agents (Cebrián et al., 2010). For example, Obe et al. (2018) verified that the exposure of *Salmonella* Heidelberg cells to sub-lethal concentrations of a chlorine solution could lead to both homologous and cross-protection, since the cells became more adapted to the same sanitizing agent and displayed less susceptibility to certain antibiotics.

Moreover, it is worth noting that, although antimicrobial films are a novel technology able to control microbial growth and extend food shelf life, they do not promote the completely inhibition of the microorganisms present in the food matrix. The surviving cell population in the food typically consists of non-affected cells and sub-lethally injured cells, which can repair themselves and recover the ability to multiply (Wu et al., 2014). Besides that, it is also possible for the microbial cell to acquire resistance during the repair period, becoming more adapted to the same stressor or another (Wu et al., 2014; Jin et al., 2020).

Despite the importance of this topic, there is a lack of studies in the literature about active antimicrobial packaging and the development of bacterial resistance. Usually, studies concerning active films are more focused on the antimicrobial effect of the manufactured materials on pathogens and spoilage microorganisms of importance in foods. However, besides knowing the antimicrobial potential of the packaging, it is equally important to verify if the active material is safe or if it could pose serious risks to public health by inducing the emergence of resistant strains.

In this sense, the present work aims to fill this gap by providing more information about active antimicrobial packaging. Aligned with the concepts of sustainable development, cellulose acetate (CA) was selected as the polymer base, and garlic essential oil (GEO) was chosen as the natural antimicrobial. *Listeria innocua* cells were exposed to the manufactured active films to verify the occurrence of cell injury and homologous resistance by changes in minimal inhibitory concentrations (MIC) values. Since *L. monocytogenes* poses a serious risk to human health due to its pathogenicity, *L. innocua,* a non-pathogenic bacterium with similarities to *L. monocytogenes*, is often used as a surrogate (Kramer et al., 2019; Bertec et al., 2021). Also, mechanical, water vapor barrier and thermal properties of films were determined. Finally, the films were tested on sliced mozzarella cheese as interfold packaging. It was hypothesized that the films would not cause any increase in microorganisms' homologous resistance, besides preserving the tested food.

## 4.2 Material and Methods

### 4.2.1 Materials

Garlic essential oil was purchased from Laszlo Aromaterapia (Brazil). Cellulose acetate (degree of substitution = 2.5; average molecular weight (Mn) = 2,024,000 $g.mol^{-1}$) was donated by Rhodia Solvay Group (Brazil). *L. innocua* ATCC 33090 was obtained from the culture collection of the Laboratory of Food Packaging, Federal University of Viçosa.

Mozzarela cheese was purchased and sliced in a local market. Before the procedure, both the slicer machine and the cheese packaging were cleaned with a sanitizer solution.

### 4.2.2 Initial assessment of GEO

#### 4.2.2.1 Gas chromatography (GC)

The EO's compounds were identified and semi quantified by gas chromatography with mass spectrometry detection (GC-MS QP2010SE, Shimadzu, Japan) and gas chromatography with flame ionization detector (GC-FID QP2010SE, Shimadzu, Japan), according to Mendes et al. (2017). The analyses were performed as follows: helium was the carrier gas for both detectors with a flow and linear velocity of 2.80 $mL.min^{-1}$ and 50.80 $cm.seg^{-1}$ (GC-FID), and 1.98 $mL.min^{-1}$ and 50.90 $cm.seg^{-1}$ (GC-MS). The injector temperature was 220 ºC with a split proportion of 1:30, a capillary column of fused silica (30 m x 0.25 mm); stationary phase Rtx®-5MS (0.25 µm film thickness); the initial oven temperature was 40 ºC for 3 min and gradually increase at 3 $ºC.min^{-1}$ until 180 ºC, then held for 10 min, with a total time of analysis of 59.67 min. The FID and MS detectors temperatures were 240 ºC and 200 ºC, respectively (Souza et al., 2017). An aliquot (1 µL) was obtained from a sample containing 3% of GEO in hexane 95% and analyzed. The GC-FID experiment was carried out with $H_2$ and atmospheric air ionization at a temperature of 300 ºC, with $H_2$ and atmospheric air with a flow of 40 $mL.min^{-1}$ and 400 $mL.min^{-1}$, respectively. Identification of GEOs compounds was based on comparisons of their retention index (RI) relative to a standard alkane series $C_7$-$C_{40}$ (Supelco, USA) and comparison of their mass spectra with reference data from the equipment database and literature (Wiley7, NIST 05 and NIST 05s) (Adams, 2007; El-Sayed, 2019; Linstrom & Mallard, 2018). The relative percentage of each compound was determined by the ratio between each peak area and the total area of all the compounds obtained by GC-FID.

#### 4.2.2.2 Minimal inhibitory concentration (MIC)

*L. innocua* was cultured twice in brain heart infusion broth (BHI, Kasvi, Italy), incubated for 24 h at 37 ± 1 ºC, streaked over plate count agar (PCA, Oxoid, England) and incubated again under the same conditions. Selected colonies were taken from the plate and suspended in 0.85% (wt/v) saline solution until obtaining a visual suspension density similar to 0.5 McFarland turbidity standard (approximately $10^7$ $CFU \cdot mL^{-1}$) and diluted 1:10. Then, we proceeded with the agar dilution method, with modifications, to investigate the MIC of GEO (CLSI, 2012; Marques et al., 2022). Samples were dispersed in 10 mL of liquefied BHI

agar (around 45 °C), resulting in GEO final concentrations ranging from 39.75 $\mu g \cdot mL^{-1}$ to 2650 $\mu g \cdot mL^{-1}$ , and subsequently poured into Petri dishes with a diameter of 60 mm. Brain heart infusion agar without GEO was the negative control. After allowing the agar to solidify, aliquots of the inoculum (20 µL) were dispensed on the agar surface (final concentration around $10^4$ $CFU.mg^{-1}$ per spot). The plates were incubated at 37 ± 1 °C for 24 h, and MIC was considered the lowest concentration capable of growth inhibition.

#### 4.2.2.3. Pre-exposure of *L. innocua* to sub-lethal concentrations of GEO and investigation of homologous resistance

After MIC determination, *L. innocua* cells were exposed to subinhibitory concentrations (1/2MIC, 1/4MIC e 1/8MIC) of GEO to verify the occurrence of homologous resistance. The experiment was carried out according to Chueca et al. (2016), with some modifications. *L. innocua* cells were cultured in tryptic soy broth with 0.6% yeast extract (TSBYE, Kasvi, Brazil), and 10 µL of the inoculum (around $10^8$ $UFC.mL^{-1}$) was added to 50 mL of TSBYE and incubated at 37 ºC ± 1 ºC for 4 h. After that, aliquots of 2.5 mL were added to the tubes containing 7.5 mL of TSBYE and GEO in subinhibitory concentrations. The tubes were incubated at 37 ºC ± 1 ºC for 24 h, and an aliquot of 100 µL was taken from each tube and added to 4.9 mL of TSBYE containing the respective subinhibitory GEO concentration, and then incubated again. This procedure was repeated for 3 days. Moreover, after every 24 h of incubation, one aliquot of 10 µL of each tube was streaked in PCA and incubated (37 ºC ± 1 ºC /24 h). Then, colonies were selected for MIC re-evaluation, and compared to the initial MIC value. Three subinhibitory concentrations were evaluated at three different times (24 h, 48 h, and 72 h), totaling nine derivate strains of *L. innocua* that were obtained for MIC re-investigation. Three results were considered: MIC value higher than initial MIC, which meant occurrence of homologous resistance; MIC equal to initial MIC, meaning there was no homologous resistance or susceptibility; and MIC lower than initial MIC, which indicated susceptibility to the same antimicrobial.

### 4.2.3 Active films elaboration

The films were prepared according to Marques et al. (2022). Three grams of cellulose acetate were added to 30 mL of acetone (ratio of 1:10 wt/v) and let disperse for 24 h. After that, 0.9 g of glycerol was added into dispersions (30% wt/wt based on polymer mass). Besides that, 0.03 g of GEO (1% wt/wt based on polymer mass) and 0.3 g of GEO (10% wt/wt based on polymer mass) were added, separately, into the polymer dispersion, producing

the treatments designated: CNT (control, 0% of GEO); GEO1 (1% of GEO); and GEO10 (10% of GEO). The films dispersions were homogenized in Ultra-turrax (2 min/5,000 rpm, model T25, IKA) and left for 30 min to stand. Subsequently, the dispersions were spread over a glass plate with the aid of a K-Paint Applicator machine (USA), and let to dry. After solvent evaporation, the manufactured films were vacuum sealed in plastic bags and stored in the dark until analysis.

### 4.2.4 Films characterization

#### 4.2.4.1 Scanning Electron Microscopy (SEM)

The films' surface morphology was analyzed with a Scanning Electron Tabletop Microscope (TM3000, Hitachi High-Technologies, Japan) with secondary electron detector, operating under low-vacuum and with an accelerating voltage of 15 KV. The uncoated samples were attached on stubs' surface with the aid of a double-sided carbon tape. Microscopic changes in films morphology due to EO presence were evaluated.

#### 4.2.4.2 Thermogravimetric analysis (TGA)

Thermogravimetric analysis was performed on a Shimadzu thermogravimetric analyzer, (Model DTG-60H, Japan), under a nitrogen atmosphere (50 $mL.min^{-1}$). Approximately 3 mg of each sample were weighed and heated from 25 ºC to 550 ºC, at 10 $ºC.min^{-1}$. The TG curves, as well their derivatives (DTG), obtained for the films (CNT, GEO1, and GEO10) and the pristine materials (CA, GEO, and glycerol) allowed the evaluation of the materials' thermal stability.

#### 4.2.4.3 Thickness, density, and grammage

Thickness, density, and grammage were determined according to Moraes et al. (2017). Thickness was measured, in µm, with the aid of a digital micrometer (model 547–401, Mitutoyo, Japan). Ten random points of film areas (175 x 25 $mm^2$) were measured. Density ($g.cm^{-3}$) was calculated as the sample weight over its volume, which, in turn, was obtained as film area x average thickness. At last, grammage was considered the quotient of the sample weight over its area ($g.m^{-2}$).

#### 4.2.4.4 Mechanical properties

Mechanical properties were also evaluated: ultimate tensile strength (UTS, in MPa), elongation at break (EB, in %), and modulus of elasticity (Young's modulus, YM, in MPa). A

Universal Testing Machine (model 4204, Instron Corporation, USA) equipped with a 1 kN load cell was used to test five specimens of each treatment (175 × 25 mm²), in three repetitions. The initial distance of grids' separation was 125 mm, and the rate of separation was 50 $mm \cdot min^{-1}$ (ASTM, 2012).

#### 4.2.4.5 Water vapor permeability (WVP)

Water vapor permeability was investigated according to ASTM E96/E96M (2010) with modifications (Marques et al., 2022). The films (Ø = 83 mm) were placed on poly(methyl methacrylate) cups containing a saturated solution of lithium chloride (12 ± 5% RH at 25 ± 2 °C) and sealed with paraffin. Subsequently, the cups were placed in desiccators containing saturated sodium chloride (75 ± 5% RH at 25 ± 2 °C), and were periodically weighted to provide at least ten data points. The gain of mass over time allowed the determination of the water vapor transmittance rate (WVTR) according to the following equation: WVTR=(m/t) x A; in which m/t is the slope of gain of mass (g) over time (h), and A is the permeation area (m²). Next, the WVP was obtained according to: WVP = (WVTR x $X_T$)/($P_S$ x($RH_1$−$RH_2$)); in which $X_T$ corresponds the film thickness, $P_S$ is the saline water saturation pressure, $RH_1$ is the RH in the desiccator containing NaCl, and $RH_2$ is the RH on the desiccator containing LiCl. Water vapor permeability was expressed as $g \cdot Pa^{-1} \cdot s^{-1} \cdot m^{-1}$.

### 4.2.5 Pre-exposure to GEO-films and investigation of sub-lethal injury and homologous resistance in *L. innocua*

The methodology used for evaluating the effect of the active films on the injury and homologous resistance of *L. innocua* was based on Miller et al. (2006), Tampau, González-Martínez, and Chiralt (2018), and Berdejo et al. (2019), and is summarized in Figure 1.

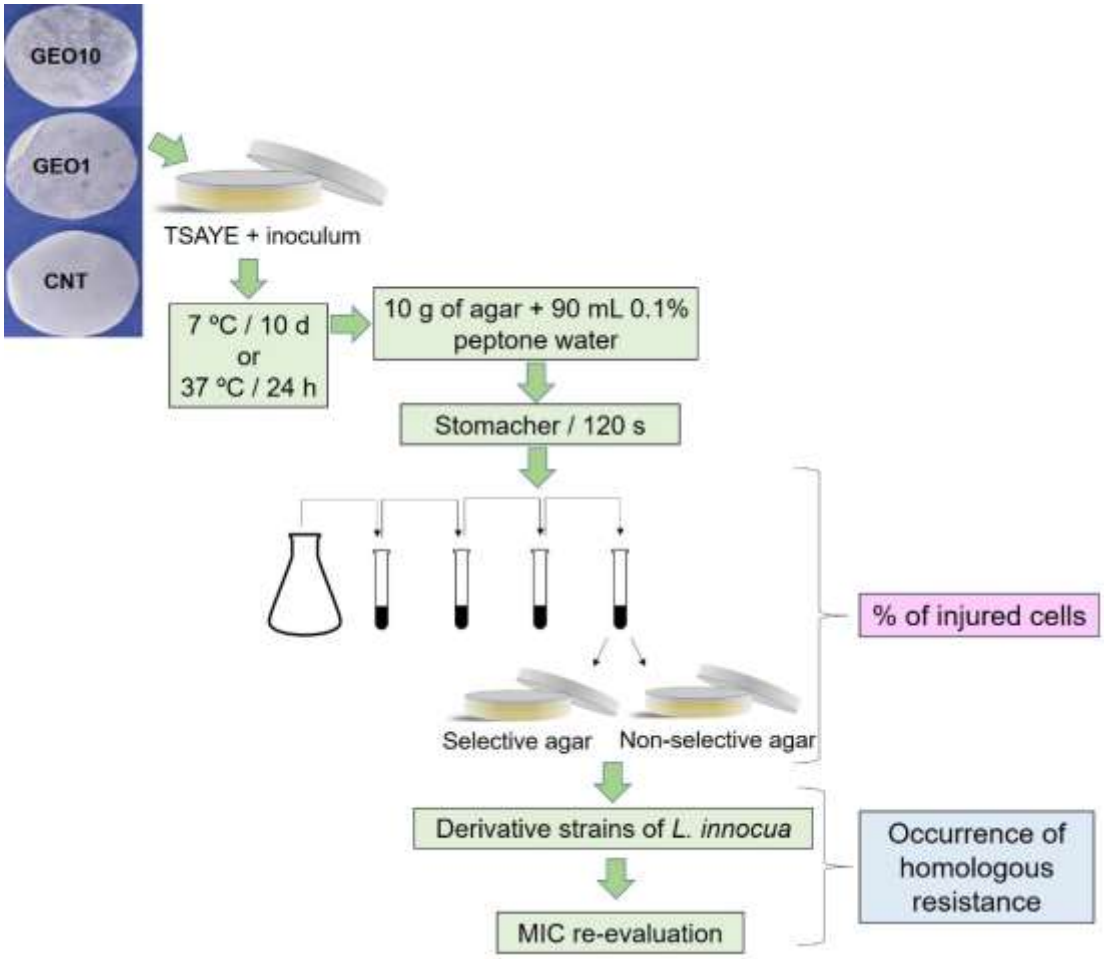


**Figure 1.** Schematic description of the methodology employed to evaluate the effect of active cellulose acetate-based films on cell injury and homologous resistance in *L. innocua*.

Firstly, the films were cut into circles at the same diameter as the used Petri dish (Ø = 60 mm), and reserved. Inoculum (Section 4.2.2.2) was diluted until approximately 1 x $10^4$ CFU.mL$^{-1}$, and 1 mL was added to 15 mL of liquefied tryptic soy agar with yeast extract (TSAYE, Kasvi, Brazil), then poured into the Petri dish. The circular films were placed on the surface of the inoculated solidified agar. The plates were incubated at 37 ºC ± 1 ºC for 24 h (optimum temperature) and at 7 ºC ± 1 ºC for 10 days (temperature recommended for psychrotrophic growth) (Downes, Ito, 2001). After the incubation period, the films were discarded, and 10 g of the agar was weighed and homogenized in a stomacher (120 s) with 90 mL of 0.1% (wt/v) peptone water. Serial dilutions were plated on a non-selective medium (TSAYE), and on the selective medium, Listeria Oxford agar (Neogen, United Kingdom) added with selective supplement (Oxoid, England). The plates were incubated at 37 ± 1 ºC for 24 h. The purpose of this step was to enumerate non-injured and injured cells. The results were expressed as colony-forming unit *per* gram (CFU.g$^{-1}$) and the percentage of the injured

cell population was calculated as: %Injured cells = 100 x ($CFU_{NS}$ – $CFU_S$)/$CFU_{NS}$; in which $CFU_{NS}$ corresponds to the total of colony forming units on non-selective medium and $CFU_S$ corresponds to colony forming units on selective medium (Espina et al., 2016).

Subsequently, at least six colonies from each plate were selected, streaked in PCA and the MIC was re-done to evaluate if the exposure to the active films incurred homologous resistance against GEO in *L. innocua* (Section 4.2.2.2). The expected results were similar to the ones described in Section 2.2.3. Since there were three films treatments, two media (non-selective and selective), and two storage conditions (7 ºC and 37 ºC), 12 derivative strains from *L. innocua* were obtained.

### 4.2.6 Test as interfold packaging

The films were tested as interfold packaging on sliced mozzarella cheese. The cheese slices were cut into 6 x 9 cm² (12.5 g) and arranged in a polystyrene tray covered with polyvinyl chloride (PVC) film. Each tray contained two slices of cheese separated by the interfold package (totaling 25 g per sample) (Figure 2). The samples were stored at 7 ± 1 ºC for 8 days, and the microbial contaminants (total mesophiles, psychrotrophics, molds and yeast) were evaluated every 2 days.

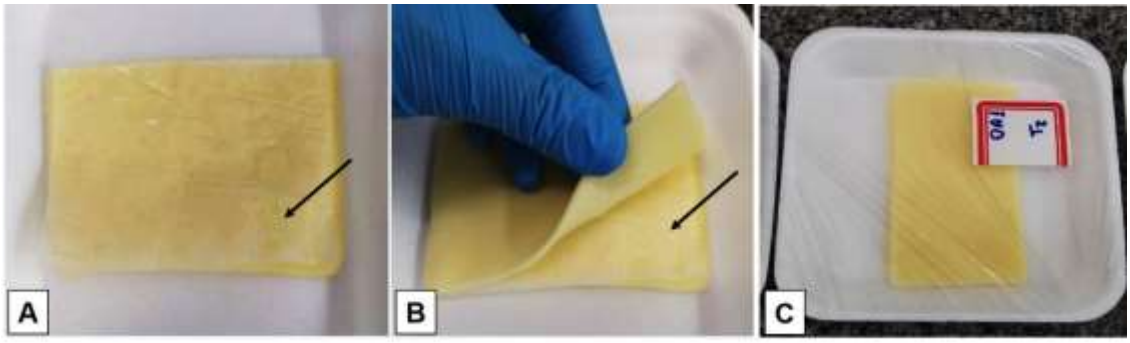


**Figure 2.** Application of cellulose acetate films incorporated with garlic essential oil as interfold packaging for sliced mozzarella cheese for 8-days storage at 7 ºC. Black arrows (A and B) emphasize the films placed between the cheese slices. Mozzarella slices arranged in a polystyrene tray covered with PVC film (C).

Samples of 25 g of mozzarella cheese and 225 mL of 0.1% peptone water and were homogenized in a stomacher (120 s). Ten-fold dilution series were made, and aliquots were inoculated onto the specific medium for each microorganism group: PCA for mesophilic aerobic bacteria, incubated at 37 ºC ± 1 ºC for 24 h, and for aerobic psychrotrophic bacteria, incubated at 7 °C ± 1 ºC for 10 days; and Potato Dextrose Agar (PDA, Sigma-Aldrich, EUA)

acidified with 1% of tartaric acid 10% (wt/v) for molds and yeasts, incubated at 25 °C ± 1 ºC for 6 days. The results were expressed as $CFU.g^{-1}$ of cheese (Downes & Ito, 2001).

### 4.2.7 Statistical analyses

The results were subjected to analysis of variance (ANOVA) followed by Tukey's test. The free software R was used (R Core, 2021).

## 4.3. Results and Discussion

### 4.3.1. Assessment of GEO

Gas chromatography identified five aromatic sulfur compounds in GEO (Table 1). According to the literature, allyl polysulfides, such as those found here, are products of allicin degradation, commonly found in EOs hydro-distillate or steam-distillate obtained from the *Allium sativum* plant (Charron, Milner, and Novotny, 2016; Satyal et al., 2017). Allicin is an unstable compound, and because of this, it has a short life that can vary from hours to days after the extraction. It breaks down forming several organosulfur compounds, such as diallyl sulfide (DAS), disulfide (DADS), and trisulfide (DATS). These allicin derivatives are more stable and accounts for the majority of GEO sulfinades (Münchberg et al., 2007; Charron et al., 2016).

**Table 1.** Major compounds (> 1%) identified in garlic essential oil.

| n | Compound[a] | Structural formula | $RI_{cal}$[b] | $RI_{tab}$[c] | $A_{rel}$ (%) |
|---|---|---|---|---|---|
| 1 | Diallyl sulfide | 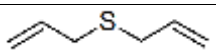 | 854 | 856 | 17.3 |
| 2 | Allyl methyl disulfide | 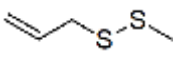 | 914 | 915 | 2.5 |
| 3 | Diallyl disulfide | 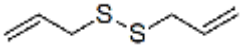 | 1078 | 1077 | 28.5 |
| 4 | Allyl methyl trisulfide | 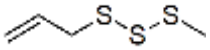 | 1134 | 1132 | 5.7 |
| 5 | Diallyl trisulfide | 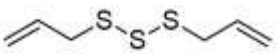 | 1298 | 1289 | 27.4 |
| | Total identified | | | | 81.4 |

[a]Major compounds in order of elution extracted with Rtx®-5MS capillary column;

[b]Retention index obtained from data by sampling of saturated n-alkanes ($C_7$-$C_{40}$);

[c]Tabulated retention index (ADAMS, 2007; EL-SAYED, 2016; NIST, 2011);

Regarding the antimicrobial activity, the determined MIC against *L. innocua* was 159 $\mu g.mL^{-1}$. Garlic compounds have been recognized as natural antimicrobial agents with a broad spectrum of action, showing activity against Gram-positive and Gram-negative bacteria (Ezeorba et al., 2022). However, an initial screening was done against different bacteria, and it was verified activity against only the Gram-positive ones (Marques et al., 2022). This result may be due to the EO composition, since the antimicrobial property of GEO depends on the type and ratio of the organosulfur compounds present (Münchberg et al., 2007; Arbach et al., 2019).

Casella et al. (2012) and Bagheri et al. (2020) reported that the GEO antimicrobial activity is attributed to disulfide bonds and diallyl groups present in the polysulfide compounds. Their action mechanism involves damage in proteins, incurred by reactions with low molecular weight thiols (like glutathione, which act as a redox buffer in cell cytoplasm), generation of reactive oxygen species (ROS), and changes in the permeability of cell membrane due to the hydrophobic nature of the compounds (Münchberg et al., 2007; Arbach et al., 2019). Thiols consumption and creation of ROS are processes that may cause levels of oxidative stress enough to injury or even kill cells (Münchberg et al., 2007).

When exposed to sub-lethal concentrations of GEO for up to 72 h, the MIC values found against pre-exposed cells and no pre-exposed cells were the same, indicating, initially, that the EO did not lead to homologous resistance in *L. innocua* cells. Chueca et al. (2016) also did not verify changes in MIC values when investigating *Escherichia coli* pre-exposed to carvacrol, citral, and (+)-limonene for 24 h. However, after 10 days of exposition, the authors found that the *E. coli* cells were more resistant to the antimicrobials. Similarly, Berdejo et al. (2019) reported that *Staphylococcus aureus* cells also became more resistant to the EOs compounds investigated after exposition to sub-MIC concentrations for 10 days. Thus, the literature suggests that a prolonged period of exposition to sub-lethal concentrations of certain antimicrobial compounds may trigger a stress response in bacterial cells leading to more resistant strains. Since active packaging usually remains in contact with the food matrix for long periods, and therefore in contact with the microorganisms present, the investigation of homologous resistance caused by active films is justified.

### 4.3.2 Films characterization

The photographs of the films, and their micrographs, are presented in Figure 3. All films elaborated were opaque and slightly white, and their micrographs showed presence of CA non-solubilized particles. It was also possible to observe presence of several circular

structures in films CNT and GEO1. Gonçalves et al. (2019) obtained similar results when studying CA films with concentrations of glycerol ranging from 0 to 50%. The authors reported opaque films and presence of micro-pores in films with 30% of glycerol, the same concentration used in the present study. Concerning the GEO10 film, the surface morphology was quite different, with a net-like surface, a behavior also verified by Gonçalves et al. (2020) in CA films added with glycerol and fennel EO.

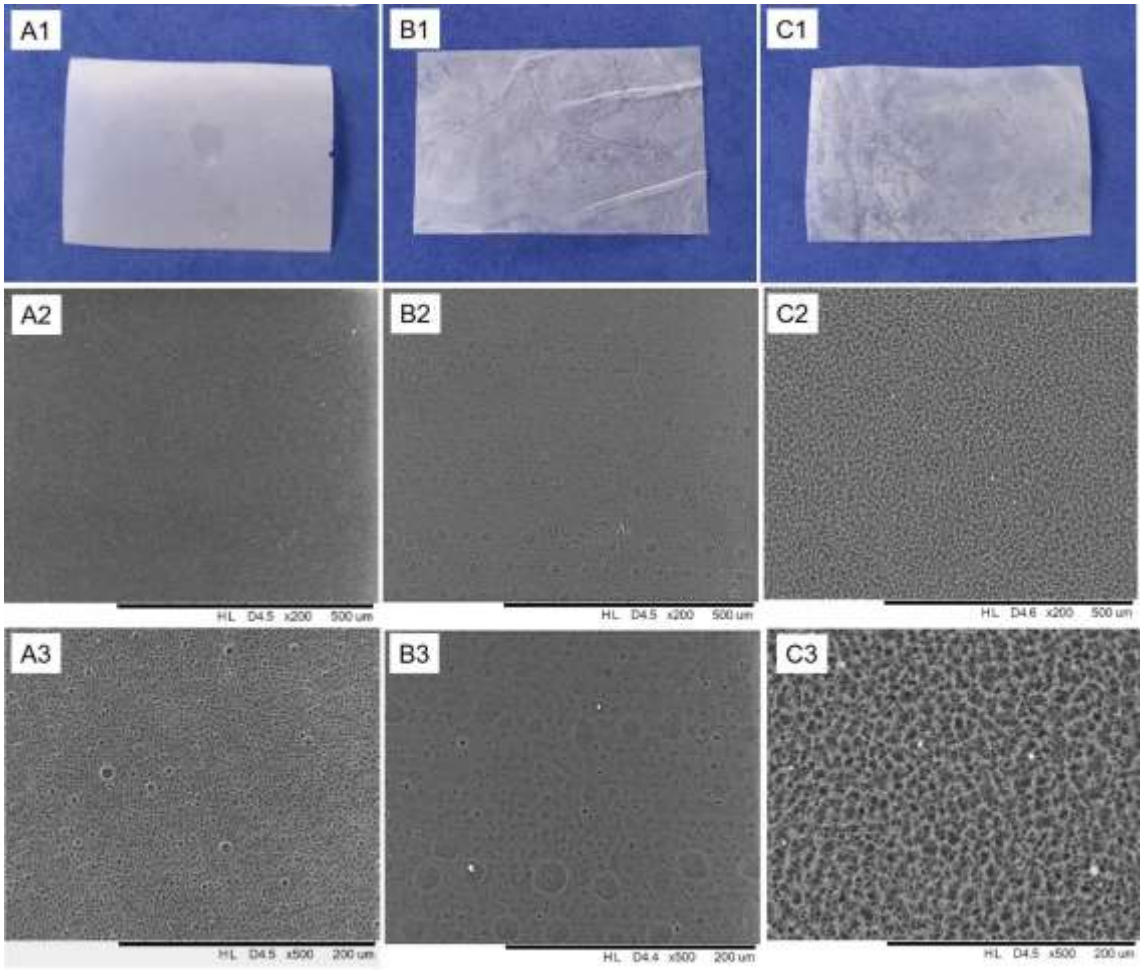


**Figure 3.** Cellulose acetate films incorporated with 0% (A), 1% (B), and 10% (C) of garlic essential oil: macrographs (A1, B1, C1) and micrographs obtained by SEM at two magnifications: 200x (A2, B2, C2) and 500x (A3, B3, C3).

The thermogravimetric curves (TG) and their derivatives (DTG) of the pristine components and the active films are shown in Figure 4. The temperatures of maximum thermal decomposition of GEO, glycerol, and CA were 98 ºC, 201 ºC, and 356 ºC, respectively. Silva et al. (2021) showed that the incorporation of water molecules into the polymer matrix is responsible for reducing the thermal stability of polymers by approximately 150 °C, since water catalyzes the fission of the polymer chain skeleton by hydrolysis. Despite

the plasticizer glycerol being widely recognized as a hygroscopic plasticizer (Basiak et al. 2018; Cazón et al., 2020; Teixeira et al. 2021), it was observed that the amount of incorporated mass was not enough to reduce the decomposition temperature of the CA when structured as films (Figure 4B). Therefore, these results confirm that the additives used had a low impact on the polymer decomposition temperature and comply with the thermal stability requirements for food packaging applications.

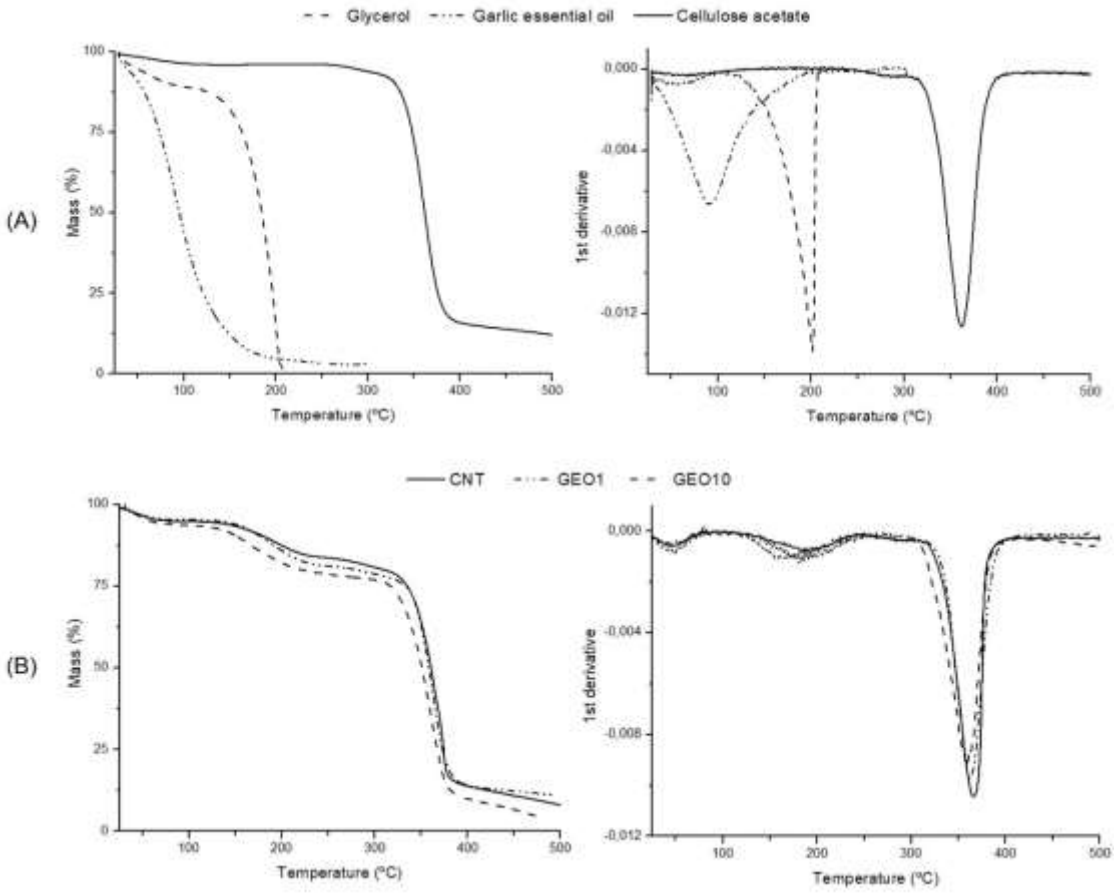


**Figure 4.** Thermogravimetric curves and their respective first derivatives for pristine materials (A) and cellulose acetate-based films incorporated with 0% (CNT), 1% (GEO1), and 10% (GEO10) of garlic essential oil (B).

The mechanical performance of the films (UTS, EB, and YM) as a function of GEO incorporation was not significantly changed (Table 2). The plasticizing effect caused by EOs when added into polymer matrices is described in the literature, however the results indicated that it was not the case in this study (Bastos et al., 2016; Biswas et al., 2020; Cázon et al., 2021). The plasticizer performance can be related to intrinsic factors (e.g. chemical composition, molecular size, branching, and polarizability) or associative factors with the

polymer (e.g. the types of intermolecular interactions) (Wypych et al., 2017). According to Marcilla et al. (2017), to insert a plasticizer between the polymeric chains, it is necessary for cohesive forces, i.e., secondary interactions between plasticizer and polymer, to overcome the cohesion energy established between the polymeric chains. Therefore, GEO (up to 10% addition) did not behave as a plasticizer in CA films due to the absence of oxygenated groups (or fluor and nitrogen atoms), preventing hydrogen bonds with the CA polymer and resulting in low cohesion energy between GEO-CA.

**Table 2.** Thickness, density, grammage, mechanical properties (ultimate tensile strength, UTS, elongation at break, EB, and Young's modulus, YM), and water vapor permeability (WVP) of cellulose acetate-based films incorporated with 0% (CNT), 1% (GEO1), and 10% (GEO10) of garlic essential oil.

| **Assay** | **Thickness** (μm) | **Density** ($g.cm^{-3}$) | **Grammage** ($g.m^{-2}$) | **UTS** (MPa) | **EB** (%) | **YM** (MPa) | **WVP** ($10^{-10}g.Pa^{-1}.s^{-1}.m^{-1}$) |
|---|---|---|---|---|---|---|---|
| CNT | 64.1 ± 5.0 [a] | 1.04 ± 0.05 [a] | 62.29 ± 4.02 [a] | 31.2 ± 2.9 [a] | 6.1 ± 5.7 [a] | 1,887 ± 139 [a] | 8.2 ± 1.0 [ab] |
| GEO1 | 76.8 ± 8.1 [b] | 1.07 ± 0.10 [a] | 85.23 ± 9.45 [b] | 32.6 ± 3.7 [a] | 5.1 ± 4.1 [a] | 1,831 ± 134 [a] | 9.5 ± 1.8 [a] |
| GEO10 | 72.9 ± 7.0 [b] | 1.25 ± 0.11 [b] | 96.15 ± 13.53 [c] | 35.0 ± 4.3 [a] | 7.6 ± 5.7 [a] | 1,802 ± 168 [a] | 6.9 ± 0.2 [b] |

Mean ± standard deviation; mean values followed by the same letter, within the same column, are not significantly different according to Tukey's test (p-value > 0.05)

In turn, the grammage and density values significantly increased with the incorporation of 10% of GEO in the polymer matrix (Table 2). This suggests a combination of factors such as (i) molecular packaging between the CA chains and (ii) the filling of the free volume of the polymer matrix by GEO (Hashemi et al., 2017; White & Lipson, 2016). Furthermore, the incorporation of GEO increased the water vapor barrier, as reported in the literature (Pola et al., 2016; Gonçalves et al., 2020). Since water vapor transfer occurs through the hydrophilic portions of the films, it explains why WVP depends on the hydrophilic/hydrophobic ratio of the constituents present in the film. Moreover, the improved water vapor barrier property can be attributed to the increase in film density and tortuosity produced with the oil phase implementation (Acevedo-Fani et al., 2015). Therefore, to mitigate the spoilage reactions of food catalyzed by hydrolysis, we believe that the increase in the GEO content could further benefit the water vapor barrier properties of the film and contribute to the increase of the food shelf life.

### 4.3.3 *In vitro* assessment of active films

*L. innocua* was exposed to films containing 0%, 1%, and 10% of GEO in two incubation conditions: 24 h at 37 ºC, and 10 d at 7 ºC. After, the plating was carried out in a non-selective and in a selective media for cell injury investigation. The viable cell counts are displayed in Table 3.

**Table 3.** Viable cell counts of *L. innocua*, expressed as $\log_{10}$ CFU.g$^{-1}$, on non-selective medium (TSAYE) and selective medium (Listeria Oxford) and percentage of injured cells after exposure to cellulose acetate-based films incorporated with 0% (CNT), 1% (GEO1), and 10% (GEO10) of garlic essential oil at 7 ºC/10 d or 37 ºC/24 h.

| Assay | Incubation at 7 ºC/10 d | | Injured cells (%) | Incubation at 37 ºC/24 h | | Injured cells (%) |
|---|---|---|---|---|---|---|
| | Non-selective medium ($\log_{10}$ CFU.g$^{-1}$) | Selective medium ($\log_{10}$ CFU.g$^{-1}$) | | Non-selective medium ($\log_{10}$ CFU.g$^{-1}$) | Selective medium ($\log_{10}$ CFU.g$^{-1}$) | |
| CNT | 9.1 ± 0.1 $^{A\,a}$ | 9.0 ± 0.1 $^{A\,a}$ | - | 9.2 ± < 0.1 $^{A\,a}$ | 9.2 ± < 0.1 $^{A\,a}$ | - |
| GEO1 | 4.8 ± < 0.1 $^{B\,b}$ | 4.8 ± 0.2 $^{B\,b}$ | - | 8.4 ± 0.1 $^{B\,a}$ | 8.3 ± < 0.1 $^{B\,a}$ | - |
| GEO10 | 3.4 ± 0.1 $^{C\,b}$ | 2.5 ± 0.2 $^{C\,c}$ | 86.3 ± 3.2 | 7.5 ± < 0.1 $^{C\,a}$ | 7.5 ± < 0.1 $^{C\,a}$ | - |

Mean ± standard deviation; mean values followed by the same uppercase letter, within the same column, are not significantly different according to Tukey's test (p-value > 0.05); mean values followed by the same lowercase letter, within the same row, are not significantly different according to Tukey test (p-value > 0.05)

*Listeria* sp. are psychrotrophic bacteria, i.e. they are able to grow at low temperatures (Kramer et al., 2019), and the growth of *L. innocua* reached the same maximum population in the control films (CNT) regardless of the incubation temperature. Conversely, in the presence of films incorporated with GEO, the incubation temperature affected the antimicrobial property and a significantly low number of cells was observed in films kept at refrigerated temperature (Table 3). The difference of up to 6.5 log cycles in the final population of *L. innocua* found when in presence of GEO10 films and incubated at 7 ºC can be attributed, in part, to the thermal stability of the EO. At 37 ºC, the logarithmic cycles reached a maximum reduction of 1.7 and this result could be due to the volatilization of antimicrobial components of the GEO.

The literature reveals that GEO compounds are more stable at low temperatures (Ezeorba et al., 2022; Fujisawa et al., 2008). Indeed, in the GEO TG curve (Figure 4), it is possible to observe its high volatility and thermal susceptibility, since the mass loss began at around 25 ºC. Fujisawa et al. (2008) observed that the antimicrobial activity of allicin decreased with the temperature increase. Even though the organosulfur compounds derived from allicin are more thermal stable than their precursor, they still are thermolabile substances. Their degradation over the incubation period may have affected their antimicrobial property when at different incubation conditions.

In addition, possible changes in the cellular membrane that occur at low temperatures may have contributed to the higher antimicrobial activity observed at 7 ºC and can also justify these findings. Exposure to cold stress lead to alterations in the membrane lipid profile of *L. innocua*, such as increase of unsaturated fat acids and shorter chain fat acids, as verified by Moorman et al. (2008). Though this change enhances membrane fluidity and allows the survival of the microorganism in low temperatures, it can also increase the cell sensitivity to certain compounds (Moorman et al., 2005; 2008; Muchaamba et al., 2021).

Concerning the concentration of EO in films, GEO10 performed better *in vitro* than GEO1, regardless of the incubation condition. Also, the combination of GEO10 film and low temperature sub-lethally injured around 86% of the *L. innocua* cells, as demonstrated by the difference in viable cell counts verified between the non-selective and the selective media. According to Espina et al. (2016), the selective medium plate technique makes it possible to estimate the percentage of damaged cell population after the offered treatment by differences found in the microbial counts. The method is based on the fact that non-selective media allows the growth of non-injured and sub-lethal injured cells, while certain compounds

present in selective media, such as dyes, antibiotics, and salts, hinder the injured cell repair, inhibiting their growth (Wu, 2014).

As stated before, sub-lethal damaged cells can repair themselves under suitable conditions and even acquire homologous and, or cross resistance to stress factors after recovery (Jin et al., 2020; Yamamoto et al., 2021). Due to this, it was also investigated if the contact with the active films would lead to homologous resistance in *L. innocua* cells. A total of 12 pre-exposed derivate strains were isolated and re-growth, and GEO MIC was evaluated against each one of them. No difference was found between the MIC values obtained for non-pre-exposed cells and pre-exposed cells regardless of the film, the incubation condition, or the kind of media used (selective or not). These findings suggest that the active films did not lead to homologous resistance in *L. innocua*, and that the cells injured by the treatments were able to recover with normal resistance to the EO.

### 4.3.4 Active films as interfold packaging

Cheese is a worldwide consumed dairy product. Due to their nutritional aspects (i.e., high protein, fat, minerals, vitamins, and moisture contents), these products are highly susceptible to the growth of both pathogenic and spoilage microorganisms during the several stages of the food chain (Christaki et al., 2021). In this context, antimicrobial packaging incorporated with EOs could act as a potential ally to maintaining the microbiological quality of cheese products (Arruda et al., 2022).

When tested on sliced mozzarella cheese as interfold packaging, almost a 1-log-unit cycle difference was found between CNT and both GEO-films for psychrotrophic bacteria, molds and yeasts on the $8^{th}$ day of storage. Although this result is interesting, it was not statistically significant (p-value > 0.05), as displayed on Table 4. The storage time, on the other hand, was significant for all microbial groups evaluated (p-value ≤ 0.05). Since there was no interaction between the factors (storage time and presence of films), and only storage time was statistically significant, the overall means obtained for each storage time were compared with one another (Table 4). After 8 days of storage, the microbial count increased by about 1.6 log $CFU.g^{-1}$ for psychrotrophics, molds and yeasts in relation to the initial values. Meanwhile, an increase of about 1 log $CFU.g^{-1}$ of mesophiles was found. This lower growth of mesophiles can be attributed to the refrigerated storage conditions of the food product.

**Table 4.** Increase in the number of log cycles, in $\log_{10}$ CFU.g$^{-1}$, of the natural microbiota (mesophilic aerobic bacteria, psychrotrophic bacteria, molds and yeasts) in sliced mozzarella cheese packaged with interfold cellulose acetate-based films incorporated with 0% (CNT), 1% (GEO1), and 10% (GEO10) of garlic essential oil, during storage time at 7 ºC.

| **Mesophiles ($\log_{10}$ CFU.g$^{-1}$)** | | | | |
|---|---|---|---|---|
| **Assay** | **Storage time (d)** | | | |
| | **2** | **4** | **6** | **8** |
| CNT | 0.2 ± 0.1 | 0.6 ± 0.6 | 0.8 ± 0.5 | 1.2 ± 0.7 |
| GEO1 | 0.3 ± 0.5 | 0.3 ± 0.2 | 0.6 ± 0.3 | 1.1 ± 0.1 |
| GEO10 | 0.1 ± 0.2 | 0.3 ± 0.4 | 0.7 ± 0.3 | 0.7 ± 0.5 |
| Overall* | 0.2 ± 0.1 $^{a}$ | 0.4 ± 0.1 $^{ab}$ | 0.7 ± 0.1 $^{bc}$ | 1.0 ± 0.2 $^{c}$ |
| **Psychrotrophic bacteria ($\log_{10}$ CFU.g$^{-1}$)** | | | | |
| **Assay** | **Storage time (d)** | | | |
| | **2** | **4** | **6** | **8** |
| CNT | 0.4 ± 1.0 | 1.1 ± 1.1 | 1.6 ± 1.3 | 2.1 ± 0.8 |
| GEO1 | 0.2 ± 0.4 | 0.2 ± 0.5 | 0.6 ± 0.1 | 1.4 ± 0.4 |
| GEO10 | 0.3 ± 0.6 | 0.2 ± 0.7 | 1.0 ± 1.2 | 1.3 ± 0.8 |
| Overall* | 0.3 ± 0.2 $^{a}$ | 0.5 ± 0.3 $^{a}$ | 1.1 ± 0.3 $^{ab}$ | 1.6 ± 0.2 $^{b}$ |
| **Molds and yeasts ($\log_{10}$ CFU.g$^{-1}$)** | | | | |
| **Assay** | **Storage time (d)** | | | |
| | **2** | **4** | **6** | **8** |
| CNT | 0.6 ± 0.7 | 0.9 ± 0.5 | 1.5 ± 1.3 | 2.2 ± 0.9 |
| GEO1 | 0.1 ± 0.7 | 0.5 ± 0.1 | 0.9 ± 0.4 | 1.3 ± 0.6 |
| GEO10 | 0.2 ± 0.5 | 0.3 ± 0.5 | 0.5 ± 0.8 | 1.4 ± 1.0 |
| Overall* | 0.3 ± 0.2 $^{a}$ | 0.5 ± 0.2 $^{a}$ | 1.0 ± 0.3 $^{ab}$ | 1.6 ± 0.3 $^{b}$ |

Mean ± standard deviation; mean values followed by the same lowercase letter, within the same row of each microbial group, are not significantly different according to Tukey's test (p-value > 0.05). *Overall mean regardless the type of film used, since presence of film was not significant.

These findings corroborate some studies in the literature that point to a lower antimicrobial effect of active packaging applied in food matrix (Oliveira et al., 2011; Ramos et al., 2012; Marques et al., 2019; Silva et al., 2021). The discrepancies between the *in vitro* tests and the application on cheese can be mainly attributed to the food matrix effect.

Considering the application of EO-loaded films on cheese, the migration of their nonpolar active compounds is improved by the system characteristics, which are composed of approximately 20% of lipids. The affinity between the mozzarella cheese and the EOs' components facilitates the migration of the these substances from the active film to the surface of the product (Dannenberg et al., 2017). However, this same feature acts as a drawback to the effectiveness of the EOs' bioactive compounds: the fat present in food could form a protective coat around the microorganisms and, or absorbs the antimicrobial agent, thus decreasing the concentration in the aqueous phase and impairing its antimicrobial effect. (Amatiste et al., 2014; Farbood et al., 1976; Silva et al., 2021).

The influence of the food fat content on the antimicrobial action of EOs was evident on the study conducted by Smith-Palmer et al. (2001). The authors investigated the effect of different EOs against *L. monocytogenes* and *Salmonella* Enteritidis inoculated on low-fat and full-fat cheese. It was observed that the fat content was a crucial factor for the EO efficacy against the pathogens. Similarly, García-Diez et al. (2017) investigated garlic and oregano EOs' antimicrobial properties against pathogenic bacteria inoculated in food model media with different fat content, and observed a decrease in the EOs' inhibitory activity when the fat level increased. Furthermore, the transfer of the nonpolar bioactive components to the target site in bacteria could be hampered due to the reduced water content in food compared to laboratory media (Smith-Palmer et al., 2001), reinforcing the differences between the *in vitro* and *in situ* results (Marques et al., 2019).

Furthermore, although the isolation and identification of the biodiversity present in the evaluated dairy product were not the aim of the present study, the complex microbial community in the samples should also be considered when evaluating the outcomes and the differences observed between the *in vitro* results and those obtained when testing the films on food. The literature reveals that the microbiota diversity found in cow mozzarella cheese depends on several factors, such as climate, geography, manufacturing conditions, acidification methods, among others (Guidone et al., 2016; Jonalla et al., 2018; Marino et al., 2019). Regardless, different microbial genera are listed composing the cheese biodiversity: *Lactobacillus*, *Streptococcus*, *Aeromonas*, *Pseudomonas*, *Lactococcus*, *Acinetobacter*, *Escherichia*, and several others (Guidone et al., 2016; Marino et al., 2019). As stated before, an initial screening showed that the GEO did not affect the tested bacteria equally. While the Gram-positive bacteria, such as *L. innocua*, had their growth impaired by the EO, none of the Gram-negative bacteria investigated appeared to be affected by it (Marques et al., 2022). In

this sense, it is possible that part of the diverse microbial population in cheese was not impacted by the active films, and was able to grow normally during the storage time.

Higher GEO's concentrations on active films could induce inhibitory effects on the natural microbiota of mozzarella cheese, preventing its spoilage. Nevertheless, this could raise concerns regarding the sensorial properties of the food, since EOs present strong flavor characteristics. Therefore, further studies of GEO-films application in different food matrices are encouraged, especially the ones with lower fat content and with the need for cold storage.

## 4.4. Conclusion

The active films manufactured with garlic essential oil and cellulose acetate performed well when tested *in vitro* against *L. innocua*, especially at low temperature. Besides, they did not lead to homologous resistance in the evaluated microorganism, the desired outcome. Conversely, when applied as interfold packaging in mozzarella cheese, the films did not differ from the control at inhibiting microbial growth, which may have been due to the food content, such as the presence of fat. Nonetheless, these findings could be of importance to the food industry since the films have potential to be used as a sustainable option to conventional plastics. Also, the active films should be tested on different food matrices, particularly low fat items, as a strategy to minimize the occurrence of undesirable interactions between the EO components and the food matrix, and exploit their antimicrobial property to the maximum. Moreover, it is also important to continue the study of resistance with other microorganisms, pathogens or food spoilage, and verify the occurrence of cross-protection, mainly against antibiotics to ensure that the active films will not lead to problems in the future.

## 4.5 References

Acevedo-Fani, A., Salvia-Trujillo, L., Rojas-Graü, M. A., & Martín-Belloso, O. (2015). Edible films from essential-oil-loaded nanoemulsions: Physicochemical characterization and antimicrobial properties. *Food Hydrocolloids*, 47, 168–177. https://doi.org/10.1016/j.foodhyd.2015.01.032

Adams, R. P. (2007). *Identification of essential oils components by gas chromatography/mass spectroscopy*. EUA: Allured Publishing Corporation.

Ahmed, L. I., Ibrahim, N., Abdel-Salam, A. B., & Fahim, K. M. (2021). Potential application of ginger, clove and thyme essential oils to improve soft cheese microbial safety and sensory characteristics. *Food Bioscience*, 42, 101177. https://doi.org/10.1016/j.fbio.2021.101177

Al-Nabulsi, A. A., Osaili, T. M., Shaker, R. R., Olaimat, A. N., Jaradat, Z. W., Elabedeen, N. A. Z., & Holley, R. A. (2015). Effects of osmotic pressure, acid, or cold stresses on antibiotic susceptibility of *Listeria monocytogenes*. *Food Microbiology*, 46, 154-160. https://doi.org/10.1016/j.fm.2014.07.015

Amatiste, S., Sagrafoli, D., Giacinti, G., Rosa, G., Carfora, V., Marri, N., Tammaro, A., Bovi, E., & Rosati, R. (2014). Antimicrobial activity of essential oils against *Staphylococcus aureus* in fresh sheep cheese. *Italian Journal of Food Safety*, 3(3), 148–150. https://doi.org/10.4081/ijfs.2014.1696

Arbach, M., Santana, T. M., Moxhama, H., Tinson, R., Anwar, A., Groom, M., & Hamilton, C. J. (2019). Antimicrobial garlic-derived diallyl polysulfanes: Interactions with biological thiols in *Bacillus subtilis*. *BBA - General Subjects*, *1863*, 1050-1058. https://doi.org/10.1016/j.bbagen.2019.03.012

Arruda, T. R., Bernardes, P. C., Moraes, A. R. F. e, & Soares, N. de F. F. (2022). Natural bioactives in perspective: The future of active packaging based on essential oils and plant extracts themselves and those complexed by cyclodextrins. *Food Research International*, 156, 111160. https://doi.org/10.1016/j.foodres.2022.111160

ASTM. ASTM E96/E96M-10. (2010). *Standard Test Method for Water Vapor Transmission of Materials*. ASTM: West Conshohocken, PA, USA.

ASTM. ASTM D882-12. (2012). *Standard Test Method for Tensile Properties of Thin Plastic Sheeting*. ASTM: West Conshohocken, PA, USA.

Bagheri, L., Khodaei, N., Salmieri, S., Karboune, S., & Lacroix, M. (2020). Correlation between chemical composition and antimicrobial properties of essential oils against most

common food pathogens and spoilers: In-vitro efficacy and predictive modelling. *Microbial Pathogenesis*, *147*, 104212. https://doi.org/10.1016/j.micpath.2020.104212

Bastos, M. do S. R., Laurentino, L. da S., Canuto, K. M., Mendes, L. G., Martins, C. M., Silva, S. M., Kim, S., Biswas, A., & Cheng, H. N. (2016). Physical and mechanical testing of essential oil-embedded cellulose ester films. *Polymer Testing*, 49, 156–161. https://doi.org/10.1016/j.polymertesting.2015.11.006

Berdejo, D., Chueca, B., Pagán, E., Renzoni, A., Kelley, W. L., & Pagán, R., Garcia-Gonzalo, D. (2019). Sub-inhibitory doses of individual constituents of essential oils can select for *Staphylococcus aureus* resistant mutants. *Molecules*, *24*, 170. https://doi.org/10.3390/molecules24010170

Berdejo, D., Merino, N., Pagán, E., García-Gonzalo, D., & Pagán, R. (2020). Genetic variants and phenotypic characteristics of *Salmonella* Typhimurium-resistant mutants after exposure to carvacrol. *Microorganisms*, 8, 937. https://doi.org/10.3390/microorganisms8060937

Berdejo, D., Pagán, E., Merino, N., García-Gonzalo, D., & Pagán, R. (2021). Emerging mutant populations of *Listeria monocytogenes* EGD-e under selective pressure of *Thymbra capitata* essential oil question its use in food preservation. *Food Research International*, *145*, 110403. https://doi.org/10.1016/j.foodres.2021.110403

Berlec, A., Janež, N., Sterniša, M., Klančnik, A., Sabotič, J. (2021). Expression of NanoLuc Luciferase in *Listeria innocua* for development of biofilms assay. *Frontiers in Microbiology*, *12*, 636421, 2021. https://doi.org/10.3389/fmicb.2021.636421.

Biswas, A., Bastos, M. S. R., Furtado, R. F., Kuzniar, G., Boddu, V., & Cheng, H. N. (2020). Evaluation of the properties of cellulose ester films that incorporate essential oils. *International Journal of Polymer Science*, 2020, 1–8. https://doi.org/10.1155/2020/4620868

Casella, S., Leonardi, M., Melai, B., Fratini, F., & Pistelli, L. (2012). The role of diallyl sulfides and dipropyl sulfides in the *in vitro* antimicrobial activity of the essential oil of garlic, *Allium sativum* L., and leek, *Allium porrum* L. *Phytotherapy Research*, *27*, 380-383. https://doi.org/10.1002/ptr.4725

Cebrián, G., Sagarzazu, R., Pagán, R., Condón, S., & Mañas, P. (2010). Development of stress resistance in *Staphylococcus aureus* after exposure to sub-lethal environmental conditions. *International Journal of Food Microbiology*, 140, 26–33. https://doi.org/10.1016/j.ijfoodmicro.2010.02.017

Cazón, P., Velazquez, G., & Vázquez, M. (2020). UV-protecting films based on bacterial cellulose, glycerol and polyvinyl alcohol: effect of water activity on barrier, mechanical and optical properties. *Cellulose*, 27(14), 8199-8213. https://doi.org/10.1007/s10570-020-03346-9

Charron, C. S., Milner, J. A., & Novotny, J. A. (2016) Garlic. In: Caballero, B., Finglas, P. M., Toldrá, F. *Encyclopedia of Food and Health*. Academic Press, 184-190. http://dx.doi.org/10.1016/B978-0-12-384947-2.00346-9

Chueca, B., Berdejo, D., Gomes-Neto, N. J., Pagán, R., & García-Gonzalo, D. (2016). Emergence of hyper-resistant *Escherichia coli* MG1655 derivative strains after applying sub-inhibitory doses of individual constituents of essential oils. *Frontiers in Microbiology*, 7, 273. http://dx.doi.org/10.3389/fmicb.2016.00273

Christaki, S., Moschakis, T., Kyriakoudi, A., Biliaderis, C. G., & Mourtzinos, I. (2021). Recent advances in plant essential oils and extracts: Delivery systems and potential uses as preservatives and antioxidants in cheese. *Trends in Food Science and Technology*, 116, 264–278. https://doi.org/10.1016/j.tifs.2021.07.029

CLSI. (2012). *Methods for Dilution Antimicrobial Susceptibility Tests for Bacteria That Grow Aerobically*, 9th ed.; CLSI: Wayne, PA, USA.

Dannenberg, G. da S., Funck, G. D., Cruxen, C. E. dos S., Marques, J. de L., Silva, W. P. da, & Fiorentini, Â. M. (2017). Essential oil from pink pepper as an antimicrobial component in cellulose acetate film: Potential for application as active packaging for sliced cheese. *LWT - Food Science and Technology*, 81, 314–318. https://doi.org/10.1016/j.lwt.2017.04.002

Downes F. P. & Ito K. (2001). *Compendium of Methods for the Microbiological Examination of Foods*. 4th ed. APHA, Washington, DC, 676 pp.

El-Sayed, A. M. *The Pherobase: Database of Pheromones and Semiochemicals*. Retrieved from http://www.pherobase.com. Accessed January 11, 2022.

Espina, L., García-Gonzalo, D., & Pagán, R. (2016). Detection of thermal sublethal injury in *Escherichia coli* via the selective medium plating technique: mechanisms and improvements. Frontiers in Microbiology, 7, 1376. https://doi.org/10.3389/fmicb.2016.01376

Ezeorba, T. P. C., Chukwudozie, K. I., Ezema, C. A., Anaduaka, E. G., Nweze, E. J., & Okeke, E. S. (2022). Potentials for health and therapeutic benefits of garlic essential oils: Recent findings and future prospects. Phamacological Research – Modern Chinese Medicine, 3, 100075. https://doi.org/10.1016/j.prmcm.2022.100075.

Farbood, M. I., MacNeil, J. H., & Ostovar, K. (1976). Effect of rosemary spice extractive on growth of microorganisms in meats. *Journal of Milk and Food Technology*, 39(10), 675–679. https://doi.org/10.4315/0022-2747-39.10.675

Fujisawa, H., Suma, K., Origuchi, K., Seki, T., & Ariga, T. (2008). Thermostability of allicin determined by chemical and biological assays. *Bioscience, Biotechnology, and Biochemistry*, *72*(11), 2877-2883. https://doi.org/10.1271/bbb.80381

García-Díez, J., Alheiro, J., Pinto, A. L., Soares, L., Falco, V., Fraqueza, M. J., Patarata, L. (2017). Influence of food characteristics and food additives on the antimicrobial effect of garlic and orégano essential oil. *Foods*, *6*(6), 44. https://doi.org/10.3390/foods6060044

Gonçalves, S. M., Santos, D. C., Motta, J. F. G., dos Santos, R. R., Chávez, D. W. H., & de Melo, N. R. (2019). Structure and functional properties of cellulose acetate films incorporated with glycerol. *Carbohydrate Polymers*, *209*, 190-197. https://doi.org/10.1016/j.carbpol.2019.01.031

Gonçalves, S. M., Motta, J. F. G., Ribeiro-Santos, R., Chávez, D. W. H., & de Melo, N. R. (2020). Functional and antimicrobial properties of cellulose acetate films incorporated with

sweet fennel essential oil and plasticizers. *Current Research in Food Science*, *3*, 1-8. https://doi.org/10.1016/j.crfs.2020.01.001

Guidone, A., Zotta, T., Matera, A., Ricciardi, A., de Filippis, F., Ercolini, D., & Parente, E. (2016). The microbiota of high-moisture mozzarella cheese produced with different acidification methods. *International Journal of Food Microbiology*, 216, 9-17. http://dx.doi.org/10.1016/j.ijfoodmicro.2015.09.002

Hashemi, G. H., Ziaee, E., Eskandari, M. H., & Hosseini, S. M. H. (2017). Characterization of basil seed gum-based edible films incorporated with *Zataria multiflora* essential oil nanoemulsion. *Carbohydrate Polymers*, 166, 93–103. http://dx.doi.org/10.1016/j.carbpol.2017.02.103

Jin, M., Liu, L., Wang, D., Yang, D., Liu, W., Yin, J., Yang, Z., Wang, H., Qiu, Z., Shen, Z., Shi, D., Li, H., Guo, J., & Li, J. (2020). Chlorine disinfection promotes the exchange of antibiotic resistance genes across bacterial genera by natural transformation. *The ISME Journal*, 14, 1847-1856. https://doi.org/10.1038/s41396-020-0656-9

Jonnala, B. R. Y., McSweeney, P. L. H., Sheehan, J. J., & Cotter, P. D. Sequencing of the cheese microbiome and its relevance to the industry. (2018). *Frontiers in Microbiology*, 9, 1020. http://dx.doi.org/10.3389/fmicb.2018.01020

Kramer, B., Muranyi, J. W. P. (2019). Inactivation of *Listeria innocua* on packaged meat products by pulsed light. *Food Packaging and Shelf Life*, *21*, 100353. https://doi.org/10.1016/j.fpsl.2019.100353.

Linstrom, P. J.; Mallard, W. G. *NIST Chemistry WebBook*. Retrieved from http://webbook.nist.gov/chemistry. Accessed January 11, 2022.

Marcilla, A. & Beltran, M. (2017). Mechanism of plasticizer action. In *Handbook of Plasticizers,* 3rd ed.; Wypych, G., Ed.; ChemTec Publishing, pp 119−134. https://doi.org/10.1016/B978-1-895198-50-8.50007-2

Marino, M., de Wittenau, G. D., Saccà, E., Cattonaro, F., Spadotto, A., Innocente, A., Radovic, S., Piasentier, E., & Marroni, F. (2019). Metagenomic profiles of different types on Italian high-moisture Mozzarella cheese. *Food Microbiology*, 79, 123-131. https://doi.org/10.1016/j.fm.2018.12.007

Marques, C. S., Grillo, R. P., Bravim, D. G., Pereira, P. V., Villanova, J. C. O., Pinheiro, P. F., Souza, J. C., & Bernardes, P. C. (2019). Preservation of ready-to-eat salad: A study with combination of sanitizers, ultrasound, and essential oil-containing β-cyclodextrin inclusion complex. *LWT – Food Science and Technology*, 115, 108433. https://doi.org/10.1016/j.lwt.2019.108433

Marques, C. S., Silva, R. R. A., Arruda, T. R., Ferreira, A. L. V., Oliveira, T. V., Moraes, A. R. F., Dias, M. V., Vanetti, M. C. D., & Soares, N. F. F. (2022). Development and investigation of zein and cellulose acetate polymer blends incorporated with garlic essential oil and β-cyclodextrin for potential food packaging application. *Polysaccharides*, 3(1), 277-291. https://doi.org/10.3390/polysaccharides3010016

Mendes, L. A., Martins, G. F., Valbon, W. R., Souza, T. S., Menini, L., Ferreira, A., & Ferreira, M. F. S. (2017). Larvicidal effect of essential oils from brazilian cultivars of guava on Aedes. *Industrial Crops and Products*, 108, 684-689. https://doi.org/10.1016/j.indcrop.2017.07.034

Miller, F. A., Brandão, T. R. S., Teixeira, P., & Silva, C. L. M. (2006). Recovery of heat-injuredy *Listeria innocua*. *International Journal of Food Microbiology*, *112*, 261-265. https://doi.org/10.1016/j.ijfoodmicro.2006.04.013

Moorman, M., Nettleton, W., Ryser, E., Linz, J., & Pestka, J. (2005). Altered sensitivity to a quaternary ammonium sanitizer in stressed *Listeria innocua*. *Journal of Food Prot*ection, 68(8), 1659-1663. https://doi.org/10.4315/0362-028x-68.8.1659

Moorman, M. A., Thelemann, C. A., Zhou, S., Pestka, J. J., Linz, J. E., & Ryser, E. T. (2008). Altered hydrophobicity and membrane composition in stress-adapted Listeria innocua. *Journal of Food Protection*, 71(1), 182-185. https://doi.org/10.4315/0362-028x-71.1.182

Moraes, A. R. F., Pola, C. C., Bilck, A. P., Yamashita, F., Tronto, J., Medeiros, E. A. A., & Soares, N. F. F. (2017). Starch, cellulose acetate and polyester biodegradable sheets: Effect of composition and processing conditions. *Materials Science and Engineering C*, 78, 932–941. https://doi.org/10.1016/j.msec.2017.04.093

Motelica, L., Ficai, D., Ficai, A., Oprea, O. C., Kaya, D. A., & Andronescu, E. (2020). Biodegradable antimicrobial food packaging: Trends and perspectives. *Foods,* 9, 1438. https://doi.org/10.3390/foods9101438

Muchaamba, F., Stephan, R., Tasara, T. (2021). Listeria monocytogenes cold shock proteins: Small proteins with a huge impact. *Microorganisms*, *9*(5), 1061. https://doi.org/10.3390/microorganisms9051061

Münchberg, U., Anwar, A., Mecklenburg, S., & Jacob, C. (2007). Polysulfides as biologically active ingredients of garlic. *Organic & Biomolecular Chemistry*, *5*, 1505-1518. https://doi.org/10.1039/B703832A

Obe, T., Nannapaneni, R., Sharma, C. S., & Kiess, A. (2018). Homologous stress adaptation, antibiotic resistance, and biofilm forming ability of *Salmonella enterica* serovar Heidelberg ATCC8326 on different food-contact surfaces following exposure to sublethal chlorine concentrations. *Poultry Science*, 97(3), 951-961. https://doi.org/10.3382/ps/pex346

Oliveira, T. L. C., Soares, R. A., Ramos, E. M., Cardoso, M. G., Alves, E., & Piccoli, R. H. (2011). Antimicrobial activity of *Satureja montana* L. essential oil against *Clostridium perfringens* type A inoculated in mortadela-type sausages formulated with different levels of sodium nitrite. *International Journal of Food Microbiology*, 144(3), 546-555. https://doi.org/10.1016/j.ijfoodmicro.2010.11.022

Pola, C. C., Medeiros, E. A. A., Pereira, O. L., Souza, V. G. L., Otoni, C. G., Camilloto, G. P., & Soares, N. F. F. (2016). Cellulose acetate active films incorporated with oregano (*Origanum vulgare*) essential oil and organophilic montmorillonite clay control the growth of phytopathogenic fungi. *Food Packaging and Shelf Life*, 9, 69–78. https://doi.org/10.1016/j.fpsl.2016.07.001

Ramos, Ó. L., Santos, A. C., Leão, M. V., Pereira, J. O., Silva, S. I., Fernandes, J. C., Franco, M. I., Pintado, M. E., & Malcata, F. X. (2012). Antimicrobial activity of edible coatings prepared from whey protein isolate and formulated with various antimicrobial agents. *International Dairy Journal*, 25(2), 132–141. https://doi.org/10.1016/j.idairyj.2012.02.008

R Core Team. R: A Language and Environment for Statistical Computing; R Foundation for Statistical Computing: Vienna, Austria, 2021; Retrieved from https://www.R-project.org/. Accessed January 29, 2022.

Satyal, P., Craft, J. D., Dosoky, N. S., & Setzer, W. N. (2017). The chemical compositions of the volatile oils of garlic (*Allium sativum*) and wild garlic (*Allium vineale*). *Foods*, *6*(8), 63. https://doi.org/10.3390/foods6080063

Silva, B. D., Bernardes, P. C., Pinheiro, P. F., Fantuzzi, E., & Roberto, C. D. (2021). Chemical composition, extraction sources and action mechanisms of essential oils: Natural preservative and limitations of use in meat products. *Meat Science*, 176, 108463. https://doi.org/10.1016/j.meatsci.2021.108463

Silva, R. R. A., Freitas, P. A. V., Teixeira, S. C., Oliveira, T. V., Marques, C. S., Stringheta, P. C., Pires, A. C. S., Ferreira, S. O., & Soares, N. F. F. (2022). Plasticizer effect and ionic cross-linking: the impact of incorporating divalent salts in methylcellulose films for colorimetric detection of volatile ammonia. *Food Biophysics*, 17, 59–74. https://doi.org/10.1007/s11483-021-09700-z

Smith-Palmer, A., Stewart, J., & Fyfe, L. (2001). The potential application of plant essential oils as natural food preservatives in soft cheese. *Food Microbiology*, 18(4), 463–470. https://doi.org/10.1006/fmic.2001.0415

Souza, T. S., Ferreira, M. F. S., Menini, L., Souza, J. R. C. L., Parreira, L. A., Cecon, P. R., & Ferreira, A. (2017). Essential oil of *Psidium guajava*: influence of genotypes and environment. *Scientia Horticulturae*, 216, 38–44. https://doi.org/10.1016/j.scienta.2016.12.026

Tampau, A., Gonzáles-Martínez, C., & Chiralt, A. (2018). Release kinetics and antimicrobial properties of carvacrol encapsulated in electrospun poly-(ε-caprolactone) nanofibres. Application in starch multilayer films. *Food Hydrocolloids*, *79*, 158-169. https://doi.org/10.1016/j.foodhyd.2017.12.021

Teixeira, S. C., Silva, R. R. A., de Oliveira, T. V., Stringheta, P. C., Pinto, M. R. M. R., & Soares, N. de F. F. (2021). Glycerol and triethyl citrate plasticizer effects on molecular, thermal, mechanical, and barrier properties of cellulose acetate films. *Food Bioscience*, 42, 101202. https://doi.org/10.1016/j.fbio.2021.101202

White, R. P., & Lipson, J. E. G. (2016). Polymer Free Volume and Its Connection to the Glass Transition. *Macromolecules*, 49(11), 3987–4007. https://doi.org/10.1021/acs.macromol.6b00215

Wu, V. C. H. (2014). Injured and stressed cells. In: Batt, C. A., Torturello, M. L. (Eds), *Encyclopedia of Food Microbiology* (Second Edition), Academic Press, 2104, 364-371. http://dx.doi.org/10.1016/B978-0-12-384730-0.00423-7

Wypych G. (2017). *Handbook of Plasticizers*, 3rd ed.; Wypych G., Ed.; ChemTec Publishing: Toronto, v. 1.

Yamamoto, K., Zhang, X., Inaoka, T., Morimatsu, K., Kimura, K., & Nakaura, Y. (2021). Bacterial injury induced by high hydrostatic pressure. *Food Engineering Reviews*, 13, 442-453. https://doi.org/10.1007/s12393-020-09271-8

# 5. ARTICLE 3: DEGRADATION IN SOIL OF CELLULOSE ACETATE AND ZEIN BLEND FILMS INCORPORATED WITH DIFFERENT PLASTICIZERS AND GARLIC ESSENTIAL OIL

## 5.1 Introduction

Cellulose is a versatile, environmentally friendly, cost-effective, and abundant polymer widely studied as a potential sustainable packaging material (Rogovina et al., 2013). Its structure can be chemically modified to improve the technological properties of the polymer, resulting in cellulose derivatives with distinguishing features and functionality (Anpilova et al., 2020; Assis et al., 2020; Silva et al., 2022).

Cellulose acetate (CA) is a cellulose ester in which some of cellulose hydroxyl groups were substituted by acetyl groups through an acetylation reaction. It can be obtained from cotton, wood, and agricultural by-products, and it is already used for several applications, such as cigarette filters, photographic films, membranes, texture industry, and dental products (Biswas et al., 2006; Fornazier et al., 2021; Yadav & Hakkarainen, 2021). Among the cellulose derivatives used as polymeric matrices to produce films, CA stands out due to its optical transparency, nontoxicity, and high hydrophobicity when compared to other biopolymers. In addition, it can be incorporated with plasticizers and blended with different polymers, giving rise to materials with distinct characteristics (Moraes et al., 2017; Gonçalves et al., 2019; Marques et al., 2022).

Since plastic pollution is a major global public health and environmental concern, biodegradable polymers obtained from renewable sources have been investigated as potential alternatives for packaging use. Despite being obtained from a natural polymer, the chemical modification may affect the biodegradability process of cellulose derivatives. It is known, for example, that the acetylation reaction undergone by cellulose to produce CA have a considerable impact on the material degradation. That way, the degree of acetyl substitution is one of the main factors governing its biodegradation rate (Haske-Cornelius et al., 2017; Yadav & Hakkarainen, 2021). Therefore, modified biopolymers, such as CA with a degree of acetyl substitution higher than 2.0, can last for a long time when disposed in nature. This feature is not desirable in terms of sustainability, however, in terms of food packaging, it is required when considering foodstuffs with high moisture content.

Blending CA with other biodegradable polymers can change the degradation rate of the material (Guruprasad & Shashidhara, 2004; Calil et al., 2006). For example, zein, a protein obtained from corn, and already used as food coating and studied as a potential

packaging material, can be used as a blend material to accelerate the biodegradability of CA (Lawton, 2002; Bayer, 2021). Thus, when developing sustainable materials from biopolymers, it is imperative to elucidate the changes that take place during this step.

The addition of plasticizers can also hasten the occurrence of degradation, while bioactive compounds can retard it (Phuong et al., 2014; Hernández-García et al.,2021). Although the main goal of plasticizer incorporation into polymer films is to alter their mechanical and thermal properties by allowing a higher polymer chain mobility, their presence can impact CA proneness to the environmental conditions (Phuong et al., 2014; Kunthadong et al., 2015). Glycerol is a plasticizer widely studied to produce packaging from biopolymers. Tributyrin has been investigated as a plasticizer as well, albeit more hydrophobic than glycerol (Gonçalves et al., 2019; Marques et al., 2022). Garlic essential oil (GEO), for example, is a natural antimicrobial extracted from garlic bulbs with recognized activity against several microorganisms, which can also be incorporated into polymeric matrices to provide active functions for the packaging (Bagheri et al., 2020). However, it could change the biodegradability rate of the films.

In a previous work, CA:zein blends and CA-based films were successfully elaborated with both plasticizers and GEO (Marques et al., 2022a, 2022b). However, their degradation was not assessed. In this sense, in the present work, we aimed to investigate the degradation of the elaborated active CA:zein blend films in soil. It was hypothesized that the blend films with zein would degrade faster than CA-based films, and that the incorporation with glycerol would hasten the degradation rate of the polymer. At last, since GEO is an antimicrobial agent and considering that the degradation is a complex phenomenon that involves the action of microorganisms, it was speculated that its presence in films would slow down their degradation rate.

## 5.2 Material and Methods

### 5.2.1 Material

CA (degree of acetyl substitution = 2.5; average molecular weight = 2,024,000 g.mol$^{-1}$) was donated by Rhodia Solvay Group (Brazil), and zein was donated by Flo Chemical Corp (F4400, molecular mass of 15–26 kDa) (USA). Glycerol (LabSynth, Brazil) and tributyrin (98%, Acros Organics, India) were used as plasticizers. The solvents used for polymer dispersion were anhydrous ethanol for zein (99.8%, Neon, Brazil) and acetone for CA (99.5%, LabSynth, Brazil). GEO was acquired from Laszlo Aromaterapia (Brazil). According

to the manufacturers, the main amino acids present in zein were glutamic acid, leucine, alanine, proline, and phenylalanine, whereas for GEO, the main compounds were diallyl polysulfides and allyl methyl polysulfides.

### 5.2.2 Experimental design and films elaboration

The experiment was arranged in a completely randomized design, in a factorial combination of two polymer matrices (CA and CA:zein blend, BL), two plasticizers (glycerol and tributyrin), and two GEO's concentrations (0% and 10%). In addition, controls with CA only and zein only were also elaborated, totaling 10 films, as described in Table 1.

**Table 1.** Manufactured films with cellulose acetate, zein, plasticizers (glycerol and tributyrin), and garlic essential oil.

| Sample | Polymer | Plasticizer | Garlic essential oil |
|---|---|---|---|
| BL-GLY | Cellulose acetate and zein | Glycerol | 0% |
| BL-GLY-GEO | Cellulose acetate and zein | Glycerol | 10% |
| BL-TRI | Cellulose acetate and zein | Tributyrin | 0% |
| BL-TRI-GEO | Cellulose acetate and zein | Tributyrin | 10% |
| CA-GLY | Cellulose acetate | Glycerol | 0% |
| CA-GLY-GEO | Cellulose acetate | Glycerol | 10% |
| CA-TRI | Cellulose acetate | Tributyrin | 0% |
| CA-TRI-GEO | Cellulose acetate | Tributyrin | 10% |
| CA | Cellulose acetate | 0% | 0% |
| Zein | Zein | 0% | 0% |

The CA:zein blend films were manufactured according to Marques et al. (2022a). Firstly, both CA and zein were dispersed separately in their respective solvents: CA in acetone, at the ratio of 1:10 (wt./v), for 24 h; and zein in ethanol 80% (v/v), for 10 min at 65 ºC stirring at 500 rpm. Subsequently, the dispersions were blended using the mass proportion of 3:2 CA:zein, and incorporated with the plasticizer of choice (glycerol or tributyrin, both at 30% wt. based on total polymer mass) and GEO (0% or 10% wt. also based on total polymer mass). The obtained dispersions were homogenized for 2 min in Ultra Turrax (5,000 rpm, model T25, IKA), allowed to rest for approximately 30 min, and spread over a glass plate with the aid of a K-Paint Applicator machine (USA). After solvent evaporation, the films were vacuum-sealed in plastic bags and stored in the dark until use. Plasticized CA-based

films incorporated or not with GEO were elaborated as well following the same instructions, aside from the mixture with zein. The control films (pure CA and pure zein) were elaborated with their respective solvent, only.

### 5.2.3 Degradation assay

The films' degradation was investigated by simulating the processes taking place under natural conditions, as proposed by Rogovina et al. (2013). Samples (dimensions of 5 cm x 3 cm) were placed inside plastic nets (Figure 1S of the Supplementary Material), to facilitate their removal, and buried in red soil (latosol), common in Brazil, with pH = 6.5, previously corrected with the incorporation of lime. The container with the samples was exposed to ambient-light, but sheltered from rain, and watered three times a week. Every 30 days, for 150 days, the samples were removed and cleaned using a brush. If necessary, a small amount of water was also used to assist in removal of dirt, and the films were immediately dried on absorbent paper. The degradation process was studied in terms of visual appearance, changes in morphology, weight loss over time, and changes in molecular structure. White sulfite paper and low density polyethylene were used as control samples since paper is a well-known biodegradable material, and polyethylene is a non-biodegradable material.

#### 5.2.3.1 Subjective visual analysis

After the removal of dirt, the films' appearance was subjectively (color, aspect, size) assessed by the research group. Photographs were taken every 30 days using a cellphone (Moto g6 Play, Motorola, camera 13 megapixels).

#### 5.2.3.2 Scanning Electron Microscopy

Micrographs of films' surfaces were obtained through a Scanning Electron Tabletop Microscope (TM3000, Hitachi High-Technologies, Japan) with a secondary electron detector, operating under low-vacuum and 15 Kv of accelerating voltage. The uncoated samples (around 25 $mm^2$) were attached to the stubs' surface with the aid of a double-sided carbon tape. Microscopic changes in films structures after burial were investigated, such as the occurrence of holes, tears and other defects.

#### 5.2.3.3 Mass loss

Mass loss over time was assessed every 30 days from the initial day to the 150$^{th}$, or until there were retrievable samples. The films were weighted in a digital scale (minimum 10 mg, e = 0,001, Bel Mark M214A, Italy).

#### 5.2.3.4 Thermogravimetric analysis (TGA)

TGA was conducted on a Shimadzu thermogravimetric analyzer, (Model DTG-60H, Japan), under an inert atmosphere of nitrogen (50 mL.min$^{-1}$). Approximately 4 mg of samples were weighed and heated from 25 to 600 ºC at 10 ºC.min$^{-1}$. The TG curves were obtained for pristine materials and films before burial in soil. This analysis allowed us to estimate the additive content in samples and the polymer decomposition temperature (Quintana et al., 2013). TG curves were also obtained for films after burial for 150 days, which allowed verifying if the burial period would entail changes in the thermal degradation profile of the samples.

#### 5.2.3.5 Fourier Transform Infrared Spectroscopy (FTIR)

The FTIR spectra of the films and pristine compounds were obtained, every 30 days during the 150-days period, with a FTIR spectrometer (Nicolet 6700, Thermo Scientific, USA) equipped with attenuated total reflectance (ATR). A total of 128 scans per sample were made, from 4000 to 800 cm$^{-1}$, at a spectral resolution of 4 cm$^{-1}$. Changes in the spectra regarding the main functional groups present in the samples were evaluated over time. In order to minimize interferences unrelated to the samples, baseline correction and normalization were applied.

#### 5.2.3.6 Statistical analysis

When appropriate, the data obtained were submitted to analysis of variance (ANOVA) followed by Tukey's test or non-linear regression (p-value $\leq$ 0.05). The freely software package R was used (RCore, 2021).

## 5.3 Results and Discussion

### 5.3.1 Macro and microscopic changes in films

Macroscopic changes in films visual appearance were verified during the soil burial period. Photographs of control samples (CA, zein, paper and polyethylene), plasticized CA-films, and BL-films before burial in soil and after the final day of burial are displayed in Figure 1. In the Supplementary Material (Figure 2S, 3S, and 4S), the photographs of films after 30, 60, 90, and 120 days buried in soil are available.

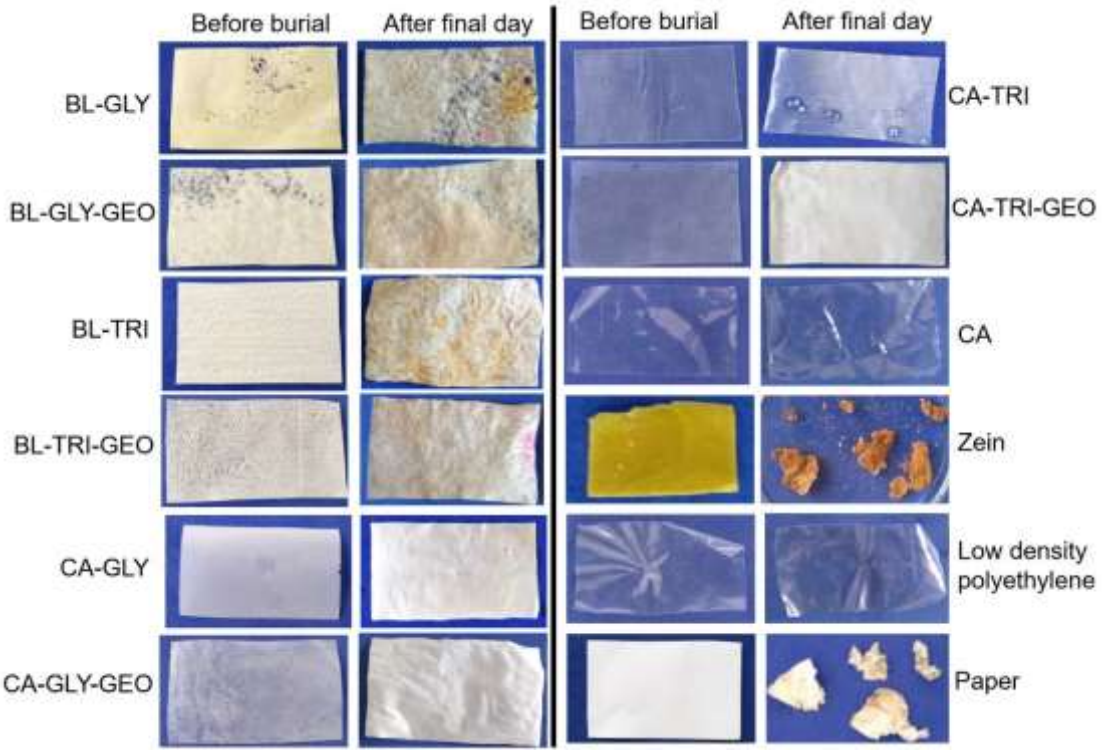


**Figure 1** Photographs of the films before burial (initial day) and after the final day buried in soil. CA: cellulose acetate; BL: cellulose acetate:zein blend; GLY: glycerol; TRI: tributyrin; GEO: garlic essential oil. Zein and paper lasted for 90 days buried. All other samples lasted for 150 days.

The visual assessment of the films before burial showed that the the CA:zein blends plasticized with glycerol presented more defects (holes and tears) than the ones plasticized with tributyrin (Figure 1). However, when compared to the pure zein film, all manufactured blends were more flexible and less brittle (Marques et al. 2022a). During the degradation assay, the blend films seemed slightly smaller in relation to their initial size, aside from the more roughened aspect and the appearance of colorful spots. As discussed by Rosa et al. (2004), roughness can be a potential parameter indicator of materials' degradation, and the increase verified could suggest that the degradation phenomenon initially takes place in the films surface. The zein control film, in turn, degraded as fast as paper (90 days) and presented

numerous adhered particles on the surface of the recovered pieces, rendering it impossible to make several analyses.

Regarding the CA-based films, before burial in soil, the samples plasticized with tributyrin seemed more transparent than the films incorporated with glycerol (Figure 1). During the burial period, all CA-based films became opaquer over time, acquiring a white coloration, with the exception of the CA control film, which no visual change was verified. Whitening of the surface was also observed by Andersson et al. (2010) when studying the hydrolytic degradation of poly(L-lactide) films. Visual changes that occur on the polymer surface, such as yellowing, whitening, and brightness reversion, are an indication of polymer degradation. This can be due to occurrence of oxidation of the hydroxyl groups that are still present in CA, since the acetylation reaction was partial. These remaining hydroxyl groups in CA chains are prone to oxidation to either keto groups or aldehydes by several abiotic factors, such as temperature, light and humidity, and the presence of plasticizers, mostly hygroscopic plasticizer, can speed up the process (Ahn et al., 2019).

Microscopic alterations were also verified in BL-films and CA-based films, and the micrographs are presented in Figures 2 and 3, respectively.

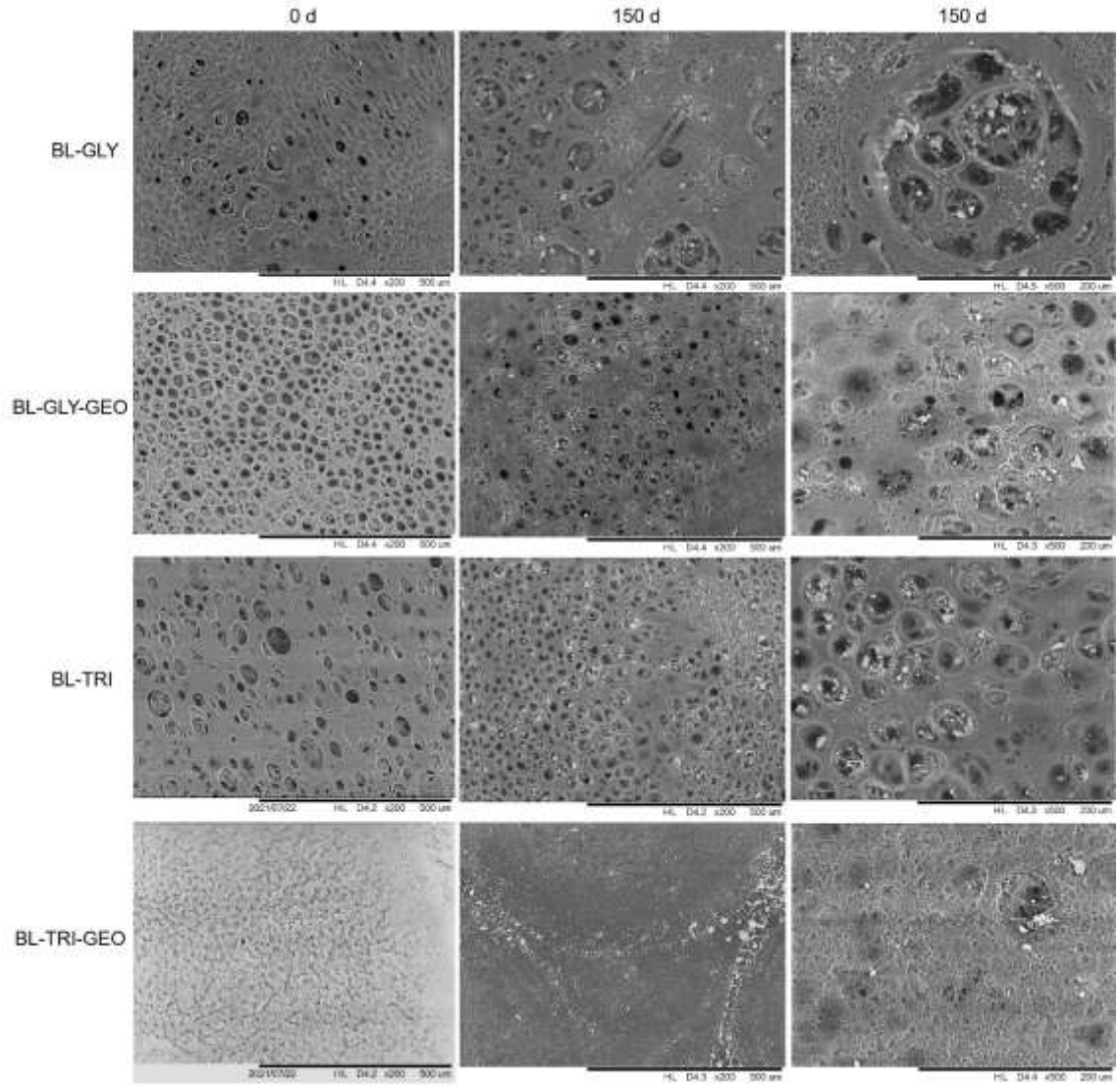


**Figure 2** Micrographs of cellulose acetate:zein blend films (BL), incorporated with plasticizers (glycerol, GLY, and tributyrin, TRI) and garlic essential oil (GEO), before burial in soil (magnification of 200x) and recovered after a burial-period of 150 days (magnification of 200x and 500x).

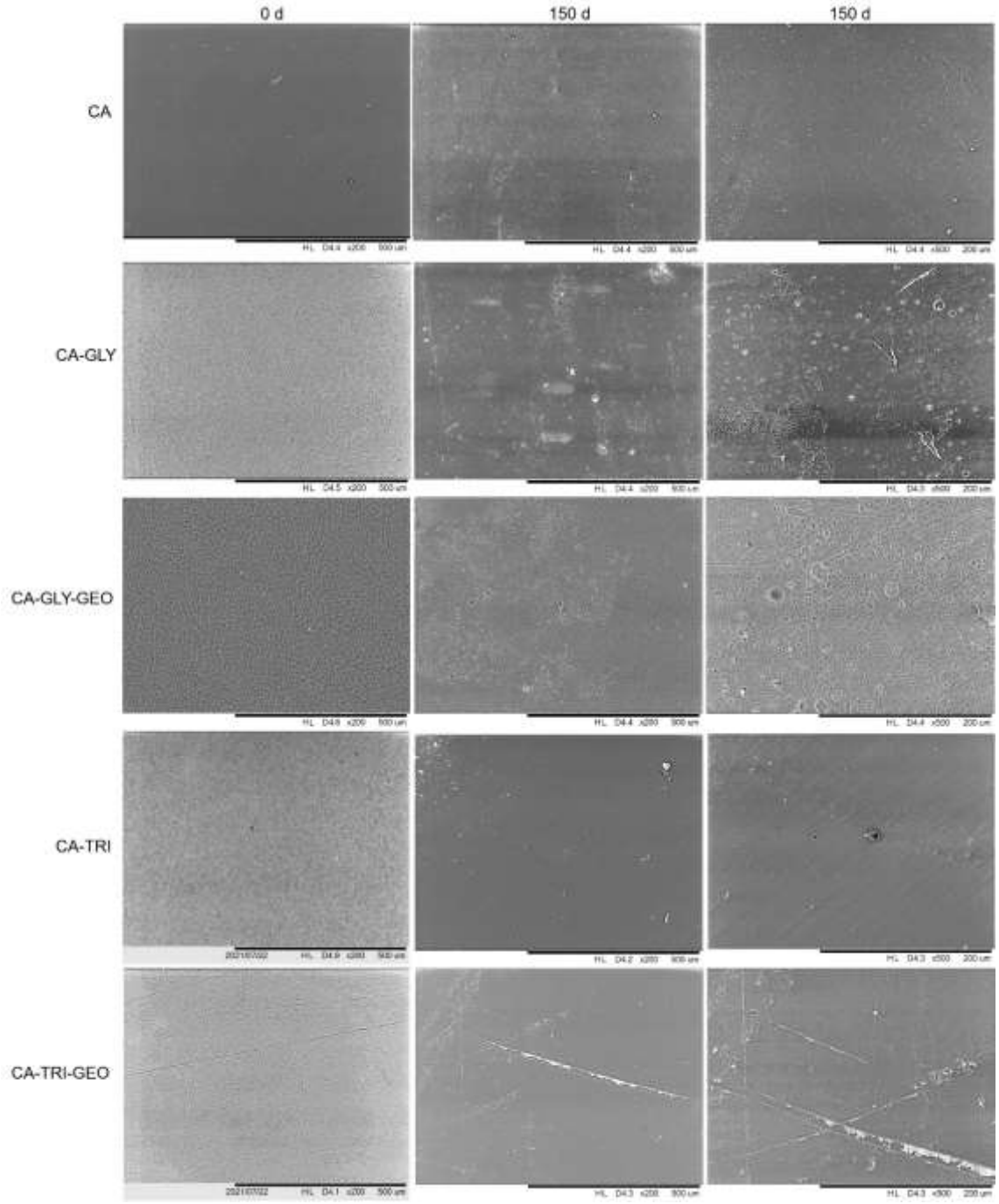


**Figure 3** Micrographs of cellulose acetate (CA) films, with or without plasticizers (glycerol, GLY, and tributyrin, TRI) and garlic essential oil (GEO), before burial in soil (magnification of 200x) and recovered after a burial period of 150 days (magnification of 200x and 500x).

Initially, the blend films (Figure 2) presented a porous structure, with exception of the sample BL-TRI-GEO, and a rough and heterogeneous surface. After 150 days in soil, it was noticed an increase in the number and size of films' pores, which could be due to plasticizer

loss/degradation and degradation of the polymer chain. Presence of small soil particles adhered inside the pores were also verified.

Regarding the CA-based films, whereas CA control film exhibited a homogeneous surface, plasticized CA films' surface appeared saturated with plasticizers microbubbles (Figure 3). A similar result was verified by Gonçalves et al. (2019, 2020) when investigating CA films incorporated with glycerol and essential oil. After the burial period of 150-days, the plasticized CA films' surface changed: the micrographs revealed loss/degradation of plasticizers and occurrence of defects resulting from erosion, such as multiple holes and scratches marks.

### 5.3.2 Mass loss

The samples' mass over time decreased exponentially, as can be seen in Figure 4. In Table 2, the non-linear models and their respective adjusted $R^2$ are presented. It is worth noting that no equations were estimated for CA an zein control films. CA control samples recovered after 150 days presented a very discreet weight loss, around 2% compared to the initial value. This result is in accordance with the literature. Although CA with a degree of acetyl substitution of 2.5 is considered a biodegradable polymer, depending on the degradation condition (composting, soil, liquid medium, reactor), it can take several days, even months, for CA to lose mass over time (Yamashita & Endo, 2005; Calil et al., 2006; Phuong et al., 2014). Regarding the zein control samples, it was not possible to quantify their mass loss due to the high amount of soil particles adhered, which would underestimate the polymer mass loss over time (Figure 1 and 2S). Either way, as stated before, these samples exhibited a more intense degradation and lasted for only 90 days.

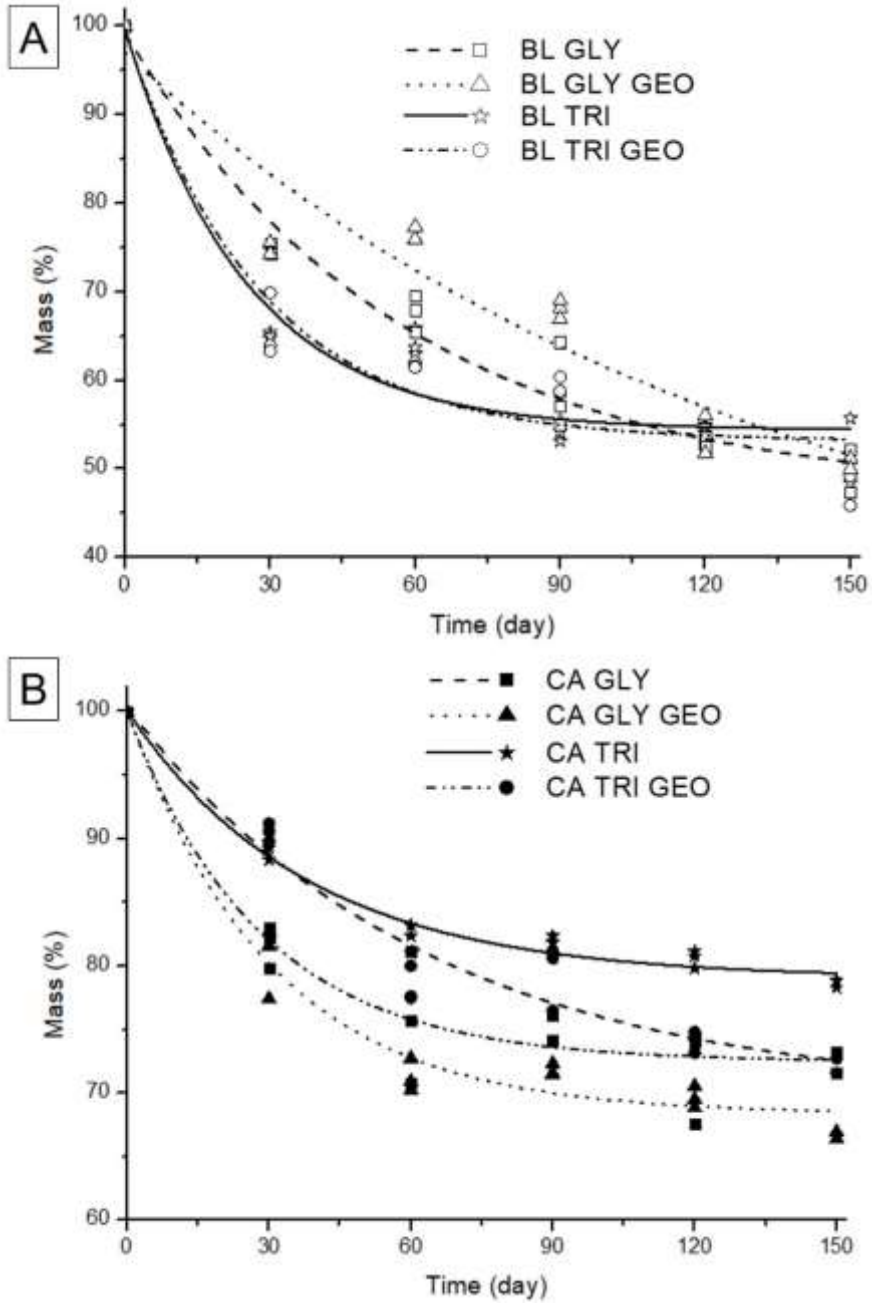


**Figure 4** Mass (%) of (A) cellulose acetate:zein blend films (BL) films and (B) cellulose acetate (CA) films incorporated with glycerol (GLY), tributyrin (TRI), and garlic essential oil (GEO) verified during 150 days buried in soil.

**Table 2** Non-linear models, and their respective adjusted $R^2$, obtained for mass (y, %) over time (x, day) during the 150-day period buried in soil, for each treatment.

| Sample | Model | $R^2adj$ |
|---|---|---|
| BL-GLY | $y = 52.208 * e^{-\left(\frac{x}{57.408}\right)} + 46.952$ | 0.972 |
| BL-GLY-GEO | $y = 66.267 * e^{\left(-\frac{x}{129.853}\right)} + 30.683$ | 0.903 |
| BL-TRI | $y = 45.205 * e^{-\left(\frac{x}{25.062}\right)} + 54.340$ | 0.957 |
| BL-TRI-GEO | $y = 46.251 * e^{-\left(\frac{x}{27.924}\right)} + 53.151$ | 0.948 |
| CA-GLY | $y = 27.468 * e^{-\left(\frac{x}{28.384}\right)} + 72.462$ | 0.946 |
| CA-GLY-GEO | $y = 31.673 * e^{-\left(\frac{x}{30.478}\right)} + 68.349$ | 0.976 |
| CA-TRI | $y = 21.049 * e^{-\left(\frac{x}{37.852}\right)} + 79.036$ | 0.981 |
| CA-TRI-GEO | $y = 30.639 * e^{-\left(\frac{x}{63.322}\right)} + 69.691$ | 0.934 |

BL: cellulose acetate:zein blend; CA: cellulose acetate; GLY: glycerol; TRI: tributyrin; GEO: garlic essential oil

After 150 days, the blend films' mass was reduced by half, regardless of the type of plasticizer or concentration of GEO. On the other hand, regarding plasticized CA films, the mass loss was less noticeable than the verified for the blends, reaching around 30% for films incorporated with glycerol and around 20% for films containing tributyrin. However, when compared to the CA control film, the mass loss was substantially higher.

According to the literature, the weight loss of CA-based films incorporated with additives can be attributed to the deacetylation process that occurred during CA degradation, as well as by loss of additives, either by degradation or exudation (Yamashita & Endo, 2005; Quintana et al., 2013). Therefore, it is more difficult to identify the degradation of the polymer in these stages only by the weight loss investigation. To elucidate the films' degradation process, TGA and FTIR techniques can be used complementarily (Quintana et al., 2013; Liu et al., 2019).

TG curves for pristine materials and films (obtained before burial), as well as the table displaying mass loss during thermal decomposition, are available in Supplementary Material (Figure 5S and Table 1S). The TG curves allowed to determine the experimental amount of additives initially present in films. With this, it was possible to estimate the amount of weight loss possible due to additive loss/degradation during the 150 days in soil and, consequently, the mass loss due to polymer degradation (displayed in Table 3). To confirm these findings,

the thermal degradation profile of the films was investigated after 150 days as well. These TG curves are also available in the Supplementary Material (Figure 6S) and showed mass loss in a single stage, indicating that the additives were no longer present in the films.

**Table 3** Films' mass loss (%) after 150 days buried in soil, experimental mass loss possible due to additive loss/degradation, and the estimated amount of mass loss due to polymer degradation.

| **Sample** | **Film mass loss after 150 days (%)** | **Additive mass loss (%)** | **Polymer mass loss (%)** |
|---|---|---|---|
| BL-GLY | 50.1 | 18.5 | 31.6 |
| BL-GLY-GEO | 49.4 | 28 | 21.4 |
| BL-TRI | 48.0 | 19 | 29.0 |
| BL-TRI-GEO | 52.4 | 22 | 30.5 |
| CA-GLY | 27.6 | 13 | 14.6 |
| CA-GLY-GEO | 33.3 | 28 | 5.3 |
| CA-TRI | 21.5 | 16 | 5.5 |
| CA-TRI-GEO | 27.9 | 24 | 3.9 |

BL: cellulose acetate:zein blend; CA: cellulose acetate; GLY: glycerol; TRI: tributyrin; GEO: garlic essential oil.

Concerning the polymer mass loss after 150 days, there was a significant interaction between the factors of polymer matrix and the kind of plasticizer (p-value $\leq 0.05$). Besides, there was also a significant interaction between the plasticizer type and the GEO concentration (p-value $\leq 0.05$). Therefore, these factors could not be studied in- dependently. The result of both interactions is displayed in Table 4.

**Table 4** Polymer mass loss (%) in films recovered after 150 days buried in soil, as a function of the type of plasticizer and the polymer matrix, and as a function of type of plasticizer and garlic essential oil (GEO) concentration.

| **Plasticizer** | **Polymer mass loss (%)** | |
|---|---|---|
| | **Cellulose acetate** | **Cellulose acetate:zein blend** |
| Glycerol | $10.0 \pm 5.4^{a\,A}$ | $26.5 \pm 6.2^{b\,A}$ |
| Tributyrin | $4.7 \pm 1.0^{a\,B}$ | $29.7 \pm 3.4^{b\,A}$ |
| **Plasticizer** | **Polymer mass loss (%)** | |

| | 0% of GEO | 10% of GEO |
|---|---|---|
| Glycerol | 23.1 ± 10.0 [a A] | 13.4 ± 9.3 [b A] |
| Tributyrin | 17.2 ± 13.9 [a B] | 17.2 ± 15.4 [a A] |

Mean ± standard deviation; Two-way interactions (polymer matrix x plasticizer and GEO concentration x plasticizer) were significant (p-value ≤ 0.05). Mean values followed by the same lowercase letter, within the same row, are not significantly different according to Tukey's test (p-value > 0.05). Mean values followed by the same uppercase letter, within the same column, are not significantly different according to Tukey's test (p-value > 0.05).

Both Tables 3 and 4 provide important information regarding the impact of the three investigated factors on films' degradation. Firstly, regarding the polymer matrix, blend films exhibited significant higher polymer mass loss than CA-films, which is in line with other studies (Guruprasad & Shashidhara, 2004; Calil et al., 2006; Herniou–Julien et al., 2019). This can be justified by the lower covalent bond of C-N present in zein, leading to greater structural instability in the CA:zein blend material (Canevarolo Junior, 2006). The C-N bond refers to the peptide bonds between the amino acids composing the zein chain, and its scission results in biofragmentation, making the CA:zein blends more exposed to assimilation by microorganisms.

Regarding the plasticizer choice, CA-based films containing glycerol showed more polymer mass loss than CA-based films incorporated with tributyrin. Glycerol is an eco-friendly hydrophilic compound used as plasticizer in several polymer matrices (Souza et al, 2016; Silva et al., 2022). Despite its lower miscibility with the solvent acetone, it is often used in CA-based films with adequate results (Melo et al., 2018; Gonçalves et al., 2019; Assis et al., 2020).

The higher mass loss observed in these films can be explained by the hygroscopic characteristic of the plasticizer (Basiak et al., 2018). According to Silva et al. (2022), the presence of water molecules in films may reduce the polymer decomposition temperature since they catalyze the scission of covalent bonds, by hydrolysis, in the polymer backbone. Hydrolysis of the acetate groups sets the beginning of CA degradation (Andersson et al., 2010; Yadav & Hakkarainen, 2021). The phenomenon takes place slowly in ambient conditions. However, presence of hydrophilic components, such as glycerol, may accelerate it due to their higher affinity with water (Yadav & Hakkarainen, 2021). This complies with the visual observations of the CA-films during the degradation period (Section 5.3.1), in which the whitening of the material was discussed. Whitening in CA-films plasticized with glycerol

occurred after the first 30 days of the degradation assay, while the phenomenon was slower in CA-films containing tributyrin. Regarding zein, albeit it is considered a protein of hydrophobic nature due to its insolubility in water, it has some hydrophilic amino acids in its structure that might contribute to hydrolysis occurrence in the blend films samples.

Regardless of the polymer matrix, either CA or CA:zein blend, the presence of GEO impacted the polymer mass loss after burial in soil when glycerol was used as plasticizer. Polymer mass loss of films incorporated with 10% of GEO was significantly lower than the verified in films without the essential oil. The recognized GEO antimicrobial activity might be associated with this result.

The biodegradation process can be defined as the degradation of the polymer and its assimilation by microorganisms, producing $CO_2$, $H_2O$, and biomass. (Calil et al., 2006; ASTM, 2018). Although assimilation tests, such as respirometry, were not performed in the present work, it is correct to say that the polymer mass loss observed resulted from abiotic degradation and, possibly, from the activity of environment naturally occurring microorganisms as well. The elaborated CA and blend films with GEO had their antimicrobial property confirmed in previous studies, in which the materials inhibited the growth of the Gram-positive bacteria *Staphylococcus aureus* and *Listeria innocua* (Marques et al., 2022a, 2022b). Therefore, it is possible that the presence of GEO in films also inhibited part of the soil microbiota responsible for polymer biodegradation.

However, when tributyrin was used as a plasticizer, a different outcome was found: GEO had no significant impact on polymer mass loss. This result is correlated with our previous findings: it was observed that active films elaborated with tributyrin showed less antimicrobial activity than films prepared with glycerol (Marques et al., 2022a). Although the explanation for this result is not entirely clear yet, it was suggested that a more hydrophobic plasticizer (tributyrin) would impair the release of the EO compounds, also of hydrophobic nature, compromising the antimicrobial performance of active films, or, in this case, having a lower impact on the soil microbiota.

### 5.3.3 FTIR

The FTIR spectra obtained for pristine compounds are displayed in Figure 5. In addition, the FTIR spectra of blend films and CA-films during the degradation period are presented in Figures 6 and 7. The spectra of GEO-films can be found in the Supplementary Material (Figure 7S). The main peaks identified for the pristine materials, summarized in

Table 5, were also observed in the films spectra and helped elucidate the phenomenon that took place during the 150-days period.

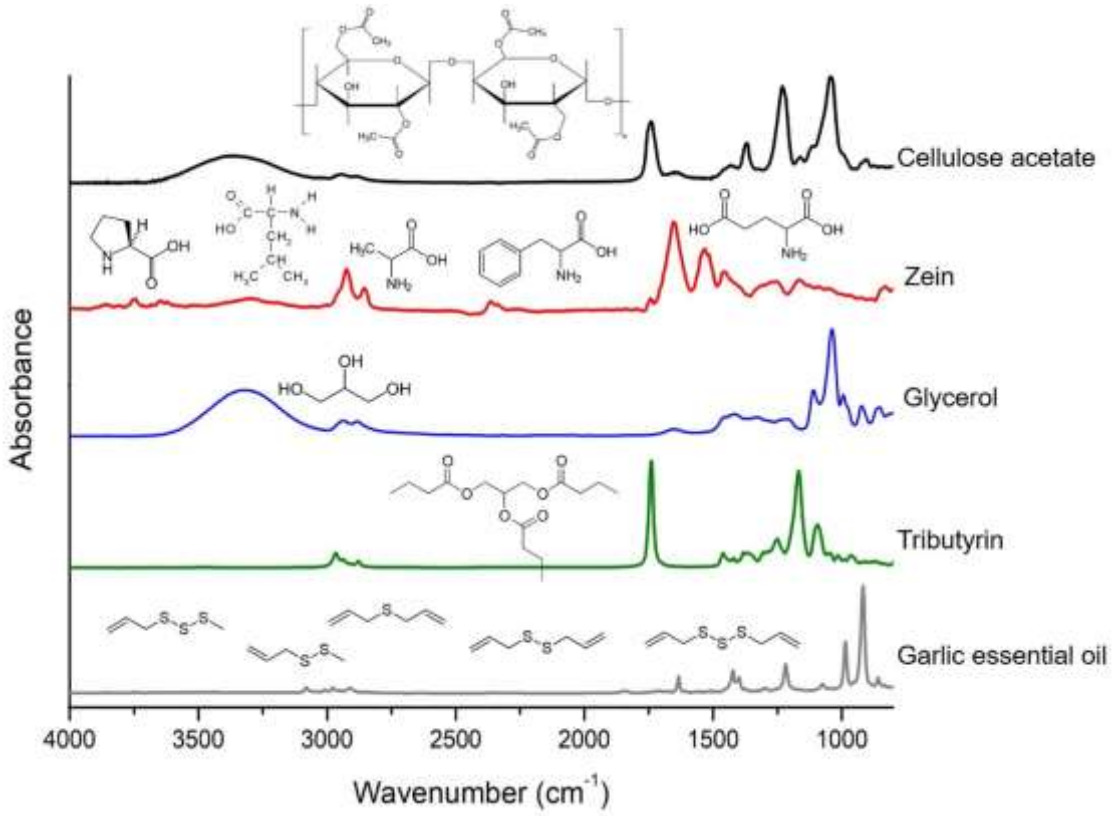


**Figure 5** FTIR spectra and structural formulas of the pristine components.

**Table 5** Main FTIR spectra peaks and bands of the pristine compounds.

| **Component** | **Group** | **Wavenumber region ($cm^{-1}$)** |
|---|---|---|
| Glycerol | O-H stretching | 3650-3100 |
| | C-H stretching | 3000-2840 |
| | C-O stretching | 1130-1040 |
| Tributyrin | C=O stretching | 1740 |
| | C-O stretching | 1170 |
| Cellulose acetate | O-H stretching | 3650-3050 |
| | C=O stretching | 1740 |
| | Asymmetric C-O-C stretching | 1240-1210 |
| | C-O stretching | 1040 |
| | C-H stretching | 1370 |

| | | |
|---|---|---|
| Zein | Asymmetric and symmetric C-H stretching | 2950-2800 |
| | C=O stretching vibration | 1650 |
| | N-H bending | 1540 |
| Garlic essential oil | C-H stretching | 3100-2900 |
| | C=C stretching | 1630 |

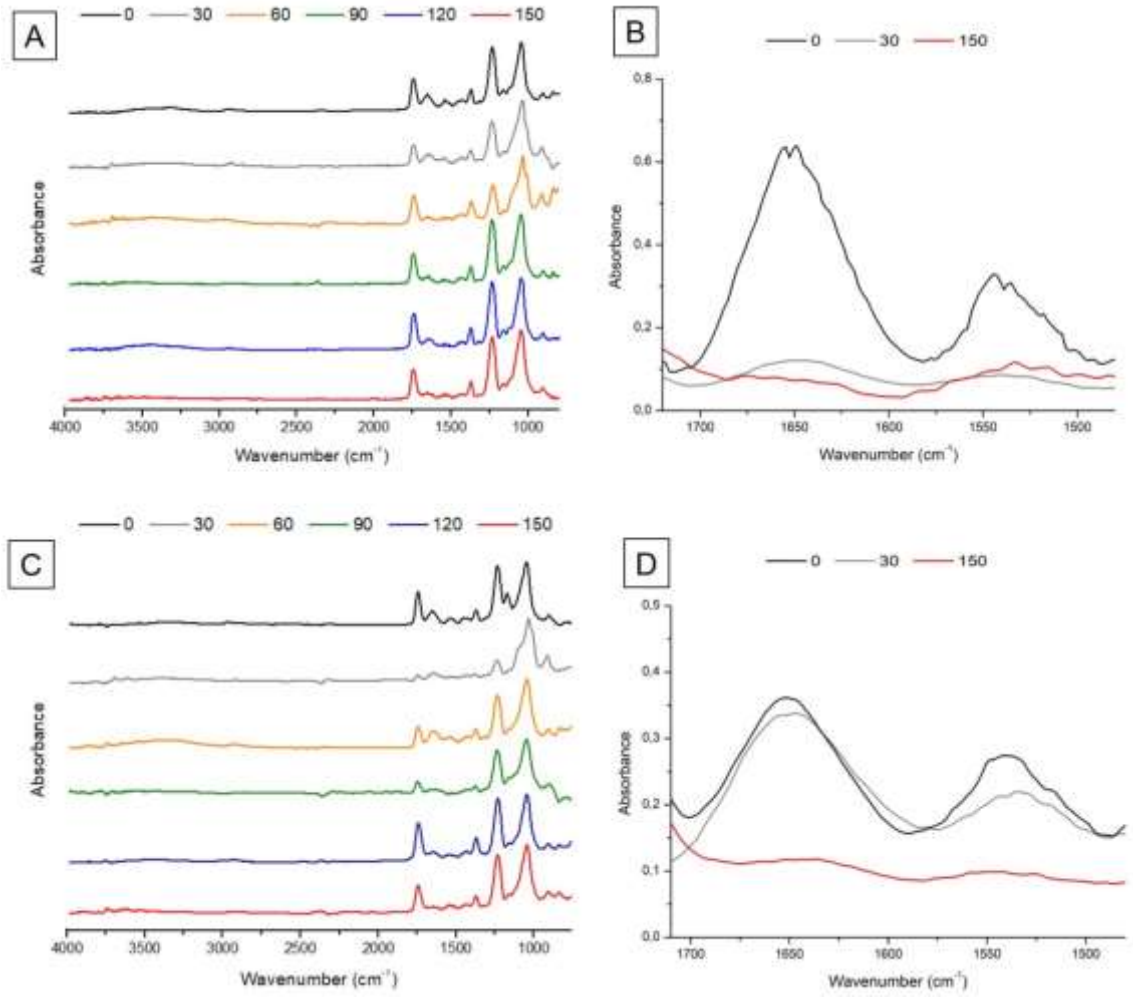


**Figure 6** Cellulose acetate:zein blend films incorporated with glycerol (A, B) and tributyrin (C, D) after burial in soil for 0, 30, 60, 90, 120, and 150 days. Zoom in FTIR spectra: 1700-1500 $cm^{-1}$ region (B, D), corresponding to the C=O stretching and N-H bending.

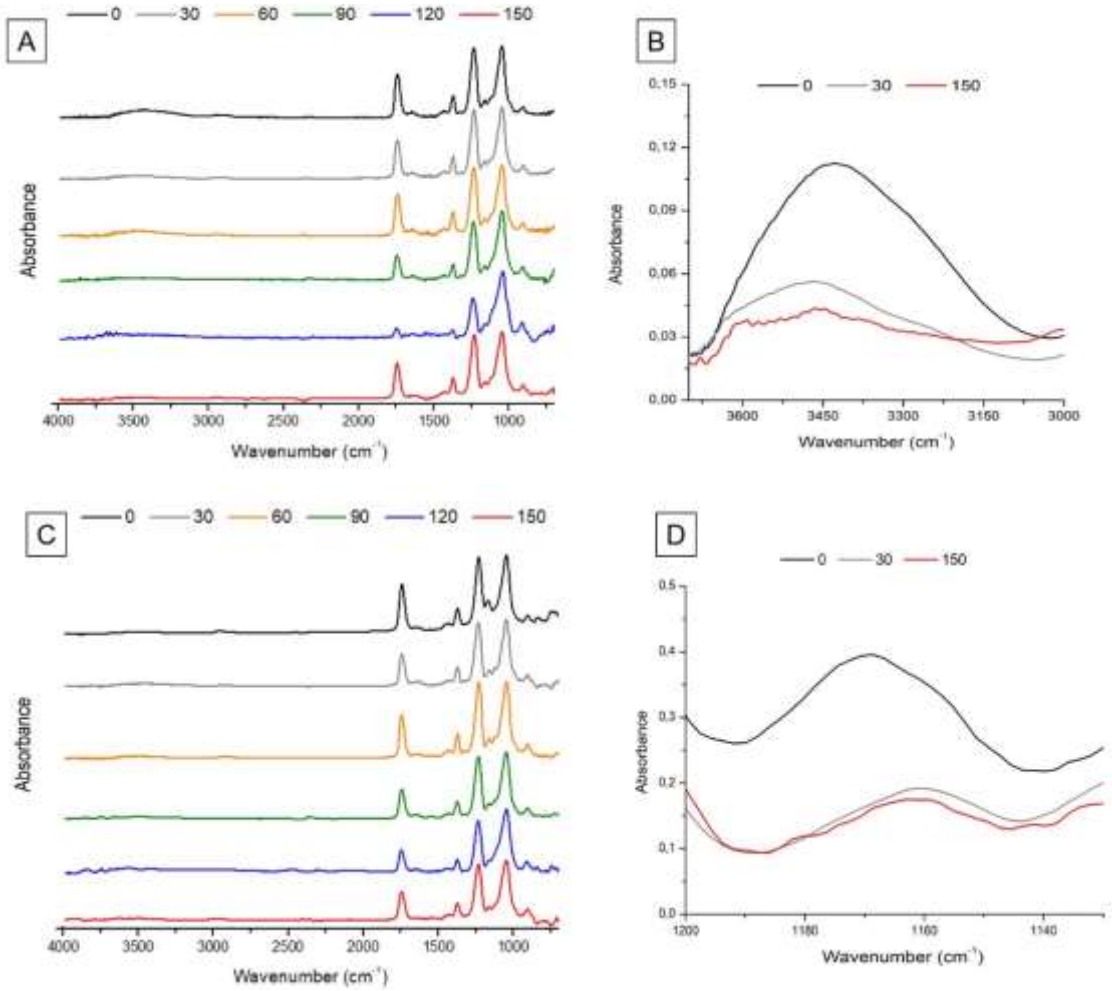


**Figure 7** FTIR spectra of cellulose acetate films incorporated with glycerol (A, B) or tributyrin (C, D) after burial in soil for 0, 30, 60, 90, 120, and 150 days. Zoom of FTIR spectra: 3600-3000 $cm^{-1}$ region (B), corresponding to the O-H stretching in films incorporated with glycerol, and at 1170 $cm^{-1}$ (D), corresponding to the peak associated with tributyrin plasticizer (C-O stretching).

In CA:zein blend films (Figure 6), it was possible to observe characteristic peaks around 1650 $cm^{-1}$, related to C=O stretching vibration, and 1540 $cm^{-1}$, attributed to N-H bending. These bands are regular in proteins and peptides FTIR spectra and correspond to amide I and II, respectively (Ali et al., 2014; Cobb et al., 2020). Over time, the magnitude of these peaks decreased (highlighted in Figure 6B and 6D), suggesting loss of the secondary structure of the protein, as well as break of peptide bonds (primary structure) due to zein degradation in the blend films, as stated before (Section 5.3.2).

The plasticizer loss was perceptible in all films' samples and confirmed the results discussed in Section 5.3.2. For both blends and CA-films plasticized with glycerol, an

intensity reduction, over time, at 3650-3100 $cm^{-1}$ band (O-H stretching) was verified. This behavior was associated with glycerol loss (evidenced in Figure 7B). Tributyrin-added films, otherwise, presented a peak at 1170 $cm^{-1}$, characteristic of the C-O stretching in the tributyrin molecule. Over time, there was a reduction in the magnitude of this peak, associated with loss of the plasticizer (Figure 7D). Along with hydrolysis, loss of plasticizer is one of the processes that occur during CA degradation (Littlejohn et al., 2013).

The assessment of CA degradation was verified, in part, by FTIR. Reduction in the intensity of the O-H stretching band was observed in all CA-based films, including the sample without plasticizers (CA control film) (Figure 8S). This finding suggests that the reduction of intensity was not only due to loss of glycerol, but also due to hydroxyl's oxidation, as discussed in Section 5.3.1 (Ahn et al., 2019). The deacetylation reaction, however, was not evidenced in the FTIR spectra, since no changes were detected in the peak related to the carbonyl group peak (1740 $cm^{-1}$). Regarding the GEO presence, the main peaks could not be observed in the films spectra probably due to polymers or plasticizers peaks that overlapped the GEO spectrum (Figure 7S).

## 5.4 Conclusion

The blend of CA with zein changed the degradation rate of the material when buried in soil, culminating in a mass loss of 50% after 150 days, a relevant value in comparison to only 2% of mass loss verified for CA control sample. Incorporation of plasticizers also speed up the process, and glycerol incorporation provided more polymer mass loss than tributyrin over time. FTIR spectra evidenced changes in the protein structure, suggesting material degradation, as well as loss of both plasticizers through the burial period and occurrence of oxidation of the remaining hydroxyl's group in CA. TGA results reinforced these findings, since the thermal profiles obtained for films recovered after 150 days were more similar to the thermal profile verified for the CA control sample, indicating absence of both additives and zein in the films. It was verified that polymer mass loss was less intense in films incorporated with GEO and glycerol, suggesting that the effect of GEO on the microbiota involved in polymer degradation is plasticizer-dependent. These findings provide important information to sustainable active packaging area, however, we highlight the need for future studies to clarify the role of different antimicrobial agents and plasticizers in biopolymers' degradation.

## 5.5 References

Ahn, K., Zaccaron, S., Zwirchmayr, N.S., Hettegger, H., Hofinger, A., Bacher, M., Henniges, U., Hosoya, T., Potthast, A., Rosenau, T., 2019. Yellowing and brightness reversion of celluloses: CO or COOH, who is the culprit?. Cellulose, 26, 429–444. https://doi.org/10.1007/s10570-018-2200-x

Ali, S., Khatri, Z., Oh, K. W., Kim, I.-S., Kim, S.H., 2014. Zein/cellulose acetate hybrid nanofibers: electrospinning and characterization. Macromol. Res., 22, 9, 971-977. https://doi.org/10.1007/s13233-014-2136-4.

Andersson, S.R., Hakkarainen, M., Albertsson, A.-C., 2010. Tuning the polylactide hydrolysis rate by plasticizer architecture and hydrophilicity without introducing new migrants. Biomacromol., 11, 3617–3623. https://doi.org/10.1021/bm101075p.

Anpilova, A.Y., Mastalygina, E.E., Khrameeva, N.P., Popov, A.A., 2020. Methods for cellulose modification in the development of polymeric composite materials. Rus. J. Phys. Chem. B, 14, 1, 176–182. https://doi.org/10.1134/S1990793120010029.

Assis, R.Q., Rios, P.D'A., Rios, A.O., Oliveira, F.C., 2020. Biodegradable packaging of cellulose acetate incorporated with norbixin, lycopene or zeaxanthin. Ind. Crop. Prod., 147, 112212. https://doi.org/10.1016/j.indcrop.2020.112212.

ASTM. ASTM D5988-18. (2018). Standard test method for determining aerobic biodegradation of plastics materials in soil. ASTM: West Conshohocken, PA, USA.

Bagheri, L., Khodaei, N., Salmieri, S., Karboune, S., Lacroix, M., 2020. Correlation between chemical composition and antimicrobial properties of essential oils against most common food pathogens and spoilers: *In-vitro* efficacy and predictive modelling. Microb. Pathog., 147, 104212. https://doi.org/10.1016/j.micpath.2020.104212.

Basiak E, Lenart A, Debeaufort F., 2018. How glycerol and water contents affect the structural and functional properties of starch-based edible films. Polymers (Basel), 10(4), 412. https://doi.org/10.3390/polym10040412

Bayer, I.S. Zein in Food Packaging. Sustainable Food Packaging Technology, First Edition. Edited by Athanassia Athanassiou. © 2021 WILEY-VCH GmbH. Published 2021 by WILEY-VCH GmbH.

Biswas, A., Saha, B.C., Lawton, J.W., Shogren, R.L., Willett, J.L., 2006. Process for obtaining cellulose acetate from agricultural by-products. Carbohydr. Polym., 64, 1, 134-137. https://doi.org/10.1016/j.carbpol.2005.11.002.

Calil, M.R., Gaboardi, F., Guedes, C.G.F., Rosa, D.S., 2006. Comparison of the biodegradation of poly(e-caprolactone), cellulose acetate and their blends by the Sturm test and selected cultured fungi. Polym. Test., 25, 597–604. https://doi.org/10.1016/j.polymertesting.2006.01.019.

Canevarolo Junior, S. V., 2006. Ciência dos Polímeros, São Paulo: Artliber. 277 p.

Cobb, J.S., Zai-Rose, V., Correia, J.J., Janorkar, A.V., 2020. FT-IR Spectroscopic analysis of the secondary structures present during the desiccation induced aggregation of elastin-like polypeptide on silica. CS Omega, 5, 14, 8403–8413. https://doi.org/10.1021/acsomega.0c00271.

Fornazier, M., Melo, P.G., Pasquini, D., Otaguro, H., Pompêu, G.C.S., Ruggiero, R., 2021. Additives incorporated in cellulose acetate membranes to improve its performance as a barrier in periodontal treatment. Front. Dent. Med., 2, 776887. https://doi.org/10.3389/fdmed.2021.776887.

Gonçalves, S.M., Santos, D.C., Motta, J.F.G., dos Santos, R.R., Chávez, D.W.H., de Melo, N.R., 2019. Structure and functional properties of cellulose acetate films incorporated with glycerol. Carbohydr. Polym., 209, 190-197. https://doi.org/10.1016/j.carbpol.2019.01.031.

Gonçalves, S.M., Motta, J.F.G., Ribeiro-Santos, R., Chávez, D.W.H., de Melo, N.R., 2020. Functional and antimicrobial properties of cellulose acetate films incorporated with sweet fennel essential oil and plasticizers. Curr. Res. Food Sci., 3, 1-8. https://doi.org/10.1016/j.crfs.2020.01.001

Guruprasad, K.H., Shashidhara, G.M., 2004. Grafting, blending, and biodegradability of cellulose acetate. J. Appl. Polym. Sci., 91, 1716–1723. https://doi.org/10.1002/app.13386.

Hernández-García, E., Vargas, M., González-Martínez, C., Chiralt, A., 2021. Biodegradable antimicrobial films for food packaging: Effect of antimicrobials on degradation. Foods, 10, 1256. https://doi.org/10.3390/foods10061256.

Herniou–Julien, C., Mendieta, J.R., Gutiérrez, T., 2019. Characterization of biodegradable/non-compostable films made from cellulose acetate/corn starch blends processed under reactive extrusion conditions. Food Hydrocoll., 89, 67-79. https://doi.org/10.1016/j.foodhyd.2018.10.024.

Kunthadong, P., Molloy, R., Worajittiphon, P., Leejarkpai, T., Kaabbuathong, N., Punyodom, W., 2015. Biodegradable plasticized blends of poly(L-lactide) and cellulose acetate butyrate: from blend preparation to biodegradability in real composting conditions. J. Polym. Environ., 23, 107–113. https://doi.org/10.1007/s10924-014-0671-x.

Lawton, J.W. Zein: a history of processing use., 2002. Cereal Chemistry, 79, 1, 1–18. https://doi.org/10.1094/CCHEM.2002.79.1.1.

Littlejohn, D., Pethrick, R.A., Quye, A., Ballany, J.M., 2013. Investigation of the degradation of cellulose acetate museum artefacts. Polym. Degrad. Stab., 98, 1, 416-424. https://doi.org/10.1016/j.polymdegradstab.2012.08.023.

Liu, L., Gong, D., Bratasz, L., Zhu, Z., Wang, C., 2019. Degradation markers and plasticizer loss of cellulose acetate films during ageing. Polym. Degrad. Stab. 168, 108952. https://doi.org/10.1016/j.polymdegradstab.2019.108952.

Marques, C.S., Silva, R.R.A., Arruda, T.R., Ferreira, A.L.V., Oliveira, T.V., Moraes, A.R.F., Dias, M.V., Vanetti, M.C.D., Soares, N.F.F., 2022a. Development and investigation of zein and cellulose acetate polymer blends incorporated with garlic essential oil and β-cyclodextrin for potential food packaging application. Polysacch., 3, 1, 277-291. https://doi.org/10.3390/polysaccharides3010016.

Marques, C.S., Arruda, T.R., Silva, R.R.A., Ferreira, A.L.V., Oliveira, W.L.A., Rocha, F., Mendes, L.A., Oliveira, T.V., Vanetti, M.C.D., Soares, N.F.F., 2022b. Exposure to cellulose acetate films incorporated with garlic essential oil does not lead to homologous resistance in *Listeria innocua* ATCC 33090. Food Res. Int., 160, 111676. https://doi.org/10.1016/j.foodres.2022.111676.

Melo, P.G., Borges, M.F., Ferreira, J.A., Silva, M.V.B., Ruggiero, R., 2018. Bio-based cellulose acetate films reinforced with lignin and glycerol. Int. J. Mol. Sci., 19, 4, 1143. https://doi.org/10.3390/ijms19041143.

Moraes, A.R.F., Pola, C.C., Bilck, A.P., Yamashita, F., Tronto, J., Medeiros, E.A.A., Soares, N.F.F., 2017. Starch, cellulose acetate and polyester biodegradable sheets: Effect of composition and processing conditions. Mat. Sci. Eng. C, 78, 932–941. http://dx.doi.org/10.1016/j.msec.2017.04.093.

Phuong, V.T., Verstichel, S., Cinelli, P., Anguillesi, I., Coltelli, M.-B., Lazzeri, A., 2014. Cellulose acetate blends – Effect of plasticizers on properties and biodegradability. Journal of Renewable Materials, 1, 35-41. https://doi.org/10.7569/JRM.2013.634136.

Quintana, R., Persenaire, O., Lemmouchi, Y., Sampson, J., Martin, S., Bonnaud, L., Dubois, P., 2013. Enhancement of cellulose acetate degradation under accelerated weathering by plasticization with eco-friendly plasticizers. Polym. Degrad. Stab., 98. 1556-1562. http://dx.doi.org/10.1016/j.polymdegradstab.2013.06.032.

R Core Team. R: A Language and Environment for Statistical Computing; R Foundation for Statistical Computing: Vienna, Austria, 2021; Retrieved from https://www.R-project.org/. Accessed January 29, 2022.

Rogovina, S., Aleksanyan, K., Prut, E., Gorenberg, A., 2013. Biodegradable blends of cellulose with synthetic polymers and some other polysaccharides. Eur. Polym. J., 49, 194-202. http://dx.doi.org/10.1016/j.eurpolymj.2012.10.002.

Rosa, D., Lotto, N., Lopes, D., Guedes, C.G., 2004. The use of roughness for evaluating the biodegradation of poly-β-(hydroxybutyrate) and poly-β-(hydroxybutyrate-co-β-valerate). Polym. Test., 23(1), 3–8. https://doi.org/10.1016/s0142-9418(03)00042-4.

Silva, R.R.A., Marques, C.S.M., Arruda, T.R., Teixeira, S.C., Oliveira, T.V., Stringheta, O.C., Pires, A.C.S., Soares, N.F.F., 2022. Ionic strength of methylcellulose-based films: an alternative for modulating mechanical performance and hydrophobicity for potential food packaging application. Polysacch., 3, 426–440. https://doi.org/10.3390/polysaccharides3020026.

Souza, A.R., Evtuguin, D.V., Gamelas, J.A.F., 2016. Xylan and xylan derivatives – Their performance in bio-based films and effect of glycerol addition. Ind. Crop. Prod., 94, 682-689. https://doi.org/10.1016/j.indcrop.2016.09.031.

Yadav, N., Hakkarainen, M., 2021. Degradable or not? Cellulose acetate as a model for complicated interplay between structure, environment and degradation. Chemosphere 265, 128731. https://doi.org/10.1016/j.chemosphere.2020.128731.

Yadav, N., Hakkarainen, M., 2022. Degradation of cellulose acetate in simulated aqueous environments: one-year study. Macromol. Mat. Eng., 2022, 2100951. https://doi.org/10.1002/mame.202100951.

Yamashita, Y., Endo, T., 2005. Biodegradation behavior of acid-containing cellulose acetate film in soil. J. Appl. Polym. Sci., 98, 466–473, 2005. https://doi.org/10.1002/app.21998.

## 5.6 Supplementary Material

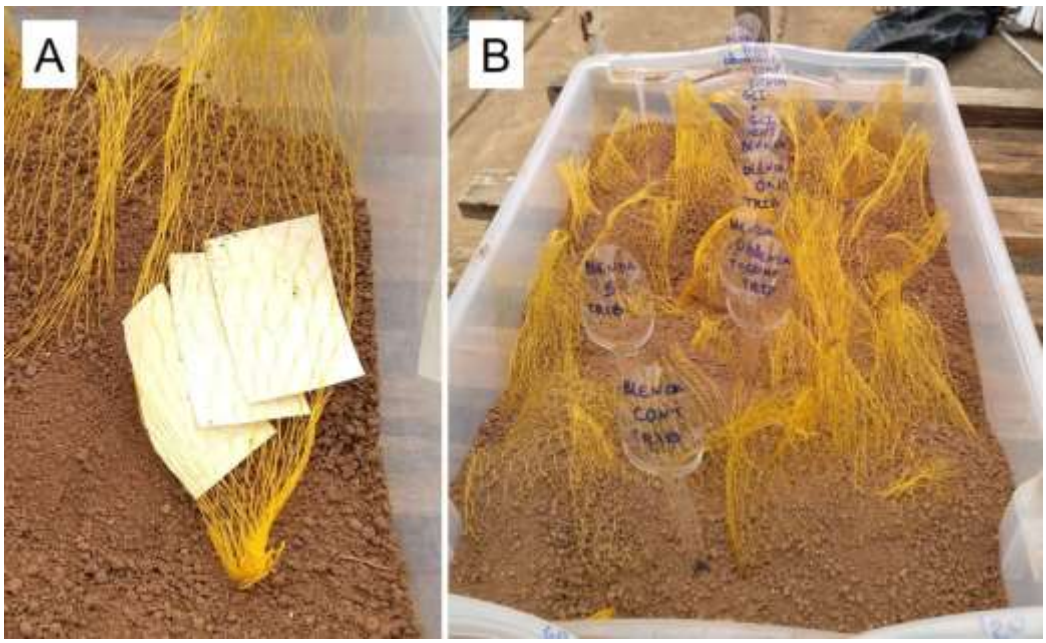


**Figure 1S** Films inside plastic nets in the degradation assay. A) Before burial in soil; B) During the 150-day period.

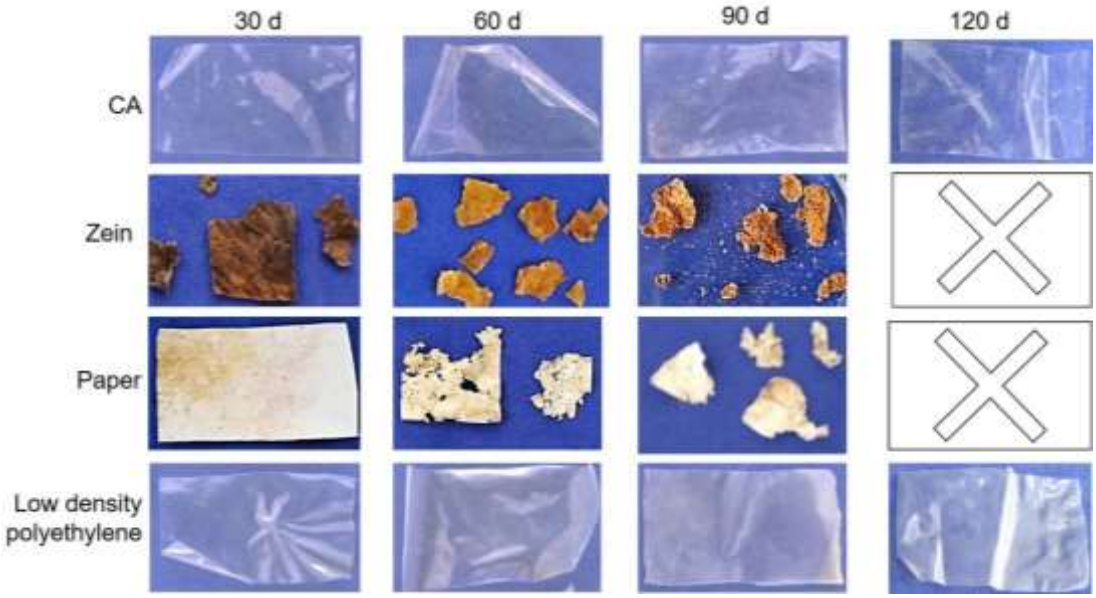


**Figure 2S** Photographs of the controls cellulose acetate (CA) and zein films after burial in soil for 30, 60, 90, and 120 days. Low density polyethylene and paper were also used as controls.

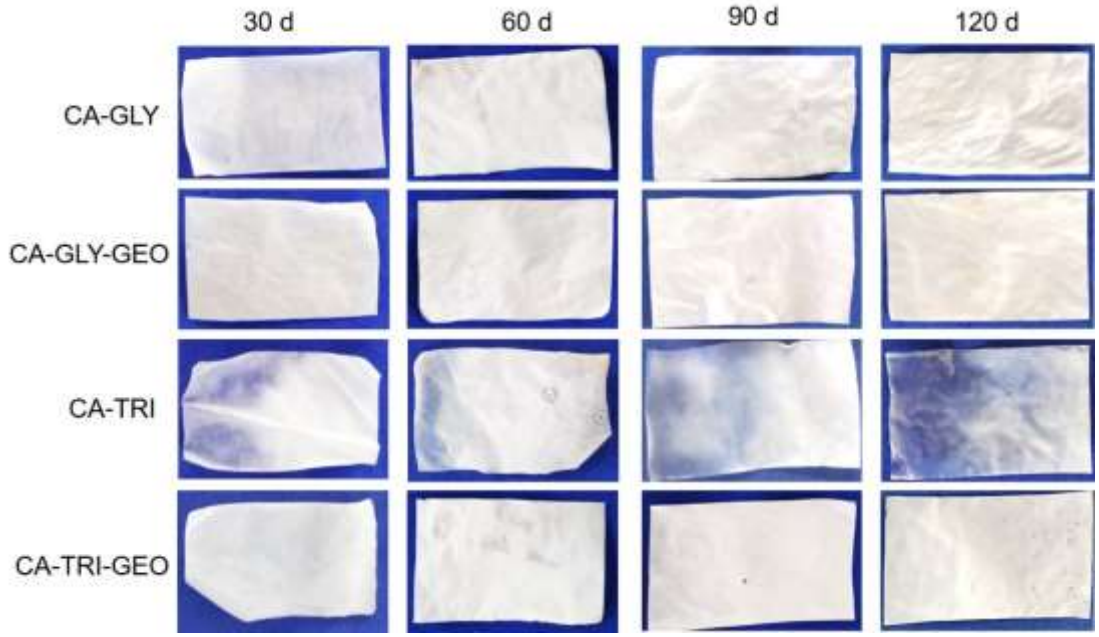


**Figure 3S** Photographs of the cellulose acetate (CA) films incorporated with glycerol (GLY), tributyrin (TRI) and garlic essential oil (GEO) after burial in soil for 30, 60, 90, and 120 days.

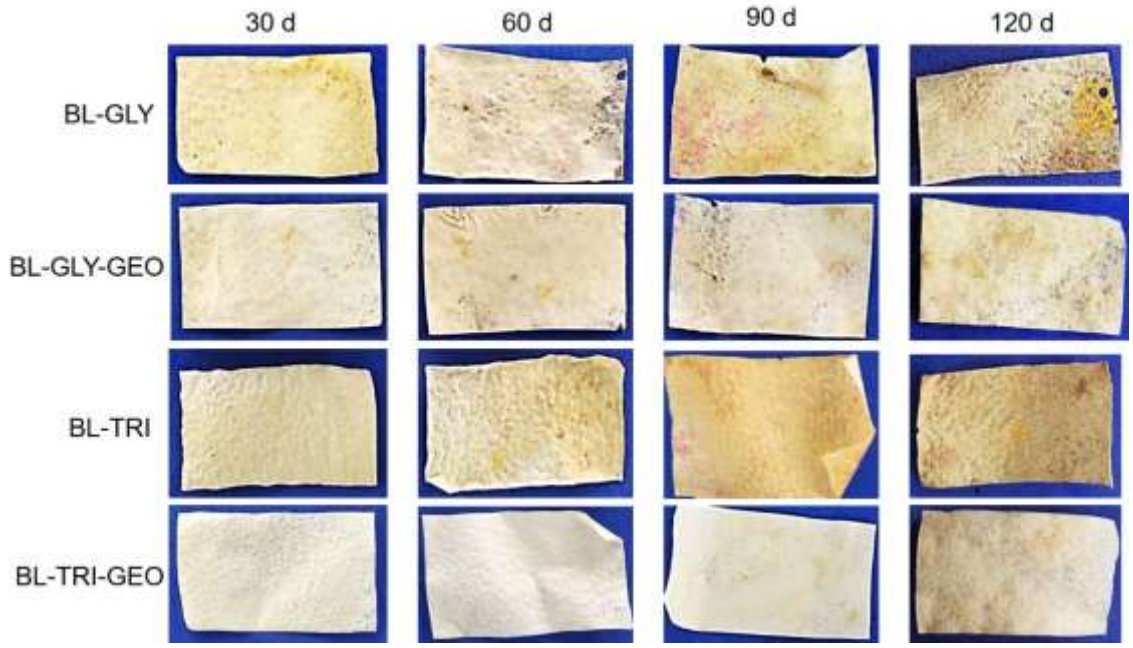


**Figure 4S** Photographs of the cellulose acetate and zein blend films (BL) incorporated with glycerol (GLY), tributyrin (TRI) and garlic essential oil (GEO) after burial in soil for 30, 60, 90, and 120 days.

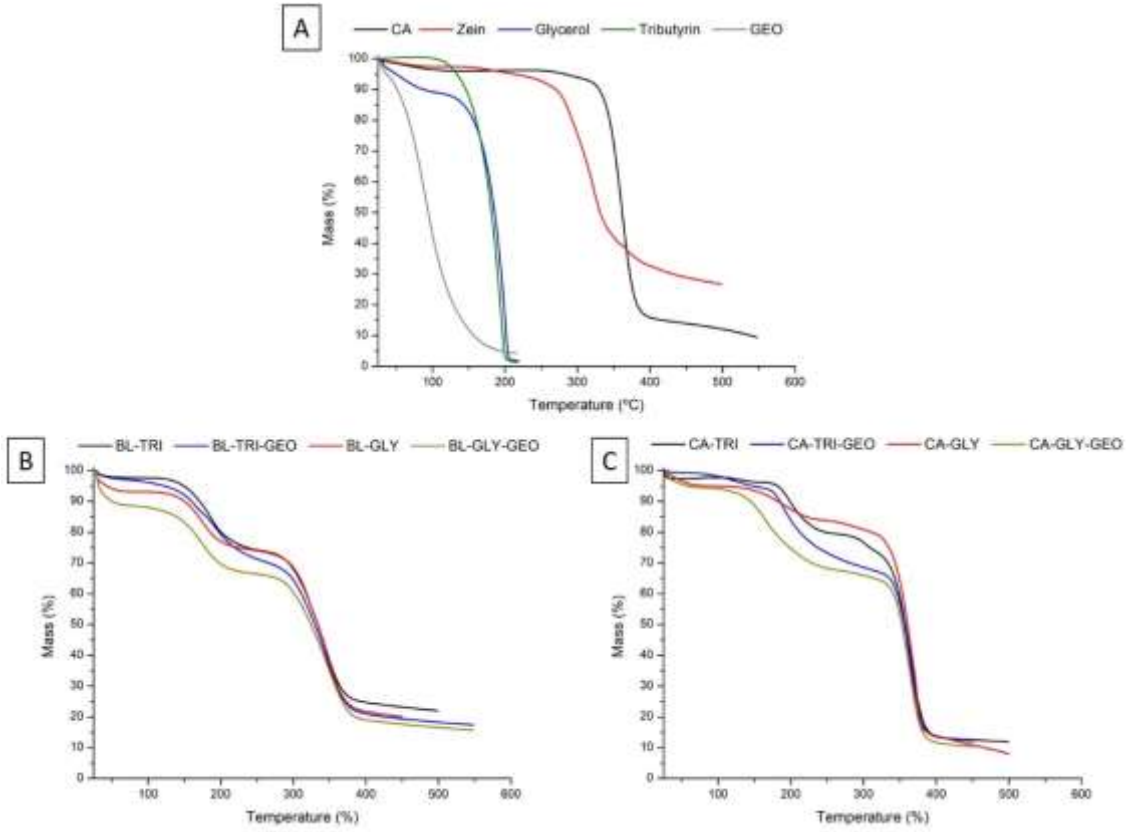


**Figure 5S** TG curves of pristine materials (A), cellulose acetate:zein blend films (B) and cellulose acetate films (C) before burial in soil (0 d).

**Table 1S** Weight loss (%) of pristine components and films samples (0 d), in different temperature ranges, obtained by TG/DTG technique.

| **Sample** | **Mass loss (%)** | | |
|---|---|---|---|
| | **25-120 ºC** | **120-260 ºC** | **260-420 ºC** |
| Cellulose acetate | 4 | - | 81 |
| Zein | 2.5 | 6.5 | 61 |
| Glycerol | - | 100 | - |
| Tributyrin | - | 100 | - |
| GEO | - | 100 | - |
| Mixture CA and zein | 4.5 | 3.5 | 65 |
| CA-GLY | 5 | 12 | 71 |
| CA-GLY-GEO | 7 | 25 | 58 |
| CA-TRI | 3 | 17 | 68 |
| CA-TRI-GEO | 4 | 24 | 60 |
| BL-GLY | 7 | 19.5 | 53.5 |

| | | | |
|---|---|---|---|
| BL-GLY-GEO | 13 | 23 | 46 |
| BL-TRI | 2.5 | 24.5 | 49 |
| BL-TRI-GEO | 5 | 25 | 50 |

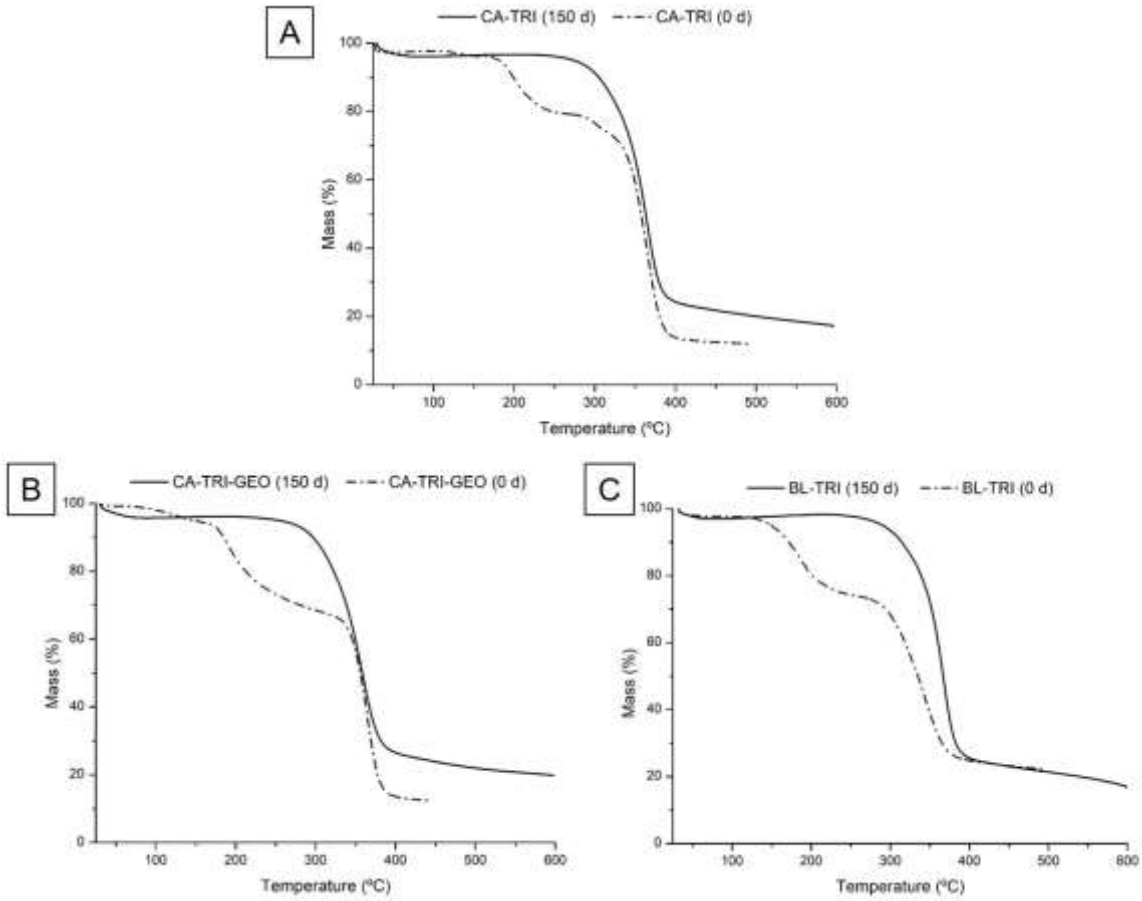


**Figure 6S** TG curves of films before (0 d) and after 150 d buried in soil: cellulose acetate incorporated with tributyrin (A); cellulose acetate incorporated with tributyrin and garlic essential oil (B); cellulose acetate:zein blend incorporated with tributyrin (C).

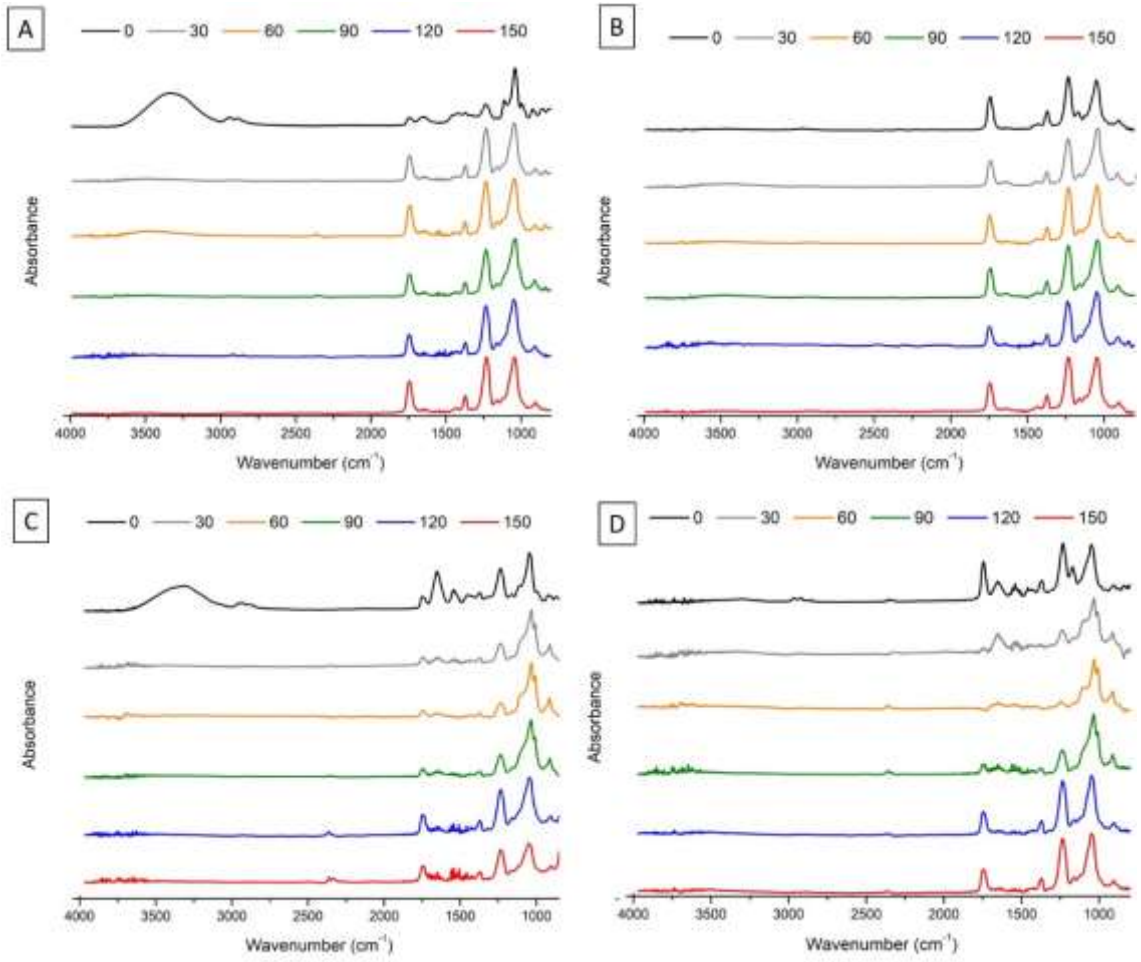


**Figure 7S** FTIR spectra of cellulose acetate films incorporated with glycerol (A) or tributyrin (B), and of cellulose acetate:zein blends incorporated with glycerol (C) or tributyrin (D) after burial in soil for 0, 30, 60, 90, 120, and 150 days. All films contained garlic essential oil.

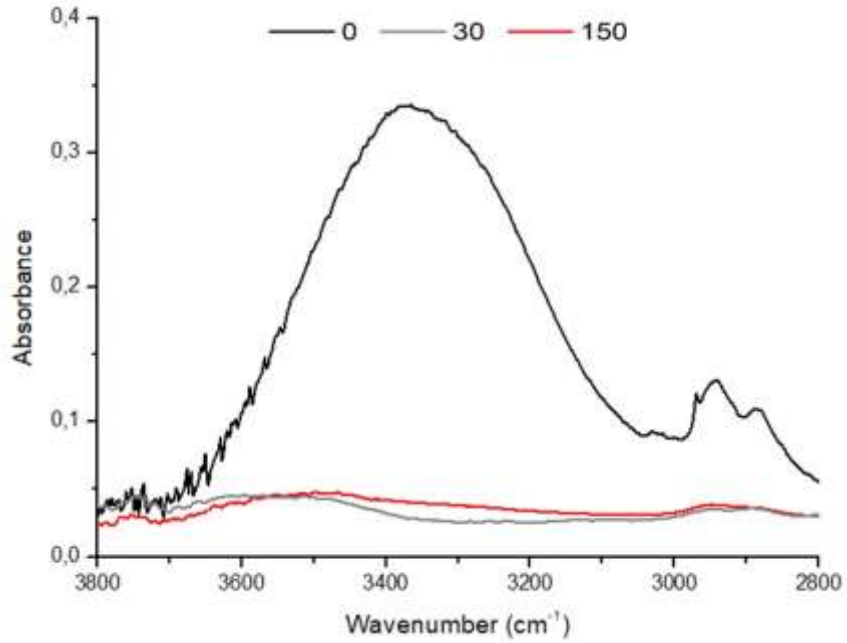


**Figure 8S** Zoom of FTIR spectra of CA control film before burial (0 d) and after 30 days and 150 days buried in soil: 3600-3000 $cm^{-1}$ region, corresponding to the O-H stretching due to presence of residual hydroxyls.

## 6. GENERAL CONCLUSION

Active CA films and their blends with zein were successfully manufactured with different plasticizers and GEO. Incorporation of tributyrin resulted in blend films with a more homogeneous aspect when compared to blends plasticized with glycerol, probably due to better compatibilization between the polymers and the plasticizer. Although the blend films underperformed the CA-based films in mechanical and water vapor permeability tests, the mixture with zein accelerated the material degradation rate, which is an important finding in terms of both sustainability and food application. Presence of plasticizers also speed up the degradation process, likely due to their effect on increasing the polymer chain mobility, whereas the effect of the EO seemed to depend on the type of plasticizer used.

Regarding the antimicrobial agent, films containing GEO showed activity against Gram-positive bacteria when tested *in vitro*. Also, the active films did not lead to homologous resistance in *Listeria innocua*, an important initial result when we take into account the capability of the microorganisms to adapt to stress factors and develop resistance against them.

It is worth noting that the present work provided important information regarding two themes still little explored in the literature (degradation of antimicrobial films, and microbial resistance related to active films) and the results achieved open doors for future researches in the Food Packaging field. For example, it would be of great importance to study if the contact with the manufactured films would lead to cross resistance in microorganisms, such as resistance to antibiotics, as well as to test the films against others microorganisms besides *L. innocua*. Moreover, to better understand how the type of plasticizer affects the EO's antimicrobial activity, and consequently their role in the polymer degradation rate, would bring valuable information to studies regarding sustainable active packaging.